National Park Service
U.S. Department of the Interior

Science Report NPS/SR—2025/324
https://doi.org/10.36967/2313756

Landscape Phenology, Vegetation Condition, and Relations with Climate at Golden Spike National Historical Park, 2000–2019



The “blue marble” image is the most detailed true-color image of Earth to date. Much of the information contained in this image came from a single remote-sensing device: NASA’s Moderate Resolution Imaging Spectroradiometer, or MODIS. Flying more than 700 kilometers above Earth onboard the Terra satellite, MODIS provides an integrated tool for observing a variety of terrestrial, oceanic, and atmospheric features of the Earth.
NASA GODDARD SPACE FLIGHT CENTER

Landscape phenology, vegetation condition, and relations with climate at Golden Spike National Historical Park, 2000–2019

Science Report NPS/SR—2025/324

David Thoma[1]

[1] National Park Service
Northern Colorado Plateau Network
P.O. Box 848
Moab, UT 84532

Eliot Rendleman[1], editor

Please cite this publication as:

Thoma, D. 2025. Landscape phenology, vegetation condition, and relations with climate at Golden Spike National Historical Park, 2000–2019. Science Report NPS/SR—2025/324. National Park Service, Fort Collins, Colorado. https://doi.org/10.36967/2313756

NPS 431/197327, June 2025

The National Park Service Science Report Series disseminates information, analysis, and results of scientific studies and related topics concerning resources and lands managed by the National Park Service. The series supports the advancement of science, informed decisions, and the achievement of the National Park Service mission.

All manuscripts in the series receive the appropriate level of peer review to ensure that the information is scientifically credible and technically accurate.

Views, statements, findings, conclusions, recommendations, and data in this report do not necessarily reflect views and policies of the National Park Service, US Department of the Interior. Mention of trade names or commercial products does not constitute endorsement or recommendation for use by the US Government.

The Department of the Interior protects and manages the nation's natural resources and cultural heritage; provides scientific and other information about those resources; and honors its special responsibilities to American Indians, Alaska Natives, and affiliated Island Communities.

This report is available in digital format from the National Park Service DataStore and the Natural Resource Publications Management website. If you have difficulty accessing information in this publication, particularly if using assistive technology, please email irma@nps.gov.

Contents

Page

Figures v
Tables x
Abstract xi
List of Acronyms xii
Executive Summary xiv
Acknowledgments xvi
1 Introduction 1
1.1 The importance of primary production 1
1.2 Satellite monitoring of primary production 1
1.3 Vegetation condition and vulnerability 2
1.4 Pivot points and responses 3
1.5 Phenology 4
2 Methods 5
2.1 Overview 5
2.2 Remote-sensing targets 6
2.2.1 Alliance polygons 6
2.2.2 NCPN alliance groups 7
2.3 Satellite imagery 8
2.4 Soil Adjusted Vegetation Index 8
2.5 Pixel time series extraction and smoothing 9
2.6 Water-balance model 9
2.7 Measures of vegetation production 11
2.8 Calculating the measures 12
2.9 Climate correlates with annual production 13
2.9.1 Single-variable analysis 13
2.9.2 Multiple-variable analysis 14
2.10 Conceptual basis of climate pivot points and responses 16
2.11 Operational use of pivot points for “now-casts” 17

Contents (continued)

Page

2.12 Phenology metrics and climate drivers 17
3 Results and Discussion 22
3.1 Completeness of satellite observations 22
3.2 Time series 22
3.3 Trends in indicators of annual production 24
3.4 Trends in indicators of growing season production 25
3.5 Climate relations 27
3.5.1 Qualitative patterns in annual precipitation and production 27
3.5.2 Single-variable drivers of production 29
3.6 Pivot points 31
3.6.1 Pivot points indicate drought tolerance 31
3.6.2 Spatial patterns of drought tolerance 33
3.6.3 Pivot points for other climate variables 33
3.7 Vegetation response 35
3.7.1 Vegetation response and climate sensitivity 35
3.7.2 Patterns within alliance groups 38
3.7.3 Production response to water and non-water variables 40
3.8 Multivariable indicators of annual vegetation production 42
3.9 Land-surface phenology trends at Golden Spike National Historical Park 45
3.10 Drivers of green-up 46
3.10.1 A priori model selection method 46
3.10.2 Random-forest method 49
3.11 Climate patterns 52
4 Tools to Inform Near-Term Management 55
5 Conclusions 56
6 Literature Cited 57
7 Appendix A. Supplemental Figures for Landscape Phenology, Vegetation Condition, and Relations with Climate at Golden Spike National Historical Park, 2000–2019 63

Figures

Page

Figure 1. NCPN alliance groups analyzed for trends in production, phenology, and climate relations at Golden Spike National Historical Park. 5

Figure 2. Measures of annual production from a time series of 16-day soil adjusted vegetation index (SAVI) derived from MODIS imagery. 12

Figure 3. Conceptual diagram of soil-moisture pivot point and response of a single vegetation-alliance map unit to variation in annual average soil moisture. 14

Figure 4. Integrated area under the growing-season curve (shaded area) for one polygon over two calendar years. 18

Figure 5. Soil-adjusted vegetation index time series by alliance group for 28 polygons analyzed for 2000–2019. 23

Figure 6. Spatial pattern of trends in mean annual iSAVI. 25

Figure 7. Trends in mean growing-season iSAVI by alliance group, determined via simple linear regression. 26

Figure 8. Co-variation in growing-season production, estimated as the iSAVI between March and October and water-year cumulative precipitation averaged within alliance groups, demonstrating the link between climate and vegetation production in the park at the annual scale. 28

Figure 9. Significant (p-value < 0.05) relationships between water-year climate variables and first difference of growing season iSAVI, 2000–2019. 30

Figure 10. The mean precipitation pivot-point values shown here represent critical water needs for the different alliance groups. 32

Figure 11. Precipitation pivot points for polygons with a significant relationship (p-value < 0.05) between water-year annual precipitation and change in annual vegetation production, assessed as the interannual difference in iSAVI. 33

Figure 12. Significant (p-value < 0.05) water-related pivot points by alliance group. 34

Figure 13. Sensitivity of growing-season vegetation production to annual water-year precipitation. 36

Figure 14. Responses of different vegetation alliance groups to precipitation. 37

Figure 15. Graphical depiction of the relationship between pivot points and responses in polygons that had a significant relationship (p-value < 0.05) between iSAVI and water-year precipitation (e.g., critical water need vs. rate of growing season iSAVI change per mm precipitation). 39

Figures (continued)

Page

Figure 16. Top models in multi-model comparison of climate correlates with interannual differences in growing-season iSAVI across all alliance groups. 41

Figure 17. Top models in multi-model comparison of climate correlates with interannual differences in growing-season iSAVI across all alliance groups. 43

Figure 18. Top models of growing-season production by alliance group in multi-model comparisons of climate correlates with interannual differences in growing season iSAVI. 44

Figure 19. Top models in multi-model comparisons of climate correlates with start of growing season at the whole-park scale. 47

Figure 20. Top models in multi-model comparisons of climate correlates with start of growing season at the alliance-group scale. 48

Figure 21. Variable importance in the random-forest model of climate drivers of the start of growing season. 49

Figure 22. Predicted start-of-season date versus observed start-of-season date in the holdout dataset used for validation of the random-forests model for all polygons in Golden Spike NHP. 50

Figure 23. Predicted start-of-season date versus observed start-of-season date in the holdout dataset used for validation of the random-forests model for alliance groups. 51

Figure 24. Long-term temporal patterns in precipitation in vegetation alliance groups. 53

Figure 25. Annual precipitation trend over time, 2000–2019. 54

Figure 26. Spatial pattern of trends in maximum annual iSAVI. 63

Figure 27. Pivot points for polygons where soil moisture was significantly related to interannual variation in production (p-value < 0.05). 64

Figure 28. A map of Golden Spike NHP showing the locations of polygons where soil moisture was significantly related to interannual variation in production (p-value < 0.05). 65

Figure 29. Pivot points for polygons where rain was significantly related to interannual variation in production (p-value < 0.05). 66

Figure 30. A map showing the locations of polygons where rain was significantly related to interannual variation in production (p-value < 0.05). 67

Figure 31. Pivot points for polygons where precipitation was significantly related to interannual variation in production (p-value < 0.05). 68

Figure 32. A map showing the locations of polygons where precipitation was significantly related to interannual variation in production (p-value < 0.05). 69

Figures (continued)

Page

Figure 33. Pivot points for polygons where water deficit was significantly related to interannual variation in production (p-value < 0.05). 70

Figure 34. A map showing the locations of polygons where water deficit was significantly related to interannual variation in production (p-value < 0.05). 71

Figure 35. Pivot points for polygons where actual evapotranspiration was significantly related to interannual variation in production (p-value < 0.05). 72

Figure 36. A map showing the locations of polygons where actual evapotranspiration was significantly related to interannual variation in production (p-value < 0.05). 73

Figure 37. Pivot points for polygons where water was significantly related to interannual variation in production (p-value < 0.05). 74

Figure 38. A map showing the locations of polygons where water was significantly related to interannual variation in production (p-value < 0.05). 75

Figure 39. Pivot points for polygons where vapor pressure deficit was significantly related to interannual variation in production (p-value < 0.05). 76

Figure 40. A map showing the locations of polygons where vapor pressure deficit was significantly related to interannual variation in production (p-value < 0.05). 77

Figure 41. Sensitivity of growing season vegetation production to soil moisture in polygons, where the relationship was significant (p-value < 0.05). 78

Figure 42. A map showing the sensitivity of growing season vegetation production to soil moisture in polygons, where the relationship was significant (p-value < 0.05). 79

Figure 43. Sensitivity of growing season vegetation production to rain in polygons, where the relationship was significant (p-value < 0.05). 80

Figure 44. A map showing the sensitivity of growing season vegetation production to rain in polygons where the relationship was significant (p-value < 0.05). 81

Figure 45. Sensitivity of growing season vegetation production to precipitation in polygons, where the relationship was significant (p-value < 0.05). 82

Figure 46. A map showing the sensitivity of growing season vegetation production to precipitation in polygons where the relationship was significant (p-value < 0.05). 83

Figure 47. Sensitivity of growing season vegetation production to water deficit in polygons, where the relationship was significant (p-value < 0.05). 84

Figure 48. Sensitivity of growing season vegetation production to water deficit, where the relationship was significant (p-value < 0.05). 85

Figures (continued)

Page

Figure 49. Sensitivity of growing season vegetation production to actual evapotranspiration in polygons, where the relationship was significant (p-value < 0.05). 86

Figure 50. Sensitivity of growing season vegetation production to actual evapotranspiration, where the relationship was significant (p-value < 0.05). 87

Figure 51. Sensitivity of growing season vegetation production to water in polygons, where the relationship was significant (p-value < 0.05). 88

Figure 52. Sensitivity of growing season vegetation production to water, where the relationship was significant (p-value < 0.05). 89

Figure 53. Sensitivity of growing season vegetation production to vapor pressure deficit in polygons, where the relationship was significant (p-value < 0.05). 90

Figure 54. A map showing the sensitivity of growing season vegetation production to vapor pressure deficit in polygons where the relationship was significant (p-value < 0.05). 91

Figure 55. Variation in precipitation pivot points as related to soil and site characteristics. 92

Figure 56. Variation in responses to precipitation as related to soil and site characteristics. 93

Figure 57. Direction and magnitude of change in land surface phenology metrics, shown as ± days per year, for each vegetation alliance group. 94

Figure 58. Direction and magnitude of change in land surface phenology metrics, shown as ± days per year, grouped by metric. 95

Figure 59. Cumulative annual precipitation over time (1980 to 2019) in vegetation alliance groups. 96

Figure 60. Cumulative annual precipitation over time (2000 to 2019) in vegetation alliance groups. 97

Figure 61. Annual average temperature over time (1980 to 2019) in vegetation alliance groups. 98

Figure 62. Annual average temperature over time (2000 to 2019) in vegetation alliance groups. 99

Figure 63. Cumulative annual actual evapotranspiration over time (1980 to 2019) in vegetation alliance groups. 100

Figure 64. Cumulative annual actual evapotranspiration over time (2000 to 2019) in vegetation alliance groups. 101

Figures (continued)

Page

Figure 65. Cumulative annual water deficit over time (1980 to 2019) in vegetation alliance groups. 102

Figure 66. Cumulative annual water deficit over time (2000 to 2019) in vegetation alliance groups. 103

Figure 67. Annual average soil moisture over time (1980 to 2019) in vegetation alliance groups..... 104

Figure 68. Annual average soil moisture over time (2000 to 2019) in vegetation alliance groups..... 105

Tables

Page

Table 1. NCPN alliance groups and corresponding National Vegetation Classification alliances, Golden Spike National Historical Park. 7

Table 2. Climate and water-balance variables used to identify correlations with vegetation production and phenology. 10

Table 3. *A priori* models of climate influence on vegetation production competed via generalized linear mixed-effects modeling to identify best correlates with production. 15

Table 4. *A priori* models of climate influence on timing of green-up (start of the growing season) 20

Table 5. Amount of park area with increasing (pos) or decreasing (neg) trends in mean annual or maximum annual SAVI by alliance group. 24

Table 6. Changes in land surface phenology in days averaged by alliance group during the 20-year study. 45

Abstract

Climate determines the vegetation composition in parks, and changes in climate will affect vegetation conditions and composition in the future. This study, which examined changes in climate, water availability, and vegetation from 2000 to 2019 in Golden Spike National Historical Park (NHP) in Utah, USA, evaluates vegetation sensitivity to weather and climate to understand climate–vegetation relationships that can be used to predict what vegetation types may change. Specifically, it evaluates where change is likely in the park, when change may happen, and why change may occur. This information is needed to anticipate changes and can be used to plan for inevitable change. Satellite images were analyzed with climate data to quantify vegetation sensitivity and drought tolerance. Historic trends in vegetation production and phenology were evaluated, and an analysis with climate data identified which aspects of climate were most important to annual production and phenology for different vegetation types. Since 2000, a very dry period, growing season primary production has increased in all alliance groups in Golden Spike NHP. The increase coincided with a slight increase in precipitation and a slight decrease in temperature over the same period. However, over this period, there were dry years and dry periods extending for several years that resulted in substantial declines in vegetation cover. These largely rebounded by the end of the study. The variation in vegetation condition across wet and dry years was evaluated to identify which alliance groups were most tolerant of low annual precipitation (Perennial Exotic Grassland), and which were least sensitive to variation in precipitation (Disturbed areas). The climate variable most strongly correlated with vegetation production was three years of soil moisture. The information generated in this study can be applied to long-term management and planning and help preserve the natural resources of the National Park System for the enjoyment, education, and inspiration of this and future generations.

List of Acronyms

AET: actual evapotranspiration

D: climatic water deficit

EOS: end of growing season

GDD: growing degree days

iSAVI: integrated growing season soil adjusted vegetation index

LOS: length of season

Meltd: date of complete snowmelt

MODIS: moderate resolution imaging spectroradiometer

NHP: national historical park

NCPN: Northern Colorado Plateau Network

NDVI: normalized difference vegetation index

NVC: National Vegetation Classification

NVCS: National Vegetation Classification Standard

P: annual precipitation

PACK: snowpack water equivalent

PET: potential evapotranspiration

POP: timing of peak growth

RAIN: rain

SAVI: soil adjusted vegetation index

SVP: saturation vapor pressure

SNOW: snow

SOIL: soil moisture

SOS: start of season/green-up

SRAD: solar radiation

T: temperature (annual average)

Tmax: temperature (maximum)

Tmin: temperature (minimum)

VP: vapor pressure

VPD: vapor-pressure deficit

W: water as rain plus snowmelt

Executive Summary

Quantitatively linking satellite observations of vegetation condition and climate data over time provides insight into climate influences on primary production, phenology (timing of growth), and sensitivity of vegetation to weather and longer-term patterns of weather referred to as climate. This in turn provides a basis for understanding potential climate impacts to vegetation—and the potential to anticipate cascading ecological effects, such as impacts to forage, habitat, fire potential, and erosion, as climate changes.

This report provides baseline information about vegetation production and condition over time at Golden Spike National Historical Park (NHP), as derived from satellite remote sensing. Its objective is to demonstrate methods of analysis, share findings, and document historic climate exposure and sensitivity of vegetation to weather and climate as drivers of vegetation change.

This report represents a quantitative foundation of vegetation–climate relationships on an annual time step. The methods can be modified to finer temporal resolution and other spatial scales if further analyses are needed to inform park planning and management. The knowledge provided in this report can inform vulnerability assessments for Climate-Smart Conservation planning by park managers. Patterns of pivot points and responses can serve as a guide to anticipate what, where, when, and why vegetation change may occur.

For this analysis, vegetation alliance groups were derived from vegetation-map polygons (Coles et al. 2011) by lumping vegetation types expected to respond similarly to climate. Relationships between vegetation production and phenology were evaluated for each alliance map unit larger than a satellite pixel (~300 × 300 m). We used a water-balance model to characterize the climate experienced by plants. Water balance translates temperature and precipitation into more biophysically relevant climate metrics, such as soil moisture and drought stress, that are often more strongly correlated with vegetation condition than temperature or precipitation alone. By accounting for the interactions between temperature, precipitation, and site characteristics, water balance helps make regional climate assessments relevant to local scales.

Key findings:

- The patterns of pivot points and responses can serve as a guide to anticipate what, where, when, and why vegetation change may occur in the future.
- Multiple indicators show that trends in annual and growing-season vegetation production increased over time in all areas of the park between 2000 and 2019.
- Growing-season production increased in all alliance groups at approximately the same rate.
- Water availability (precipitation, actual evapotranspiration, rain, and soil moisture) were positively correlated with production. Water deficit and vapor pressure deficit were negatively correlated with production.

- Perennial exotic grassland required less annual precipitation to maintain productivity than other alliance groups.
- Disturbed areas were least sensitive to annual precipitation, whereas other alliance groups were similar in their response to changes in precipitation.
- The best multivariable indicator of production was three years of soil moisture at the park scale. This was also generally true at the alliance-group scale.
- By the end of the study period, the growing season was starting 6.2 days earlier on average across all alliance groups and ending 4.5 days later. The length of the growing season was 10.6 days shorter on average. The timing of peak growth was occurring 15.2 days earlier. Change in length of the growing season in this analysis is questionable due to disturbance and/or small sample size.
- Precipitation, actual evapotranspiration, growing degree days, and day of snow melt were correlated with start of growing season.

This report provides a foundation for interpreting weather and climate as drivers of changes in primary production over a 20-year period at the polygon and alliance group scale. Additionally, it demonstrates how vegetation type and site characteristics, such as soil properties, slope, and aspect, interact with climate at local scales to determine trends in vegetation condition. This report quantitatively defines critical water needs of vegetation and identifies which alliance types, in which locations, may be most susceptible to changes in climate in the future.

Acknowledgments

Thoughtful reviews from Dustin Perkins improved this report.

1 Introduction

This report provides baseline information about vegetation production and condition over time as derived from satellite remote sensing at three scales: the park, vegetation-alliance group, and vegetation-alliance polygon. The objective is to demonstrate methods of analysis, share standardized findings, and document historic climate exposure and sensitivity to weather and climate as drivers of vegetation change at Golden Spike National Historical Park.

This study quantitatively defines critical water needs of vegetation and demonstrates how vegetation type and site characteristics interact with climate at local scales to determine change in vegetation condition.

It provides a foundation for interpreting weather and climate as drivers of change in primary production over a 20-year period at local scales. It can be used to quantitatively determine which alliance types, in which locations, may be most susceptible to changes in climate in the future, providing a basis for vulnerability assessments.

1.1 The importance of primary production

Photosynthesis is the process in plants that converts sunlight, CO_2, water, and minerals into the chemical forms of energy (carbohydrates and sugars) essential to life. All terrestrial life depends on photosynthesis, also called "primary production" because it is the foundation of food webs. As the first step in creating food and habitat for wildlife, vegetation production is an important indicator, or "vital sign," of ecosystem health that can be tracked over time to assess conditions that support higher life forms in parks. The complex temporal and spatial patterns of primary production are influenced by many factors, including disturbances, such as wildfire and drought; differences in precipitation across space or over time; vegetation assemblages that differ in response to change; topography and soil properties; land use; and invasive species (Kariyeva and van Leeuwen 2011).

Sunlight provides the energy used to synthesize organic compounds from CO_2 and water. In semiarid environments like the Colorado Plateau, sunlight and CO_2 are abundant and rarely limit production. But primary production is controlled by different environmental variables in different places. In tropical forests, primary production may be controlled by availability of sunlight (due to cloud cover and dense canopy) or soil nutrients. In deserts, primary production is mostly controlled by water availability. At the highest elevations on the Colorado Plateau, it may be controlled by cold temperatures and a short growing season. Changes in primary production may indicate changes in ecological structure (e.g., change in vegetation assemblage) or ecological function (e.g., loss of vegetation cover, resulting in erosion and loss of soil nutrients).

1.2 Satellite monitoring of primary production

Assessing the rate of photosynthesis and the condition of vegetation at broad landscape scales provides insight into the cycles of energy, nutrients, and water that sustain life in parks. Sunlight reflected from vegetation provides information about photosynthetic rates, leaf area, and biomass accumulation, as well as conditions of habitat and forage for animals. High-frequency satellite

remote sensing of vegetation condition provides a broad-scale view of spatial patterns in vegetation condition, production, and change in response to climate, disturbance, and management actions over time.

The Northern Colorado Plateau Network (NCPN) monitors landscape-scale vegetation condition and trends using satellite imagery collected more frequently than ground-based data (which are also collected). The high frequency of observations and complete spatial coverage of satellite images are ideal for assessing seasonal as well as annual conditions and trends. The imagery also provides insight into the response of vegetation to climate patterns and disturbance (e.g., fire and forest disease, often mediated by climate) that cannot be obtained at broad scales in any other cost-effective way.

Quantitatively linking satellite observations of vegetation condition and climate data over time provides insight into climate influences on primary production, phenology (timing of growth), and sensitivity of vegetation to weather and long-term weather patterns referred to as climate. This, in turn, provides a basis for understanding potential climate impacts to vegetation and the potential to anticipate cascading ecological effects, such as impacts to forage, habitat, fire potential, and erosion, as climate changes in the future.

Primary production assessed via satellite remote sensing does not indicate which species are present, or which species are performing well or poorly. It is also not a "good" or "bad" judgment (i.e., increased or decreased production is not inherently good or bad). Monitoring primary production is analogous to monitoring river flow. Flow monitoring measures the timing and abundance of water that provides habitat for animals and other essential ecological functions. It does not indicate which organisms are present, or how different species are faring.

1.3 Vegetation condition and vulnerability

Vegetation condition and trend are monitored as changes in vegetation production, or the cumulative green biomass of leaves that grow via photosynthesis. Green biomass is strongly correlated with near-infrared and red wavelengths of solar energy reflecting off vegetation measured by satellites (Thoma et al. 2002). The satellite imagery reveals repeating seasonal fluctuations in growth and senescence, as well as annual trends or abrupt changes due to disturbances. Although disturbances can be detected, it is beyond the scope of this analysis to do so, because it requires different methods than those used here. However, all the data used to detect disturbances is available and can be made available via the author.

Climate is a strong driver of vegetation distributions (Stephenson 1998). Variation in weather strongly affects vegetation condition through stress (e.g., drought) and disturbance (e.g., wildfire). Linking changes in vegetation production to climate provides important information about resistance to disturbance (resilient or susceptible) and recovery from disturbance (fast or slow).

Vegetation that is susceptible to disturbance and slow to recover is considered the most vulnerable to change (Kariyeva and van Leeuwen 2011). This kind of information can be used to assess the vulnerability of vegetation assemblages to changes in climate.

1.4 Pivot points and responses

In semiarid environments, vegetation persists when there is a positive balance between growth and resistance to drought (Noy-Meir 1973). Vegetation traits, such as rooting depth, xylem diameter, and stomatal density and resistance, interact with climate and site conditions to determine how vegetation responds to climate. Understanding these interactions provides insight into potential changes in vegetation condition and composition as the climate changes. When coupled with climate data, two important ecological characteristics, pivot points and responses, can be derived from measuring change in vegetation condition over time (Munson 2013).

A pivot point is the value of a climate variable at which annual vegetation production teeters between above- or below-average condition. For water variables, pivot points determine whether vegetation production increases or decreases given the water available for growth. A pivot point is analogous to the recommended eight glasses of water per day for adults: Except in extreme cases, more water is generally not bad—but less can have detrimental effects, even when unmet needs are slight. Semiarid plants generally respond more positively than humans to water that exceeds minimum needs. But as with people, receiving less than the minimum can cause deterioration in condition. As such, the pivot point can be considered a critical water need as well as an indicator of drought tolerance. A species' basic water needs, and the rate of change when those needs are unmet or exceeded, are important ecological variables that determine how plants respond to weather and climate.

Plant traits determine how much water vegetation needs to maintain production. How much water is available depends on climate, weather, soil, and site properties. These interactions can cause variation in the magnitude of pivot points for the same climate variable across vegetation types. Some types may be more tolerant of drought conditions than others.

Vegetation response is the sensitivity of vegetation to a climate variable or, more specifically, the amount of change in vegetation production per unit change in a climate variable. This rate of change is a quantitative measure of vegetation sensitivity to climate. Cumulative annual vegetation production and phenology are indicators of vegetation response to a suite of environmental conditions. Some conditions are spatially variable but stable over time, such as slope, aspect, and soil properties. Others, such as climate, vary both temporally and spatially. The vegetation growing at any location reflects adaptations suited to the environment where it persists. If conditions change, either abruptly or gradually, plants respond. The change can be spatial, due to differences in soil type or elevation. It can also be temporal, as weather and climate change over time.

Differences in vegetation response rates, or sensitivity, to water availability reflect survival strategies for persisting through drought or responding rapidly when water is available, making species more competitive if water needs are met. The survival strategies are a consequence of vegetation traits, including rooting depth, stomatal density, leaf area, and perennial versus annual growth forms that confer competitive advantage under different climate conditions. Generally, plant traits that favor one strategy preclude the other (Noy-Meir 1973; Thoma et al. 2019).

Individual plant responses to environmental conditions cumulatively scale up, resulting in spatial and temporal landscape patterns that can be detected in satellite imagery (Thoma et al. 2019). Because vegetation production and phenological responses are interrelated, it is useful to measure and report the two simultaneously. It is not always possible to know what caused a change noted in satellite imagery, but communication with park staff and ground-based monitoring can help interpret findings in this report.

1.5 Phenology

The annual cycle of vegetation growth and senescence, and recurring biological phenomena such as seasonal migrations, are collectively known as phenology. Commonly known measures of vegetation phenology include timing of bud burst, first leaf, and spring bloom, all observed from the ground (de Beurs and Henebry 2010). The high-frequency observations from satellites make it possible to track vegetation phenology (Dunn and de Beurs 2011) at broad spatial scales that include an assemblage of different vegetation species, referred to as "land surface phenology." Land surface phenology is an indicator of ecosystem health because it regulates dependent ecological functions, such as pollination and onset of forage production (Dunn and de Beurs 2011). On the Colorado Plateau, springtime vegetation growth is preceded by warming temperatures and snowmelt. In drier regions, onset of springtime growth may be limited if there was insufficient accumulation of fall and winter soil moisture (Workie and Debella 2018).

Changes in land surface phenology can provide an early indication of cascading climate-change impacts that may result in changing species assemblages and shifting range boundaries (Workie and Debella 2018). These may affect pollinators, as well as bird and mammal migrations. Determining the drivers of phenology, and changes in phenology over time, provides insights into cascading effects on pollinators and migrating animals that depend on growth initiation, forage production, and the length of the growing season.

2 Methods

2.1 Overview

Golden Spike NHP vegetation was sampled, plant communities and land use interpreted, and the data mapped to the actual (fenced) boundaries of each unit. Areas authorized by Congress for acquisition but still privately owned were not sampled or mapped. The mapping area is approximately 1,144 hectares (2,826 acres) (Figure 1). The privately owned lands surrounding Golden Spike NHP were not included in the classification or mapping. Logistical and budget considerations limited the vegetation mapping project boundary to the Golden Spike NHP administrative boundary, which includes a few areas still in private ownership.

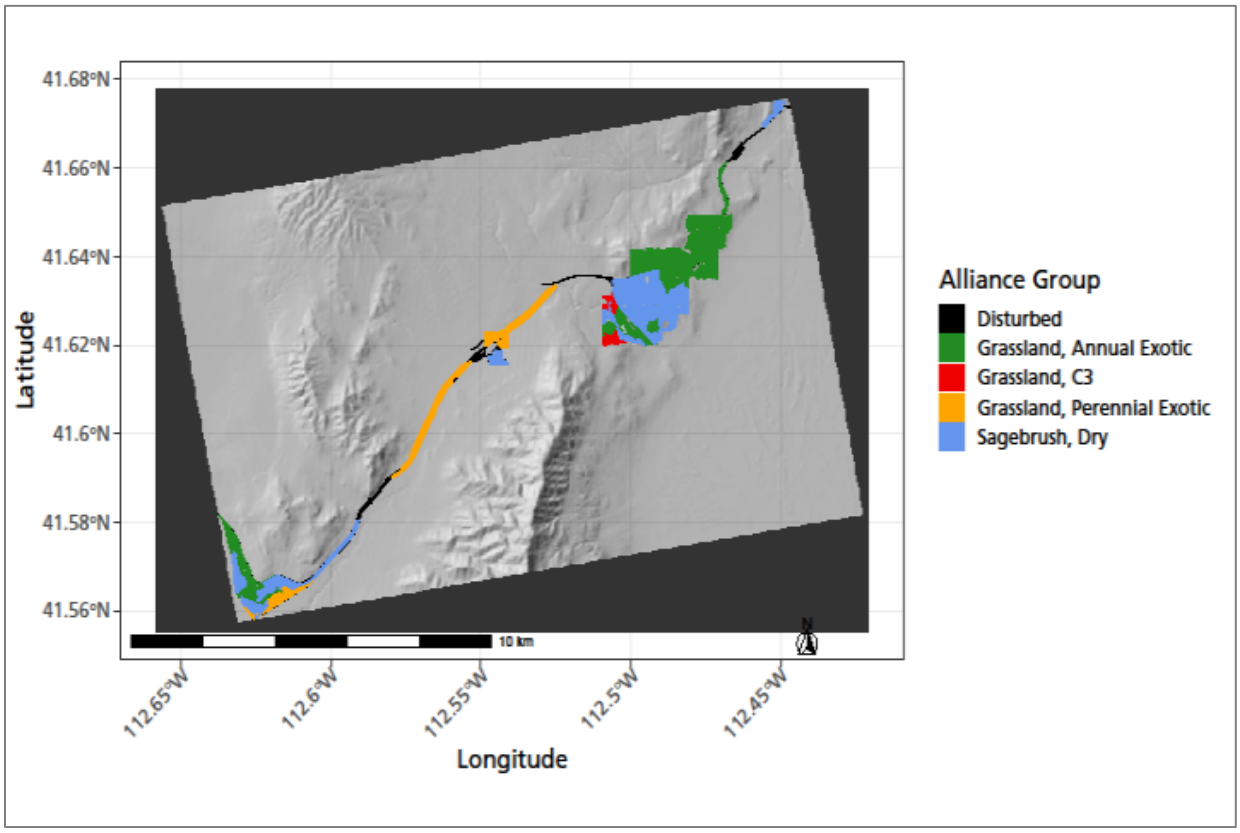


Figure 1. NCPN alliance groups analyzed for trends in production, phenology, and climate relations at Golden Spike National Historical Park. Areas not colored within the study boundary are alliance polygons smaller than the minimum target area of 8.3 hectares or are outside the study area.
NPS / DAVID THOMA

This report was compiled by comparing climate data with variation in land-surface greenness over time, as measured in satellite imagery of the park's vegetation-mapping project area (Coles et al. 2011). A large archive of 460 remotely sensed satellite images was downloaded and processed in the statistical analysis software R. A large amount of gridded climate data for the same area was downloaded and processed in Excel to estimate water-balance variables, such as soil moisture,

evapotranspiration, and water deficit from temperature and precipitation (see Section 2.6). The imagery and water-balance/climate data were merged in R separately for each vegetation alliance polygon (see Section 2.2) and analyzed statistically for spatial patterns across park landscapes and over time for trends.

2.2 Remote-sensing targets

Three scales of analysis are presented in this report: vegetation-alliance polygon, vegetation-alliance group, and parkwide. Vegetation-alliance polygons were derived from vegetation-map polygons by lumping together vegetation types expected to respond similarly to ecological disturbances, such as climate change (Coles et al. 2011; Jennings et al. 2009). The polygon scale features finer spatial resolution—but with higher resolution comes more complexity in interpretation. The group scale lumps similar alliances together for broader-scale interpretations but is not always as accurate as the polygon scale, because lumping even slightly dissimilar objects introduces variation. The park-scale analysis is achieved by lumping all alliance polygons into a single analysis or by averaging analysis results across alliances to the park scale.

It is important to note that satellite-based proxies for primary production reflect production from all vegetation within a sampling unit, regardless of the alliance name (which identifies the dominant or diagnostic vegetation types). For example, a forested alliance type may include shrub or graminoid understory that influences the satellite signal. Untangling the proportional influence of the named alliance components from background components is beyond the scope of this report.

2.2.1 Alliance polygons

The National Vegetation Classification Standard (NVCS) identifies eight hierarchical levels of classification, ranging from Formation Class (Level 1, the broadest scale) to Association (Level 8, the finest scale). The finest scale used in this report was the vegetation Alliance (Level 7). The NVCS defines a vegetation alliance as "a characteristic range of species composition, habitat conditions, physiognomy, and diagnostic species, typically at least one of which is found in the uppermost or dominant stratum of the vegetation. Alliances reflect regional to subregional climate, substrates, hydrology, moisture/nutrient factors, and disturbance regimes" (FGDC 2008).

Vegetation alliances are useful targets for tracking production and phenology because they are spatially repeating, relatively homogenous in type composition, and share similar affinities and responses to environmental conditions, such as climate. They are also mapped consistently across park units, making them an ideal classification level for cross-park analysis. Polygon boundaries for the alliances were obtained from park vegetation maps (Coles et al. 2011).

Analysis at the alliance, rather than association level, resulted in larger and fewer polygon targets that contained a larger number of satellite pixels. This helped ensure that satellite-image pixels fell mostly within target polygons and improved the signal-to-noise ratio necessary for tracking change in response to climate. Improving the signal-to-noise ratio in remote sensing of sparsely vegetated environments is achieved by spatially averaging pixels within relatively homogenous areas (Thoma et al. 2017). For this reason, the analysis in this report relies primarily on aggregated pixel means

across the spatial extent of each target polygon, rather than per-pixel analysis. More detail on pixel screening to exclude low-quality observations and outliers can be found in Sections 2.3 and 2.5, below.

2.2.2 NCPN alliance groups

For purposes of this study, alliances that respond similarly to climate based on structure and life-history traits were further grouped by NCPN ecologist Dana Witwicki (personal comm.) to simplify interpretations and reporting.[1] We created our own grouping system to simplify the alliance naming conventions and reduce the large number of alliances, which were too numerous for meaningful reporting.

Beginning with 98 different National Vegetation Classification (NVC) alliances mapped consistently across NCPN park units, we created 32 alliance groups based on floristics, canopy structure, and local environmental conditions. Of those, 5 occurred in Golden Spike NHP (Table 1, Figure 1). The alliance group names are shortened representations of the dominant alliance(s) in each group. Hereafter, we refer to the grouped alliance categories as "NCPN alliance groups" or "alliance groups," but it should be noted that these groups are similar to, but different than, Level 6 of the NVC. A key that links each NCPN alliance group to vegetation-mapping units familiar to NCPN managers can be found in Table S-1 of NPS (2025). The image-analysis targets were the ungrouped alliance polygons, so while results reported in the body of this report are for NCPN alliance groups, results are also available by polygon for ungrouped alliances in the supplemental tables (NPS 2025).

Table 1. NCPN alliance groups and corresponding National Vegetation Classification alliances, Golden Spike National Historical Park.

NCPN alliance group	National Vegetation Classification alliance(s) [A]
Disturbed	Non-natural
Grassland, Annual Exotic	Cheatgrass - Medusa-head Ruderal Annual Grassland Alliance
Grassland, C3	Idaho Fescue - Bluebunch Wheatgrass - Sandberg Bluegrass Dry Grassland Alliance
Grassland, C3	Needle-and-Thread Grassland Alliance
Grassland, Perennial Exotic	Crested Wheatgrass - Smooth Brome - Kentucky Bluegrass Ruderal Grassland Alliance
Sagebrush, Dry	Basin Big Sagebrush - Foothill Big Sagebrush Mesic Steppe & Shrubland Alliance
Sagebrush, Dry	Sagebrush species - Mixed Shrub Ruderal Understory Shrubland Alliance

[A] The alliance names shown in this table do not match those found in Coles et al. (2011) because alliance names and codes in that report were subsequently updated to USNVC Version 2.01, released March 30, 2017. The names from 2011 were cross-walked to the current names displayed here. For information on nomenclature, see FGDC (2008).

[1] Although there is an NVC Group level (6), the "NCPN alliance groups" discussed in this report were developed independently from the NVC for purposes of this study.

2.3 Satellite imagery

Since early 2000, the moderate resolution imaging sensor (MODIS) on the Terra satellite, operated by NASA, has collected daily imagery of Earth at a spatial resolution of 250 meters (820 ft). Because cloud cover, cloud shadows, aerosols, smoke, and water vapor can interfere with clear views of Earth's surfaces, daily images are composited into a single image for 16-day windows of time (product MOD13Q1). The 16-day composite images are created from values obtained from the clearest view during the 16-day window. They are generally the best quality observations for every pixel during the 16-day window.

Even so, during extended periods of poor atmospheric viewing conditions, some pixel values are unreliable. For this reason, each pixel in the composite image is tagged with a quality rating that can be used to screen out unreliable values influenced by poor viewing conditions. Sophisticated algorithms are used to assess the quality of every pixel value based on measurements of atmospheric conditions made by the satellite during image acquisition (Didan et al. 2015).

There are 23 fixed, 16-day window periods in a year (with a few overlapping days at year's end to account for leap years). Thus, there were 457 viewing opportunities and 23 observations per year for every pixel in the NCPN during the period of record covered in this report. Observation completeness was calculated on an annual and seasonal basis (March–November) for the 20-year study period as the percentage of pixels in each polygon that were observed under high-quality viewing conditions. In semiarid environments, there are typically many high-quality observations during the growing season, but fewer in winter due to clouds and snow cover.

2.4 Soil Adjusted Vegetation Index

The Soil Adjusted Vegetation Index (SAVI) is a measure of primary production (Bunting et al. 2019; Qi et al. 1994) obtained from reflectance in red and near-infrared wavelengths, adjusted for soil backgrounds in semiarid environments (Huete 1988). It is calculated as

$$SAVI = \frac{(1 + \mathrm{L})(\mathrm{NIR} - \mathrm{Red})}{(\mathrm{NIR} + \mathrm{Red} + \mathrm{L})}$$

where L is the soil background adjustment factor (L=0.5), NIR is reflectance in the near infrared wavelengths, and Red is reflectance in red wavelengths.

These wavelengths were selected specifically because they are sensitive to the abundance of green vegetation and optimized for detecting spatial and temporal changes in vegetation. We use SAVI in this report, rather than the normalized difference vegetation index (NDVI), because of the thin vegetation cover and soil background reflectance in most NCPN parks. This combination of factors results in unfavorable signal-to-noise ratios that can make remote sensing of spatial and temporal change difficult in semiarid environments. However, in addition to working with a vegetation index specifically designed to reduce the background noise caused by soil variability (SAVI), there are many steps in the processing workflow that help further alleviate these issues.

2.5 Pixel time series extraction and smoothing

Despite precautions taken by the imagery providers to minimize noise and provide an analysis-ready product from the MODIS sensor, there were lingering issues that required attention prior to analysis (Thoma et al. 2017). Each polygon larger than 8.3 hectares (the area of a MODIS pixel at NCPN latitude) was analyzed independently for trends in production and phenology and for its relationship with multiple climate variables. Pixels extracted from target polygons above the 90th percentile or below the 10th percentile of average greenness were removed from analysis. This step served several purposes. First, it removed pixels that fell on alliance-group boundaries if the reflectance was very different across the boundary, such as riparian ribbons adjacent to dry uplands. Second, it eliminated areas that may have been classified incorrectly in the vegetation maps if the result of misclassification included an area of substantially different reflectance. It also eliminated inclusions of contrasting reflectance if any occurred.

After outliers were removed, each pixel was weighted according to its proportional area that fell within the target (see Section 2.2). This step further minimized the effect of any remaining pixels that overlapped target boundaries. After computing an area-averaged value at each timestep for the pixels within a polygon target, missing polygon-average values were interpolated.

Missing daily values were a consequence of the 16-day periodicity of observations and quality screening in earlier steps. Finally, a smoothing filter was used to remove high-frequency noise from the time series of each polygon. After smoothing across large gaps in winter, prominent dips in time series (artificially low values that were an artifact of the smoothing) were truncated to a minimum winter value based on pixel values that were likely reflectance from bare soil or senesced vegetation (Wang et al. 2018). This process resulted in a smoothed and complete daily time series for each polygon.

2.6 Water-balance model

Vegetation responds to seasonal and interannual variations in temperature and water availability depending on adaptations and site conditions (Munson et al. 2015; Thoma et al. 2019). To understand climate drivers of vegetation condition and potential impacts across large environmental gradients (hot/dry to cold/wet), we used a water-balance model to determine how different aspects of climate and site characteristics affected vegetation production and phenology. The water-balance model quantitatively accounts for temperature, precipitation, and their interactions with local site conditions (such as soil water-holding capacity, slope, and aspect) that affect soil moisture, evapotranspiration, and drought stress (Thoma et al. 2020). To calculate the water-balance variables in the model, we used 1-kilometer, gridded, Daymet temperature and precipitation data (Thornton et al. 2018).

The model partitions precipitation (P, mm) into rain (RAIN, mm) or snow (SNOW, mm of water), which accumulates until warming temperature (T, °C) causes it to melt. Soil moisture (SOIL, mm) is stored in the top meter of soil, which was treated in the model as a single layer with a maximum storage defined by its water-holding capacity. Water-holding capacity was obtained from soil surveys where data were available (NRCS 2015) but was fixed at 100 millimeters otherwise. This fixed value accommodated analyses where soil surveys have not yet been conducted and accounted for some

water storage in geologic structures (cracks or porous, rocky material) that may be mapped as having no water-holding capacity, but support sparse vegetation detected by the satellite sensor. Water input that exceeds the storage capacity becomes runoff.

Potential evapotranspiration (PET, mm), calculated via the Oudin method, is the amount of water that could be evapotranspired from a short grass with available energy if water was unlimited. The Oudin method calculates PET using daily mean temperature, daylength, and solar radiation (Oudin et al. 2005). Actual evapotranspiration (AET, mm) is the loss of water from soil via evapotranspiration, limited by soil-water availability. Climatic water deficit (D, mm) is the unmet water need of vegetation and a measure of drought stress calculated as the difference between PET and AET (Stephenson 1998).

Water-availability variables include P, RAIN, SNOW, and SOIL. Variables that estimate water use include AET and PET; however, AET is limited by dry soil. Two aspects of heat that influence vegetation growth are average annual temperature (T) and growing degree days (GDD) (McMaster and Wilhelm 1997).

This study also evaluated two variables that could influence vegetation production and phenology: vapor-pressure deficit (VPD, Pa) and solar radiation (SRAD, W m^{-2}), available from Daymet. Vapor-pressure deficit is the difference between the amount of water vapor air can hold and the amount of vapor in the air. Solar radiation is the energy plants receive from the sun that can be used for photosynthesis (Grossiord et al. 2020; Seager et al. 2015; Stephenson 1990).

In the following sections, state variables, representing condition at a point in time (e.g., SOIL, T, VPD), are averaged (Table 2). Variables representing fluxes of water (water passing through the environment) are summed annually or seasonally—except for SOIL, which is presented as an average value because soil water-holding capacity has an upper limit that summation could exceed, which is physically impossible.

Table 2. Climate and water-balance variables used to identify correlations with vegetation production and phenology.

Variable	Abbreviation	Units	Type	Temporal summary
Precipitation	P	mm	flux	sum
Rain	RAIN	mm	flux	sum
Snow	SNOW	mm	flux	sum
Snow Pack Water Equivalent	PACK	mm	flux	sum
Water as Rain plus Snow Melt	W	mm	flux	sum
Date of Complete Snowmelt	Meltd	day-of-year	state	day
Actual Evapotranspiration	AET	mm	flux	sum
Potential Evapotranspiration	PET	mm	flux	sum
Climatic Water Deficit	D	mm	flux	sum

Table 2 (continued). Climate and water-balance variables used to identify correlations with vegetation production and phenology.

Variable	Abbreviation	Units	Type	Temporal summary
Solar Radiation	SRAD	W m^{-2}	state	mean
Temperature	T	°C	state	mean
Temperature Maximum	Tmax	°C	state	maximum
Temperature Minimum	Tmin	°C	state	minimum
Soil Moisture	SOIL	mm	state	mean
Vapor Pressure	VP	Pa	state	mean
Vapor-pressure Deficit	VPD	Pa	state	mean
Growing Degree Days	GDD	°C	state	sum

The effects of summing or averaging have important implications for interpreting results. Whereas additional precipitation can substantially change the cumulative magnitude of annual precipitation, it takes a large amount of water input to change an annual average soil-moisture value even a small amount. For example, 10 millimeters of additional precipitation falling on dry soil on one day in one year would increase annual precipitation by 10 millimeters but increase average annual soil moisture by just 0.027 millimeters (10/365). Temperature and pressure variables are also summarized as means in this analysis. Units of measure are millimeters for water terms, degrees Celsius for temperature, and pascals for pressure.

Snowmelt date (Meltd) used in the phenology analysis was determined from the water-balance model variable, PACK. This term is the daily snow water equivalent (mm) stored in the snowpack that accumulated over winter. In spring, PACK declines rapidly with warming temperature. Determining the day of complete melt is somewhat subjective due to flashy spring snow events that may linger for one to a few days, even in late spring after the initiation of vegetation growth. The algorithm used to identify the day of melt begins by searching backward from May 1 (user-specified date) for PACK values greater than four millimeters (user-specified depth) for a span of three days (also user-specified). In the water-balance model, the combination of depth and span are the minimum degree days necessary to yield the user-specified depth of snowmelt water. Visual inspection of snowmelt date plotted on time series of daily PACK values confirmed this was a reasonable approach to differentiating between periods that were predominantly snow-covered or snow-free.

2.7 Measures of vegetation production

Because net primary production is generated through photosynthesis and spectral indexes are responsive to the abundance of photosynthetically active vegetation, vegetation indexes are good proxies for primary production (Paruelo et al. 2000). Characteristics of the annual repeating cycle of SAVI curves were used as proxies for production and phenology (Figure 2). We determined trends in three variables derived from the SAVI time series for each polygon: mean annual SAVI, maximum annual SAVI (maximum value regardless of month in which it occurred), and iSAVI (or sum of daily interpolated SAVI), the area under the curve during the growing season (February through October).

Daily interpolation was made via linear regression with a maximum gap size of 16 days. Mean annual SAVI (sum of 16-day observations/23 periods per year) is a measure of average productivity across the calendar year. Maximum annual SAVI is an indication of peak instantaneous rate of vegetation production, or rate of maximum biomass accumulation. It is strongly correlated with both green cover and leaf-area index. Sum of SAVI (iSAVI) is a proxy for vegetation production during the growing season. It is most strongly correlated with biomass production and cumulative productivity (Garroutte et al. 2016; Johnson et al. 2018; Thoma et al. 2002).

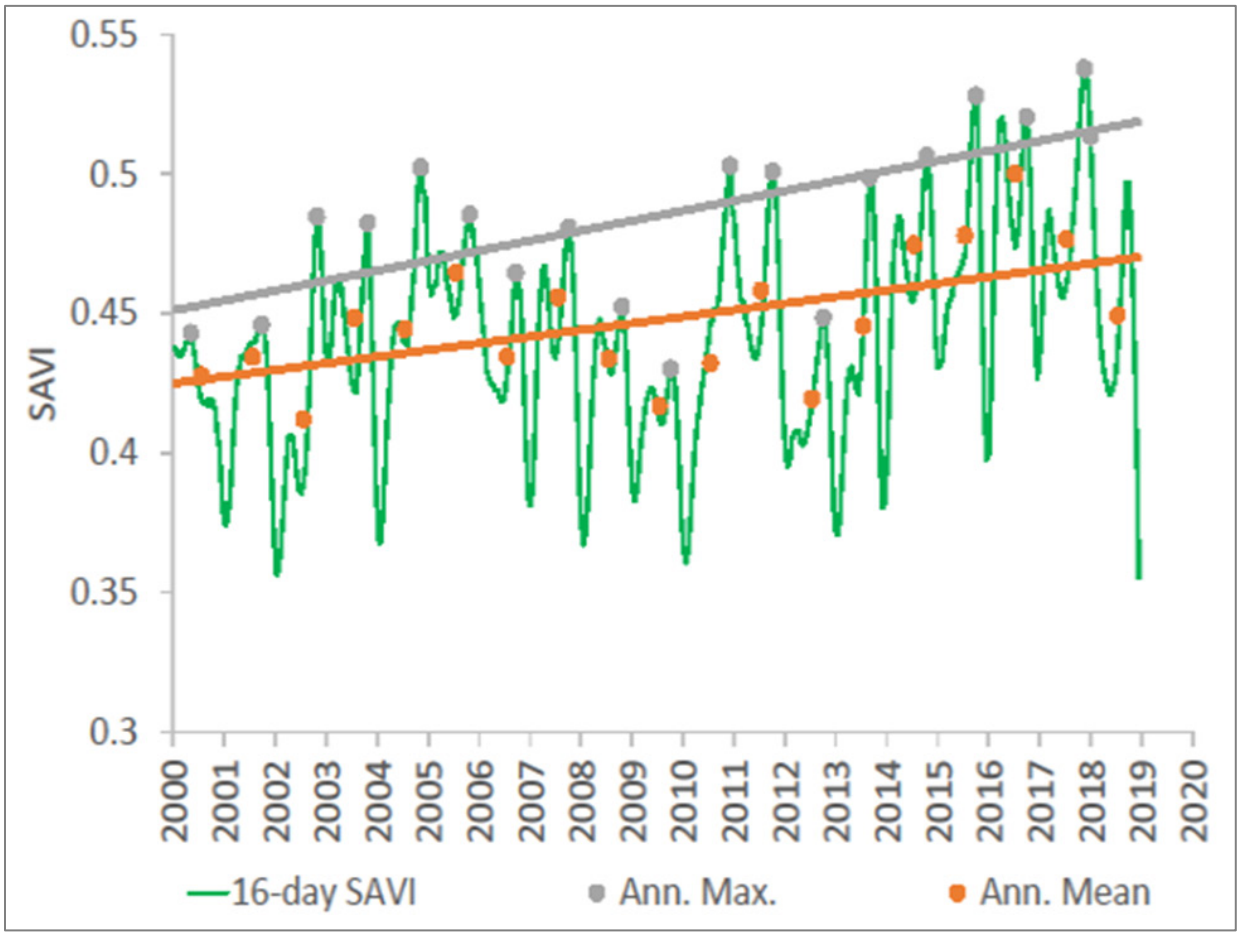


Figure 2. Measures of annual production from a time series of 16-day soil adjusted vegetation index (SAVI) derived from MODIS imagery. Linear trends against time for annual maximum and annual mean values are shown as straight lines.

NPS / DAVID THOMA

2.8 Calculating the measures

Trends in production were assessed by tracking changes in maximum and mean annual SAVI for 2000–2019, using the annual-aggregated time series method (AAT) and Mann-Kendall trend test (Forkel et al. 2013) (see Figure 2). The rate of change (regression slope) was estimated via linear regression. Significance of change was estimated by the Mann-Kendall trend test (Forkel et al. 2013). Trends in annual maximum values were more reliable than changes in mean annual values due to use

of the full annual curves that include screened and gap-filled winter values. Trends in growing-season greenness were considered in the annual pivot-points analyses below.

Representing the sum of daily interpolated SAVI values during the growing season, iSAVI is a holistic measure of the cumulative production of actively photosynthesizing vegetation (Mendez-Barroso et al. 2009; Reed et al. 1994). This proxy for aboveground net primary production results from the intentional construction of spectral indexes, such as SAVI, that are strongly responsive to absorbed, photosynthetically active radiation used by plant canopies to capture and store carbon and energy during growth.

Trends in iSAVI time series were noted in some polygons, which confounds relationships with climate unless the trend in iSAVI is removed before analysis. For this reason, we used the first difference in iSAVI, which represents the change in growing-season production from one year to the next, as an indicator of response to weather on an annual basis. This helps guard against overfitting when a trend exists in a time series. The annual change in iSAVI was calculated as

$$\Delta iSAVI = \frac{iSAVIt_2 - iSAVIt_1}{t_2 - t_1}$$

where $iSAVIt_1$ is sum of the growing-season SAVI for year t_1, and $iSAVIt_2$ is the sum of growing-season SAVI for year t_2. Positive values indicate increasing growth from one year to the next. Negative values indicate decreasing growth. This framing of the response variable makes increase or decrease in growth contingent on conditions in the previous year, allowing change to be linked to variation in weather from one year to the next. This is essentially equivalent ($r^2 \sim 0.99$) to the specific-growth concept used in plot-based studies of vegetation response to climate over long periods of time (Munson 2013).

2.9 Climate correlates with annual production

Two types of analysis were used to explore climate relations with annual production (iSAVI).

2.9.1 Single-variable analysis

First, simple linear-regression models compared a single climate variable to the annual increase or decrease in production relative to the prior year. The adjusted r^2 measured the strength of relationships between the climate variable and vegetation production in a range between 0 and 1, with stronger relationships closer to one. This revealed the proportion of variation in ΔiSAVI explained by variation in climate.

Simple linear regression was used to determine pivot points and production responses (Figure 3; see Section 1.4). Every polygon was tested against every climate and water-balance variable. After screening out relationships that were not significant (p-value > 0.05), the adjusted r^2 terms were averaged across polygons from the same alliance group to see if any one climate variable outperformed the others as a predictor of vegetation production.

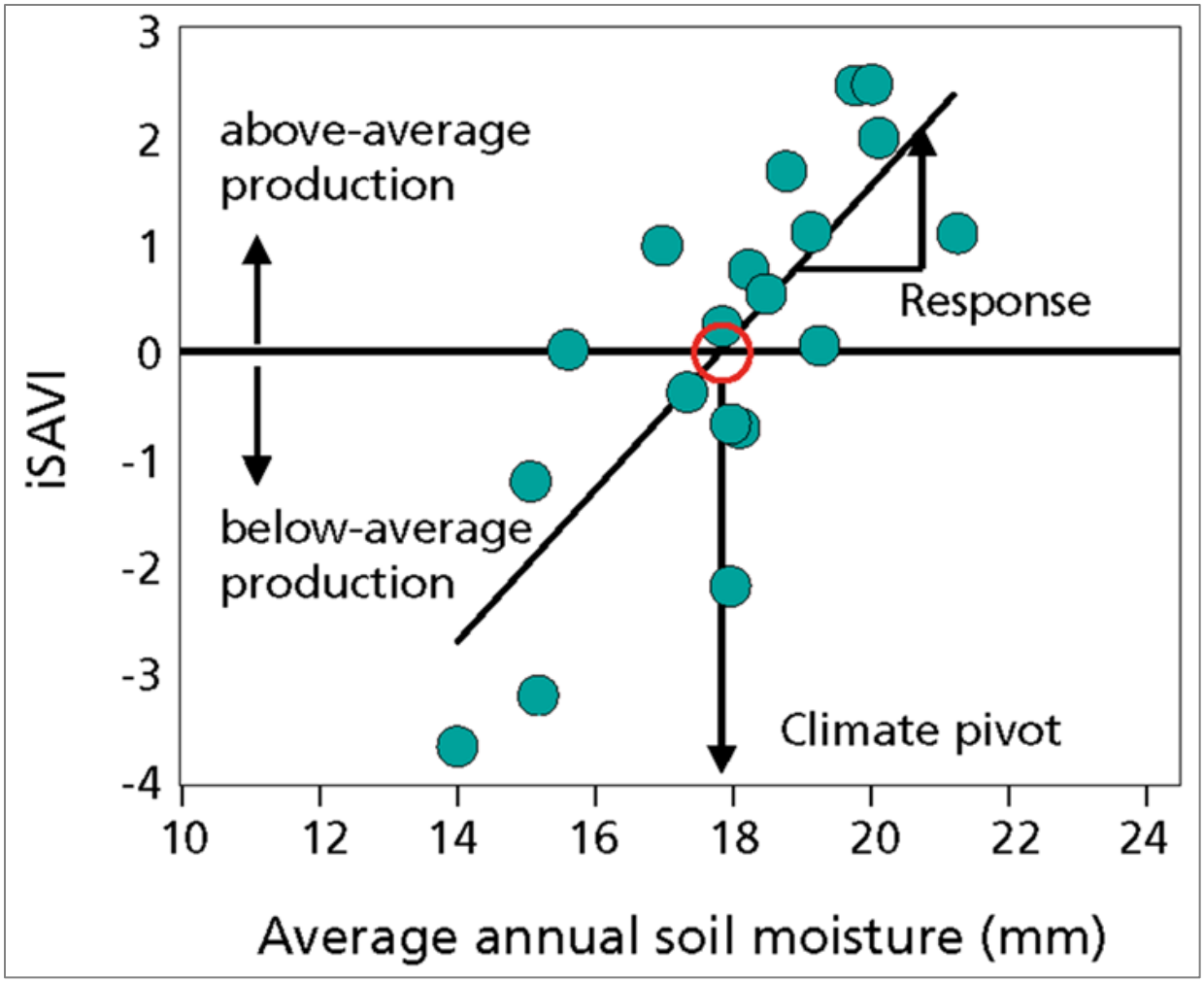


Figure 3. Conceptual diagram of soil-moisture pivot point and response of a single vegetation-alliance map unit to variation in annual average soil moisture. Vegetation production transitions from below- to above-average condition at the soil moisture pivot point. The response is the rate of change in iSAVI per millimeter of change in average soil moisture. Pivot-point figures like this can be constructed for other climate variables.
NPS / DAVID THOMA

2.9.2 Multiple-variable analysis

Second, multiple-regression models compared multiple climate variables simultaneously with production. These included lagged climate effects characterizing climate condition 1–2 years prior to an observation. This modeling framework helps account for legacy effects, or conditions in prior years that set limits on production in a current year (Sala et al. 2012). By accounting for legacy effects, the longer-term cumulative effects of drought or good growing conditions in prior years can be considered.

Additionally, this approach can help determine if climate variables interact in important ways to influence production. Whereas the linear-regression framework used to determine pivot points only considers the influence of a single variable, such as AET, on production, multiple regression can

determine interactions of AET and D, or other interactions and lags that include effects from prior years.

To account for multiple interacting factors that collectively influence vegetation production on an annual basis, we established a suite of *a priori* candidate models (Table 3) based on expected vegetation responses to climate variables and lags from our earlier experience working in semiarid landscapes. In those studies (Thoma et al. 2019; Witwicki et al. 2016), we found water-balance variables to be better predictors of vegetation response than temperature and precipitation. In addition, lag effects were apparent as much as two years prior to a given satellite observation.

Table 3. *A priori* models of climate influence on vegetation production competed via generalized linear mixed-effects modeling to identify best correlates with production.

	Climate variables [B]											
Model [A]	**AET**	**AET (lag1)**	**AET (lag2)**	**D**	**D (lag1)**	**D (lag2)**	**SOIL**	**SOIL (lag1)**	**SOIL (lag2)**	**P**	**P (lag1)**	**P (lag2)**
AET1	X	–	–	–	–	–	–	–	–	–	–	–
AET12	X	X	–	–	–	–	–	–	–	–	–	–
AET123	X	X	X	–	–	–	–	–	–	–	–	–
AET123_D1	X	X	X	X	–	–	–	–	–	–	–	–
AET123_D12	X	X	X	X	X	–	–	–	–	–	–	–
AET123_D123	X	X	X	X	X	X	–	–	–	–	–	–
SOIL1	–	–	–	–	–	–	X	–	–	–	–	–
SOIL12	–	–	–	–	–	–	X	X	–	–	–	–
SOIL123	–	–	–	–	–	–	X	X	X	–	–	–
AET1_D1	X	–	–	X	–	–	–	–	–	–	–	–
AET12_D12	X	X	–	X	X	–	–	–	–	–	–	–
D1_SOIL1	–	–	–	X	–	–	X	–	–	–	–	–
D1_SOIL2	–	–	–	X	–	–	–	X	–	–	–	–
D1_SOIL12	–	–	–	X	–	–	X	X	–	–	–	–
P1	–	–	–	–	–	–	–	–	–	X	–	–
P12	–	–	–	–	–	–	–	–	–	X	X	–
P123	–	–	–	–	–	–	–	–	–	X	X	X

[A] See Table 2 for acronyms.

[B] X = variable used in model, – = variable not used in model. Lags refer to models that include the water balance term for the preceding one (lag1) or two (lag2) years.

We then competed the models against each other using multiple-regression models and identified competitive models based on ΔAICc values < 4 to determine the combination of climate variables acting over one or more years that have the most influence on growing-season production. Models that did not compete well (ΔAICc > 4) were excluded. Several models could be competitive in any given polygon because every *a priori* model was evaluated for every polygon. We first looked for a

global best model of primary production at the park level by aggregating results from all polygons in the park. Then, we tabulated how frequently the top model occurred by NCPN alliance group to determine the best climate correlates and lags or cumulative duration of effect on production at the alliance-group level.

2.10 Conceptual basis of climate pivot points and responses

Using the pivot-point framework, annual change (ΔiSAVI) was regressed (linear regression) with climate data to determine the degree to which annual variation in weather affected production (Munson 2013). In this analysis, a pivot point is the critical magnitude of a climate or water-balance variable where vegetation "teeters" between above or below-average condition. Generally, water pivot points are important in water-limited environments. Temperature pivot points are important at higher elevations, where cold temperature limits growth (Thoma et al. 2020).

Vegetation response, or sensitivity to climate or water balance, is the rate of change in condition per unit change in water or temperature. In this analysis, vegetation response is the slope of the regression line when interannual change in iSAVI is related to the corresponding change in climate or water balance for the same period (see Figure 3).

Pivot points and responses are depicted graphically (see Figure 3) as the x-axis value where each linear-regression line crosses the horizontal line, indicating no change from one year to the next. Production values plotting above the x-axis indicate that vegetation increased in production from the previous year. Points below the line indicate vegetation production decreased from the previous year. If a deficit pivot point was exceeded during the growing season, vegetation production was likely below average, because vegetation has an inverse or negative relationship with water deficit, a measure of drought stress. If an AET pivot point was exceeded during the growing season, vegetation production was likely above average, because production is positively related to AET. Thus, the interpretation of exceeding a pivot point depends on the influence the climate variable has on vegetation (negative for water deficit, positive for water-availability variables).

Polygons that cross the horizontal line further to the left, where the x-axis variable is a water-availability metric, are considered more dry-tolerant. That is, their performance is above average at lower water availability than a polygon that crosses the horizontal line further to the right. For example, a vegetation assemblage with a precipitation pivot point of 250 millimeters is more dry-tolerant than a vegetation assemblage with a pivot point of 300 millimeters. The opposite is true if the x-axis is deficit. In that case, polygons that cross the horizontal line further to the left are less dry-tolerant; that is, their production declines to below average condition when drought stress is relatively low.

The slope of the regression line quantifies the expected change in iSAVI per millimeter of water or degree of temperature. Polygons with steeper regression slopes are more sensitive to a change in water availability. For each unit change in a climate or water balance variable, a more sensitive vegetation type will have a larger change in growing-season iSAVI.

Together, pivot points and responses determined from historical observations of vegetation condition and weather are two important ecological indicators of critical water amounts (in arid environments) or heat (in alpine environments) needed for growth, and how growth changes per unit change in the climate variable. For this reason, pivot points and responses are indicators of expected change in vegetation production as the climate changes in the future (Munson et al. 2011). When linked with projections of future climate, these two important ecological variables can be used in quantitative vulnerability assessments as part of the Climate-Smart planning framework (Stein et al. 2014), which helps managers set long-range goals achieved by near-term tactical actions (see Section 3.8).

2.11 Operational use of pivot points for "now-casts"

This report provides information for estimating vegetation condition using climate data. By tracking the climate variable with the strongest relationship to production in real time relative to its corresponding pivot point, we can determine if weather conditions are below, near, or above predetermined pivot points, and by what amount. In this way, we can use climate data to provide real-time "now-casts" indicating when weather conditions suggest production is likely to be above or below that of the previous year.

The interpretation of climate conditions against a pivot-point value requires consideration of pivot-point precision determined by the standard error around the regression line where it crosses the horizontal axis. The range is larger in polygons where the relationship between climate and vegetation growth is more variable. At the alliance group level, pivot-point range is caused by variability in plant assemblages in different polygons of the same alliance, as well as variations in soil and site properties. Additional variation is caused by noise in the MODIS sensor near its sensitivity limits in sparsely vegetated environments, errors in the gridded climate data, and vegetation legacy effects that cause plants to respond differently to the same weather, depending on what happened in the recent past. All these factors contribute to the observed standard error of a pivot point that brackets weather conditions determining if vegetation is likely performing above or below average.[2]

Vegetation performance when weather conditions are within the standard error of the pivot point is best described as "near average." When weather conditions exceed the standard error of the pivot point (above or below the pivot point), there is higher confidence that vegetation production is above or below average.

2.12 Phenology metrics and climate drivers

Phenology metrics were determined using the derivative method in the greenbrown R package (Forkel 2015) after smoothing and interpolation to daily values. The derivative method identifies growing-season phenology by recognizing inflections in the annual curves where growth rate accelerates (start), peaks (maximum) and decelerates (end) (Figure 4). Length of growing season is the span of time between start and end. These values were determined for every polygon-year

[2] Although not shown graphically, the standard error of pivot points is available for every polygon (Table S-2 in NPS 2025).

combination where possible. In some cases, phenology metrics could not be determined because the amplitude of annual variation was small, which made it impossible to find inflection points. The length-of-season metric was dropped if either start or end of season could not be determined. Start, end, and length-of-season metrics were also dropped if start of season occurred in winter between November 1 and April 1 due to vegetation shadows that confound satellite-based phenology assessments (Norris and Walker 2020).

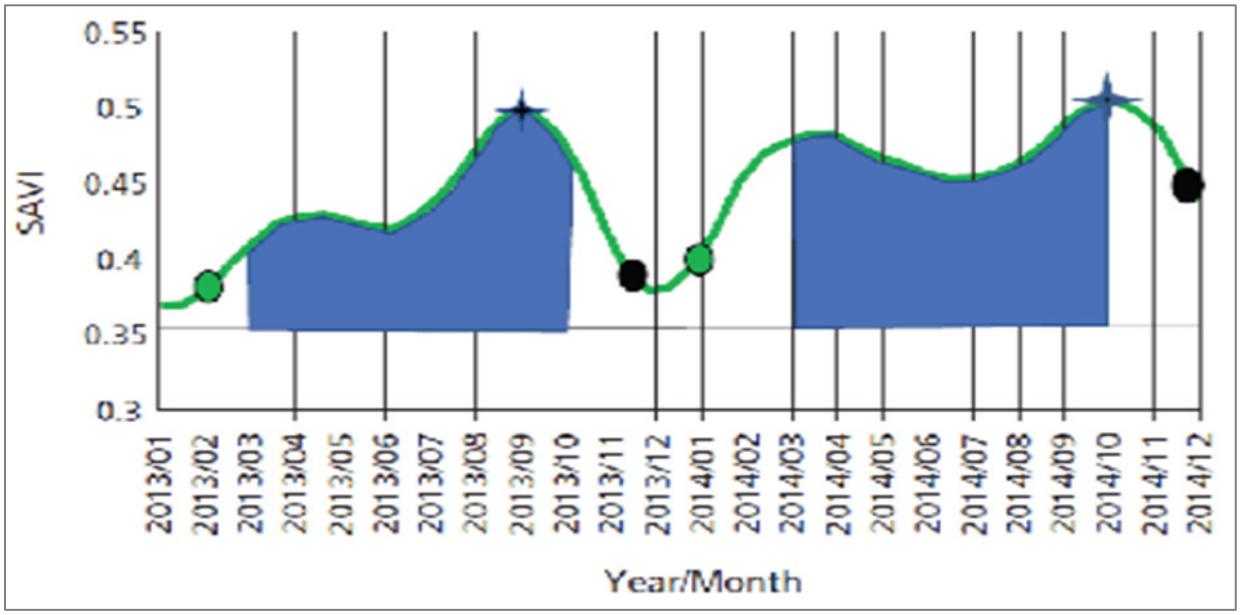


Figure 4. Integrated area under the growing-season curve (shaded area) for one polygon over two calendar years. The months used to calculate growing season production are fixed and include March through October. Phenology metrics are derived using a process that determines inflection points on the annual curves using the derivative (rate of change in growth rate) method. In some years, phenology cannot be determined in semiarid environments due to weak or noisy signals. The fixed growing-season duration used for calculating iSAVI and the start and end of growing season determined from phenology analysis may not always agree. Start of growing season (green point), peak (star), and end of growing season (black point) indicate important annual milestones in vegetation growth over two consecutive years.

NPS / DAVID THOMA

Polygon-level phenology metrics were summarized across alliance groups. The summary involved averaging linear regression slopes (days of change per year) across polygons within an alliance type, then multiplying the slope by the number of years (20 years) in the study to determine the average days of change in each phenology metric over the course of the study. Due to variation in the regression relationships and using regression slope to convert to days of change in each metric, the change in length of season in summary tables is similar to, but not equal to the length of time between start and end of season.

Climate drivers of phenology were identified by focusing on start-of-season, because plant growth in spring is most sensitive to climate (Fu et al. 2014). A suite of climate variables was reduced by

dropping variables highly correlated with day-of-year ($r^2 > 0.7$) and determining pairwise correlations between remaining explanatory variables. In the case of correlated variable pairs, the more integrative variable was retained.

The timing of SOS, peak greenness and its magnitude, senescence, and LOS were derived from the full annual curves for each polygon with winter-period minimums truncated to 60% of the winter maximum during the period of record. The cutoff value of 60% was determined via trial and error that both minimized lengths of winter gaps and included growing-season SAVI in every year. This prevented long periods of snow or winter cloud cover from having undue influence on the timing of phenology. The truncation of winter minimum values described above was a simplified version of published methods (Wang et al. 2018).

Some vegetation types (primarily conifer and shrublands) in the western US exhibit a peak satellite-observed greenness (measured using the normalized difference vegetation index, or NDVI) in winter months that is an artifact of shadows when the angle between reflected sunlight and the satellite is large (Norris and Walker 2020). It is unknown how this issue affects SAVI. The bands used to calculate SAVI are the same as those used to calculate NDVI, but a soil-correction factor is applied in SAVI to account for variable background reflectance. There is currently no known solution for resolving this shadowing effect. Thus, polygon-year combinations that exhibit winter peaks cannot be used in phenology analysis. These polygon-years were removed by determining if their annual peak of greenness occurred during winter months, defined as the period between November 1 and April 1. If any winter peaks in SAVI occurred during any year of the study period, the polygon-year was removed from analysis for that year. This allowed retention of polygon-year combinations that did not result in spurious satellite observations, rather than removing a polygon from analysis if only a few years failed the screening rules.

Two statistical methods were used to identify climate drivers of SOS, or green-up. This helped identify multiple lines of evidence for drivers if both methods yielded similar results. The first method relied on preconceived notions of phenology drivers. The second method, a machine-learning approach, let the data tell the story. In the first method, *a priori* models thought to be important in western rangelands were identified (Table 4) (St. Peter 2015). These models were competed against one another to determine top models of SOS.

Table 4. *A priori* models of climate influence on timing of green-up (start of the growing season).

Model [A]	Climate variable [B]											
	AET	GDD	P	RAIN	D	VPD	SRAD	Tmax	Tmin	VP	SOIL	Meltd
AET	X	–	–	–	–	–	–	–	–	–	–	–
GDD	–	X	–	–	–	–	–	–	–	–	–	–
P	–	–	X	–	–	–	–	–	–	–	–	–
RAIN	–	–	–	X	–	–	–	–	–	–	–	–
D	–	–	–	–	X	–	–	–	–	–	–	–
VPD	–	–	–	–	–	X	–	–	–	–	–	–
SRAD	–	–	–	–	–	–	X	–	–	–	–	–
Tmax	–	–	–	–	–	–	–	X	–	–	–	–
Tmin	–	–	–	–	–	–	–	–	X	–	–	–
VP	–	–	–	–	–	–	–	–	–	X	–	–
GDD_P	–	X	X	–	–	–	–	–	–	–	–	–
GDD_RAIN	–	X	–	X	–	–	–	–	–	–	–	–
GDD_SOIL	–	X	–	–	–	–	–	–	–	–	X	–
GDD_AET	X	X	–	–	–	–	–	–	–	–	–	–
SRAD_AET	X	–	–	–	–	–	X	–	–	–	–	–
SRAD_P	–	–	X	–	–	–	X	–	–	–	–	–
Meltd	–	–	–	–	–	–	–	–	–	–	–	X
Meltd_SRAD	–	–	–	–	–	–	X	–	–	–	–	X
Meltd_P	–	–	X	–	–	–	–	–	–	–	–	X

[A] Models were competed via generalized linear mixed-effects modeling to identify best correlates with green-up. All climate variables were summed or averaged from January 1 to the day of year when green-up began. See Table 2 for acronyms.

[B] X = variable used in model; en dash (–) = variable not used in model.

Second, the random-forests machine-learning technique was used to determine important drivers of phenology and provide predictive models of SOS (Breiman 2001). Random forests is a learning method for regression that constructs a multitude of decision trees until the optimum combination of factors describing a result is obtained. In this case, *a priori* candidate models were not specified beforehand. Rather, the random-forests algorithm used climate and water balance variables to identify a top model using a subset consisting of 70% of the data, which was randomly selected. The random-forests algorithm generated 2,000 decision trees with a maximum of four variables randomly chosen per split, which is the recommended number for a model testing the utility of 12 predictors. Sampling was done with replacement, which is the default setting.

The top model was validated against a holdout dataset consisting of the remaining 30% of observations. Variable-importance plots were used to identify which variables had the most predictive power. They consisted of percent increase in mean square error (%IncMSE), which is a measure of model improvement when adding each variable to the model, and increase in node purity

(IncNodePurity), which is the difference in residual sum-of-squares in regression with or without each variable.

After model fitting with the training data, predictions for the start of the growing season were made using the validation dataset, where SOS predictions could be compared against observations in the validation dataset. The accuracy of predictions for SOS were characterized by the mean absolute error (MAE), which is the mean value of differences between predictions and observations with units of days. The MAE is the average magnitude of error in days without specifying direction of error, thus specifying the average plus or minus error rate of predictions.

3 Results and Discussion

3.1 Completeness of satellite observations

Completeness of growing-season observations was 96.2% across all targets for the 20-year period of analysis. Clouds, aerosols, and snow cover reduced the average completeness of high-quality observations to 86.1% of potential observations on an annual basis across all polygon targets. The minimum completeness for any single polygon on an annual or seasonal basis was 55.1% and 59.6%, respectively.

Before analyzing satellite observations with climate and water balance, gaps were linearly interpolated to a daily time step prior to smoothing, which removed high-frequency noise in the time series that could not be removed via quality screening. There were no missing climate or water-balance data.

3.2 Time series

At Golden Spike NHP, SAVI observations reflected differences in vegetation response to climate that were apparent when observations were organized by NCPN alliance group (Figure 5). Some polygons were generally greener than others (indicating higher productivity and biomass accumulation), but within alliance groups there was considerable variation. That variation can be due to species assemblages within the alliance and site properties that modify the local effects of climate. Some outlier polygons within alliance groups might need to be considered separately in future analyses if interest is in the central tendency of an alliance group.

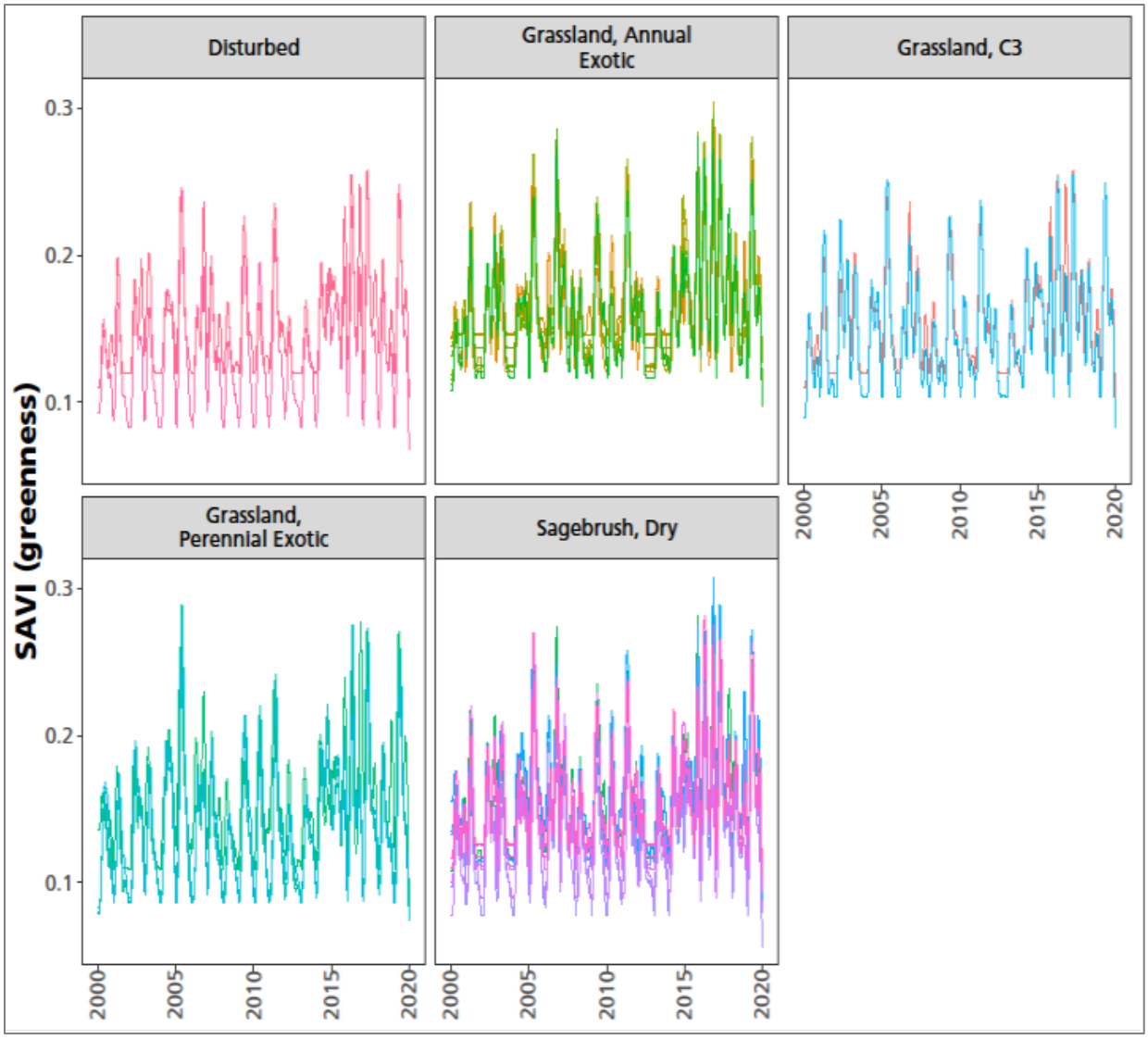


Figure 5. Soil-adjusted vegetation index time series by alliance group for 28 polygons analyzed for 2000–2019. Colors help differentiate individual polygon time series traces. Each polygon time series was filtered to include only high-quality pixel values, with minimum values truncated to winter minimum, gap-filled, and then smoothed with a Savitsky-Golay moving-window filter to remove high-frequency noise. Analysis was limited to polygons of > 8.3 hectares. A single-line trace indicates either all polygon units have similar seasonality and interannual variation, or only one polygon of the alliance group was sampled.
NPS / DAVID THOMA

Gap-filled and smoothed time series illustrated a broadly similar slightly-upward trend in most alliance groups during the study period (Figure 5). However, the alliance groups showed a high degree of variability in amplitude and timing of peak values. It was typical for some polygons in an alliance group to exhibit "outlying character," indicating they were not a good fit with other polygons in the group. This issue was most notable in the Disturbed, Ponderosa Pine, Sparsely Vegetated, and Dry Shrubland, as well as the Water alliance groups. Despite filtering outlying polygons that had an annual average value greater than the 90th percentile or less than the 10th percentile, this could happen

for several reasons. Grouping vegetation types into alliance groups forces some dissimilarity among group members. This can result from misclassification in the vegetation-mapping process, or, less commonly, disturbance after mapping that caused different vegetation to respond differently than expected of the group.

It is important to evaluate "outlier" polygons carefully, with consideration given to potential effects of land use or disturbance. For instance, time series can be affected by grazing or herbicide application that alter the growth and abundance of vegetation Disturbed areas. Disturbed areas likely have a mixture of vegetated and non-vegetated areas within pixel footprints, which may include roads, parking lots, and buildings that affect the time series. However, the dominant contribution to the time series in Disturbed areas is from dynamic vegetation growth and senescence rather than from the spectrally invariant non-living surfaces that do not vary over time.

3.3 Trends in indicators of annual production

Significant upward trends (p-value < 0.05) in maximum and mean annual SAVI occurred across 100% of the study area (Table 5; Figure 6; Appendix A). Results by polygon for significant trends in maximum and mean annual SAVI are in Table S-3 in NPS (2025).

Table 5. Amount of park area with increasing (pos) or decreasing (neg) trends in mean annual or maximum annual SAVI by alliance group. Since there are two variables that can trend in the same or opposite directions, there can be more than one row of information for each alliance group.

Alliance Group	Annual Trend Maximum	Annual Trend Mean	Hectares	# of polygons	% of park area
Sagebrush, Dry	pos	pos	271.4	10	33.8
Grassland, Perennial Exotic	pos	pos	101.3	5	12.6
Grassland, C3	pos	pos	21.3	2	2.7
Grassland, Annual Exotic	pos	pos	379.8	9	47.3
Disturbed	pos	pos	29.1	2	3.6

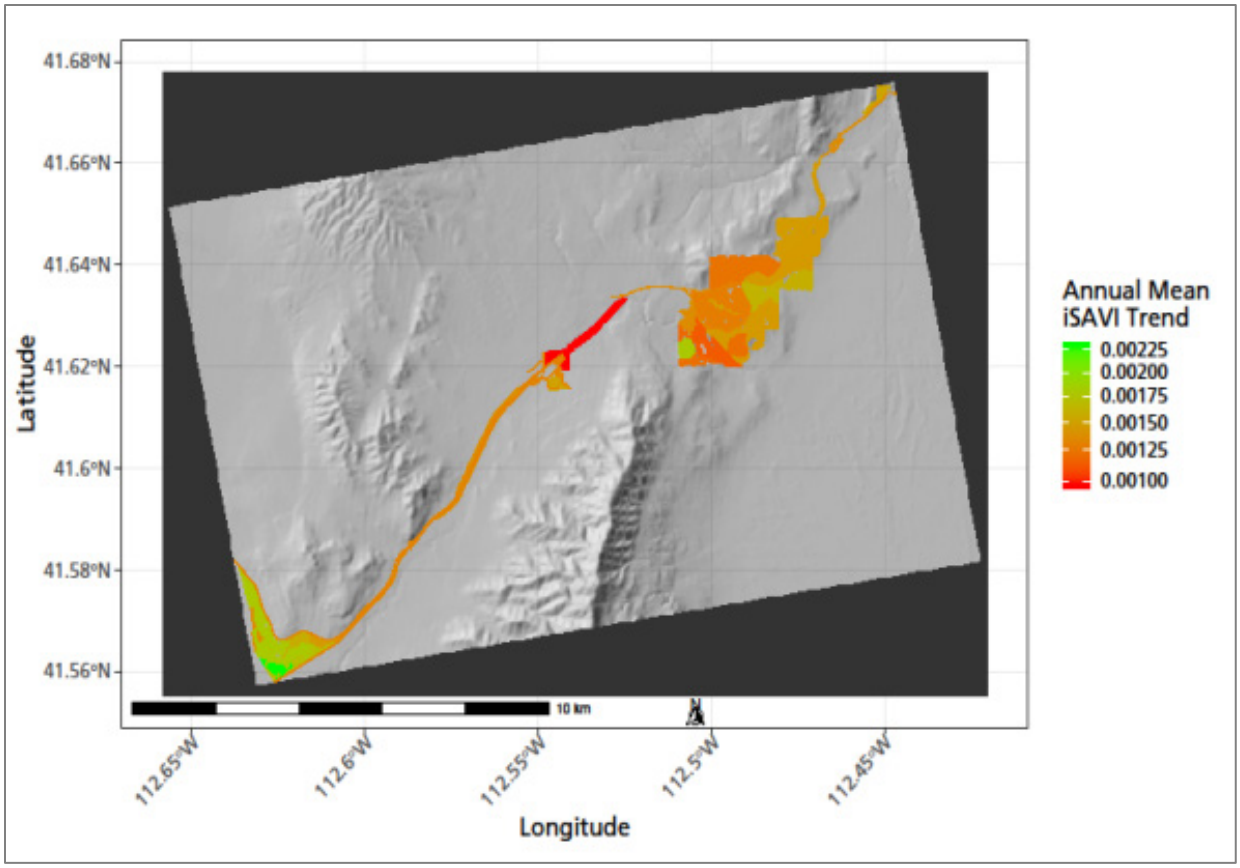


Figure 6. Spatial pattern of trends in mean annual iSAVI. Trend is average change in iSAVI per year for 2000–2019. Greener colors indicate more positive change in annual mean SAVI.
NPS / DAVID THOMA

3.4 Trends in indicators of growing season production

Across the 20-year period of study, upward trends (positive slope coefficient) in growing season iSAVI, determined via simple linear regression, were found at the alliance group level for all alliance groups, and trends were significant (p-value < 0.05) for all groups except for C3 Grassland and Perennial Exotic Grassland alliance groups (Figure 7). Interestingly, these two alliance groups were highly responsive to interannual variation in annual precipitation, like all groups at Golden Spike NHP, so the lack of significance at the 0.05 level may be more indicative of high sensitivity to precipitation more so than a lack of "significant" change over time (see Section 3.7).

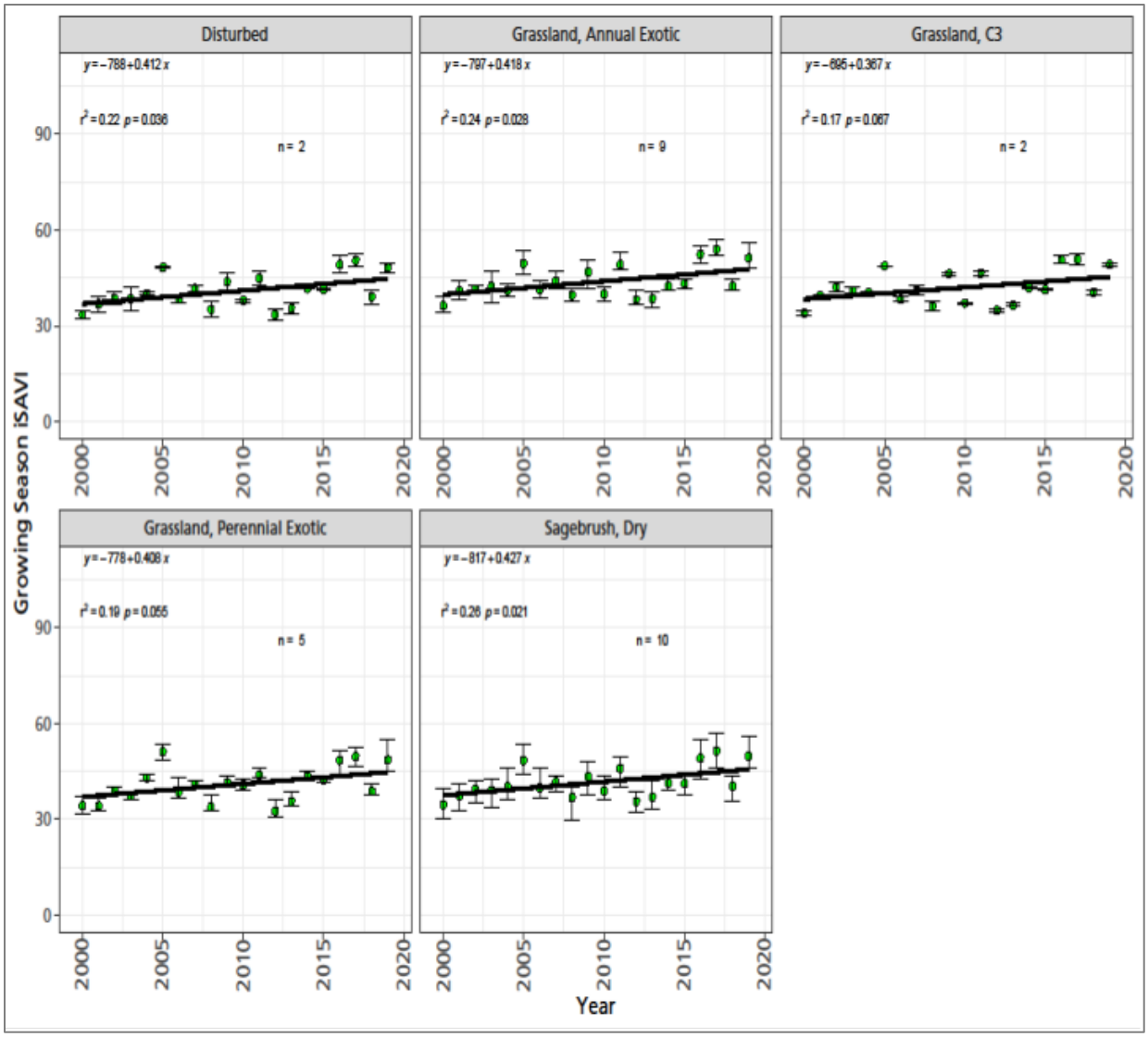


Figure 7. Trends in mean growing-season iSAVI by alliance group, determined via simple linear regression. Error bars are standard error among polygons within each alliance group. n = number of polygons analyzed in each alliance group, r^2 = coefficient of determination, p = p-value, y = growing season iSAVI, x = year.

NPS / DAVID THOMA

As a subset of the annual period, the growing-season iSAVI focused on the March through October period reveals climate-driven increases in all alliance groups. The study began in 2000, which was a low production year. Other low production years include 2008 and 2012, corresponding with dry periods. Most dry periods were followed by recovery. By the end of the study above-average levels of production were observed in most alliance groups, demonstrating the resilience of Golden Spike NHP vegetation production to short-term drought stress during the study. Although it is not clear what species represent the "recovery" after drought disturbance in all cases, some may be non-native.

The upward production trend for Dry Sagebrush at Golden Spike NHP was consistent with other research findings on the Colorado Plateau, which showed shrubs as dominant where winter soil moisture was high and seasonal temperature variable, and grasses as dominant where summer moisture was available (Gremer et al. 2018). That study pointed out that rising temperature and increasing temperature variability, associated with climate change, will result in conditions more favorable to shrubs because the change in temperature is expected to overwhelm the role of available soil moisture by late century. It also noted that shrubs are better adapted to large temperature fluctuations than grasses. A review of woody-plant proliferation (Barger et al. 2011) found that seasonality of precipitation, land use, and atmospheric CO_2 concentrations were all important drivers of woody-plant expansion in semiarid regions where annual PET was greater than annual P, as is the case at Golden Spike NHP.

3.5 Climate relations

3.5.1 Qualitative patterns in annual precipitation and production

Between 2000 and 2019, precipitation increased in most alliance groups, as did many measures of production in all alliance groups. This is the expected relationship in semiarid and water-limited environments. When precipitation exceeds potential evapotranspiration plants are not stressed by water shortage and production may be more limited by cold temperatures than lack of precipitation.

Improved water-use efficiency due to the fertilization effect of rising atmospheric CO_2 concentrations may explain some of the increase in production, but precipitation increase was likely the largest contributor at lower elevations (Sorokin et al. 2017). Plotting the iSAVI difference from long-term average iSAVI with precipitation shows the temporal correspondence of interannual variation in annual precipitation and production (Figure 8), whereas global CO_2 concentrations increased monotonically on an annual basis during the study period (https://gml.noaa.gov/ccgg/trends/). The link between precipitation and production, or covariation in precipitation and production is strong and apparent in all alliance groups (Figure 8).

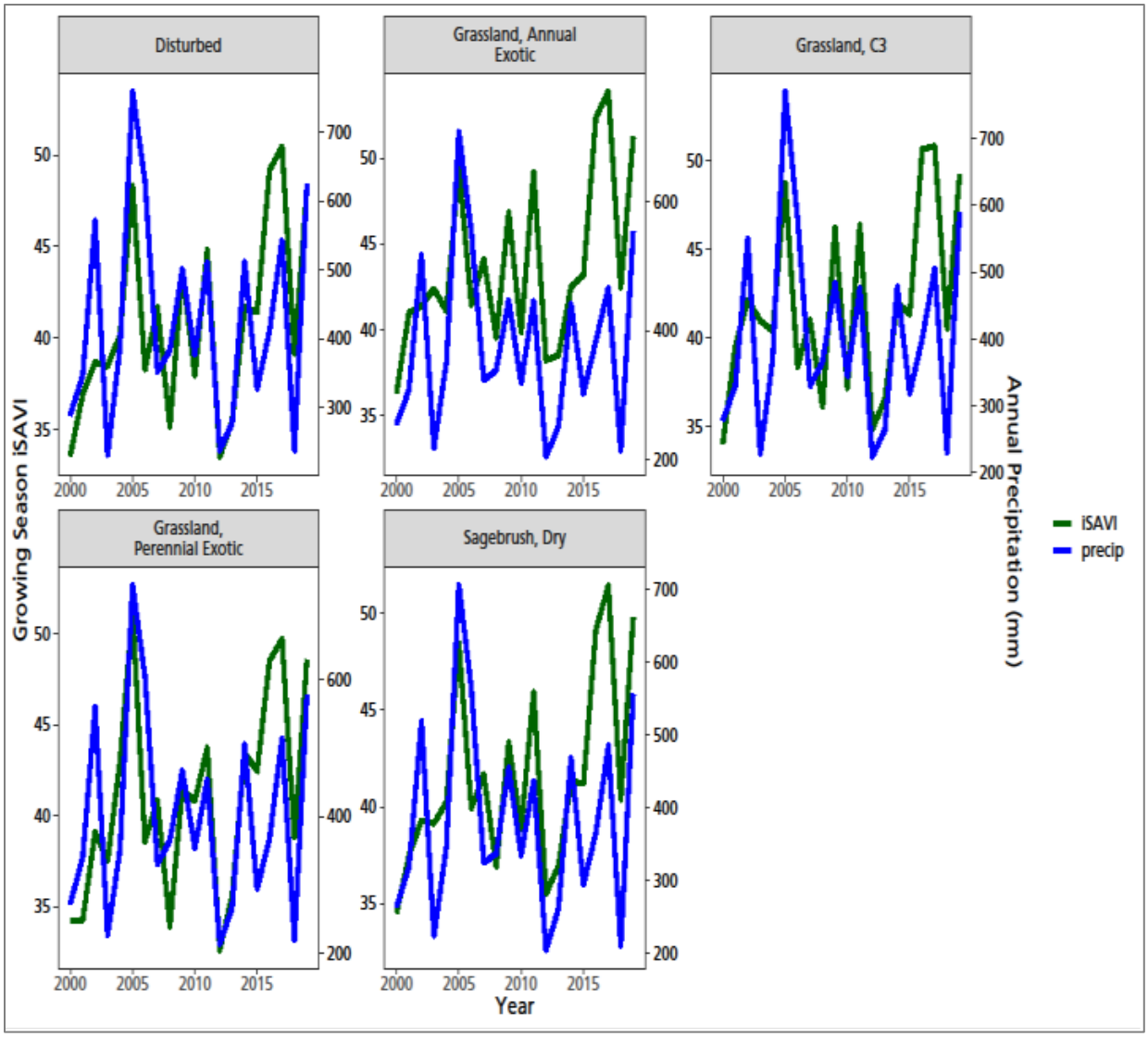


Figure 8. Co-variation in growing-season production, estimated as the iSAVI between March and October and water-year cumulative precipitation averaged within alliance groups, demonstrating the link between climate and vegetation production in the park at the annual scale. The time series shown here is intended to illustrate precipitation as a master climate driver of production in semiarid environments. Statistical analyses of the relation of production to precipitation and all other climate variables is the subject of following sections.

NPS / DAVID THOMA

iSAVI peaks in annual production corresponded with interannual precipitation peaks in most semiarid alliance groups, but a lag in vegetation response can be caused by legacy effects of vegetation condition in prior years that carry over to subsequent years.

Such legacy effects have been noted in semiarid vegetation response to precipitation where prior conditions set the stage for current-year production. For example, a wet year following a drought may not be as productive as a wet year following an average precipitation year due to legacies in

tillers, stems, root density, and seed production, which are limited in a drought (Noy-Meir 1973; Thoma et al. 2016). Because of prior conditions, the largest peaks in annual production do not always coincide with the largest peaks in annual precipitation.

In addition, the timing and magnitude of response to precipitation are affected by the structural and physiological traits of plants, including rooting depths, stomatal control of gas exchange, leaf morphology, annual or perennial life cycle, and the site conditions where they grow (Munson et al. 2015). Plant physiology may explain why peaks and valleys in annual production are more pronounced in grasslands and shrublands at Golden Spike NHP than in forested alliances in other NCPN parks. Evergreens like Pinyon and Juniper that retain leaves for multiple years have lower-amplitude seasonal cycles (Yang et al. 2019). Grasslands are generally more responsive to interannual weather variation, while woodlands with deeper rooting systems can be buffered from short-term droughts. Additionally, variation in the magnitude of vegetation response to variation in precipitation could be due to higher runoff in high precipitation years if a large proportion of precipitation fell in a few storm events.

Collectively, the response of vegetation to interannual variation in weather is complex. The study of these interactions across space and time is greatly aided by the high frequency of satellite observations coupled with continuous daily climate observations over the same period. Organizing the remotely sensed observations by management-relevant vegetation types provides insights that may be useful in climate adaptation planning.

3.5.2 Single-variable drivers of production

Vegetation in all alliance groups responded positively to measures of water abundance (precipitation, rain, actual evapotranspiration and soil moisture), and negatively to indicators of drought stress (water deficit and vapor pressure deficit). There were no significant correlations between measures of temperature (average annual temperature or growing degree days). The water-abundance variables (P, RAIN, SNOW, AET, SOIL) were positively correlated with annual production which is expected where P/PET ratios were < 1. Variables representing unmet water need, or atmospheric dryness (D, VPD) were negatively correlated with production. At the park level, relationships between growth and climate variables were generally weak due to the highly variable response relationships with climate across vegetation types (not shown). When examined by alliance groups, better relationships emerged (Figure 9).

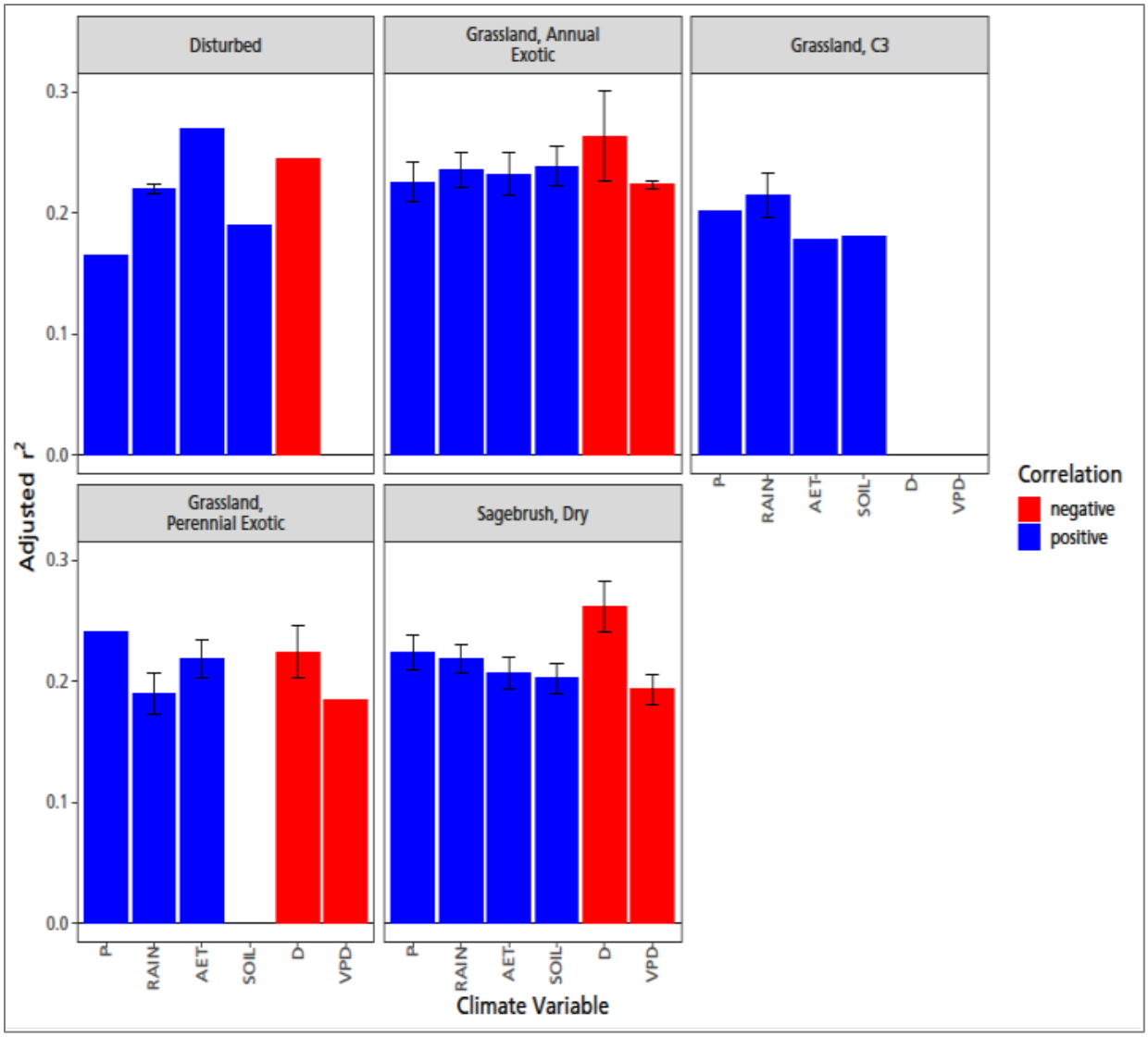


Figure 9. Significant (p-value < 0.05) relationships between water-year climate variables and first difference of growing season iSAVI, 2000–2019. Bar height is the mean variation in iSAVI explained by variation in climate or water-balance variable on the x-axis. Error bars are standard error. Blue bar color indicates positive correlation. Red bar color indicates negative correlation. P = precipitation (mm), RAIN = precipitation as rain (mm), AET = actual evapotranspiration (mm), SOIL = average soil moisture (mm), D = water deficit (mm), VPD = vapor-pressure deficit (Pa).

NPS / DAVID THOMA

Vegetation production in all alliance groups was correlated with multiple aspects of climate, all of which are related to water availability. This suggests that alliance groups at Golden Spike NHP will respond positively if water availability increases in the future, or negatively if water availability decreases (see Section 4 for projections).

Within alliance groups with multiple polygons, there was variation in relationship strength among polygons, indicated by error bars in Figure 9 (also see Table S-2 in NPS 2025). This can be caused by variation in species assemblages and abundances that differ among map units of the same alliance.

Some vegetation types respond more strongly to seasonal weather than annual conditions. For these plants, warming temperatures in the spring initiate growth. Then, as soil moisture decreases throughout the growing season, other variables, such as water deficit, typically take on greater importance. Depending on the species, most growth may occur in spring or late summer. Thus, the timing of seasonal water and energy availability may be more important to annual vegetation production than annual water and energy availability (Barnes et al. 2016). These kinds of seasonal responses to weather are difficult to characterize on an annual basis with a single variable because the important climate drivers switch seasonally and there may be long-term memory effects from earlier growing seasons that affect current-year production (Thoma et al. 2016).

In other words, multiple aspects of climate and water balance act over both short and long periods to affect annual production. Thus, a simple linear-regression approach that considers single-variable influences on production over the course of an entire year is an oversimplification of important vegetation–climate relations. This may explain coefficients of determination < 0.5 (Figure 9), which may seem unimpressive but are similar to results of species responses to single variables in plot studies (Munson et al. 2011).

Nevertheless, there is value in determining single-predictor regressions because they can identify important drivers that result in increases or decreases in annual production and represent a practical way to derive critical water needs and drought-stress indicators (Munson et al. 2016; Thoma et al. 2019) that can be tracked using data from weather stations. The best single-variable indicator of annual vegetation production can be determined by alliance group from visual inspection of Figure 9 (tallest bar = best relationship), or by polygon from Table S-2 in NPS (2025).

Annual precipitation at Golden Spike NHP was generally among the climate or water-balance variables most strongly correlated with annual production (in four of five alliance groups), so it is used in the following sections that further explore climate/vegetation relationships. Multiple predictors and time lags of annual production response are considered in a later section.

3.6 Pivot points

3.6.1 Pivot points indicate drought tolerance

Plant species with smaller pivot points for water-abundance variables (e.g., precipitation, rain, snow, actual evapotranspiration, soil moisture) demonstrated a higher degree of drought tolerance, because less water was needed to achieve above-average production (NPS 2025, Tables S-2 and S-4).[3]

[3] The pivot points differed among water-abundance variables because they represent different pools, periods and magnitudes of water availability. For example, soil moisture is a fraction of total precipitation (P), because some P runs off and is not available to plants. Similarly, rain and snow represent fractions of total P that supply water for

Conversely, larger pivot points for variables representing heat, unmet water need, or atmospheric dryness also indicated a higher degree of drought tolerance, because more drought was tolerated before production dropped below average.

At Golden Spike NHP, the most drought-tolerant alliance group (i.e., the one with the lowest precipitation pivot point) was Perennial Exotic Grassland, while the least drought tolerant group was Disturbed (Figure 10).

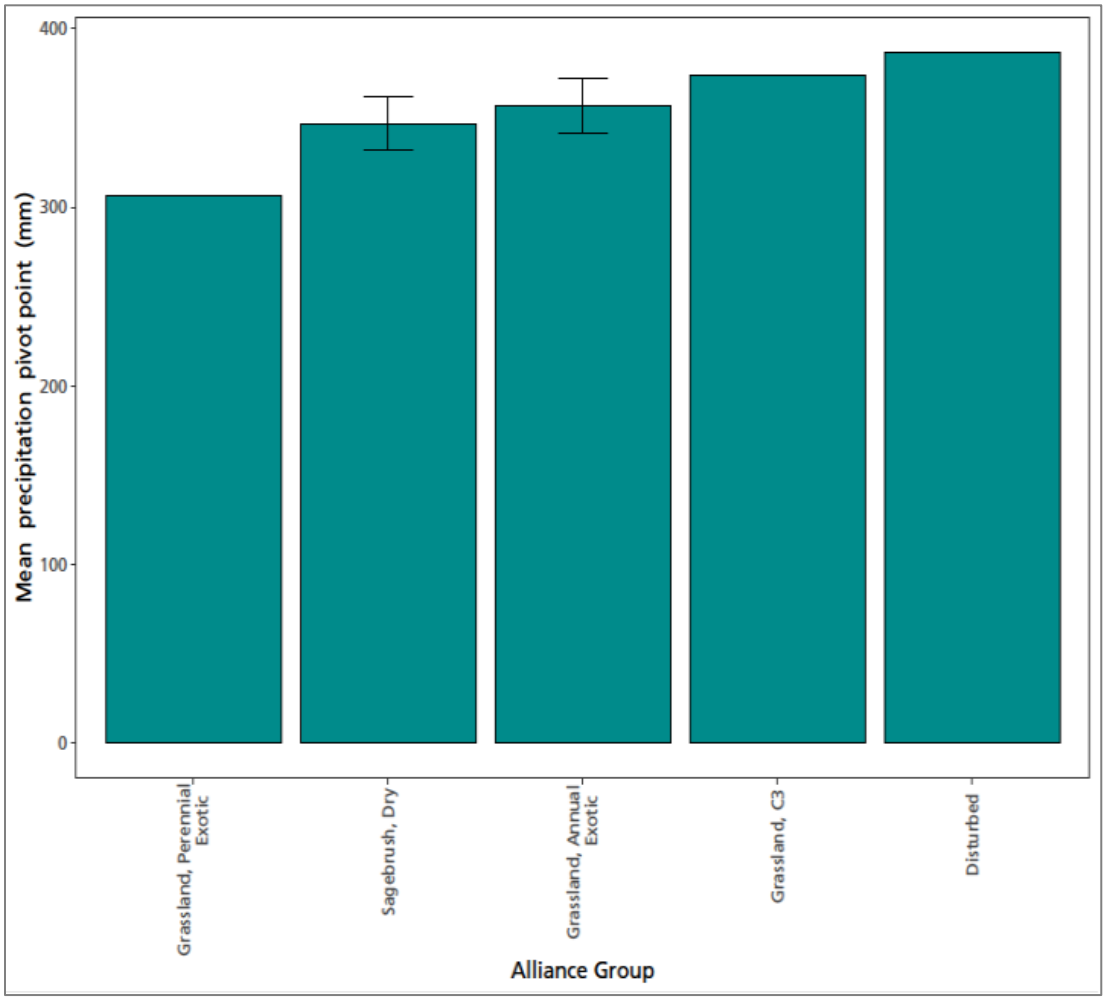


Figure 10. The mean precipitation pivot-point values shown here represent critical water needs for the different alliance groups. Standard error bars indicate range in variability of pivot points among polygons of an alliance group if more than one polygon had a statistically significant relationship (p-value < 0.05) with precipitation. Pivot points identify the critical precipitation need that achieves average production for each alliance group.
NPS / DAVID THOMA

vegetation at different times of the year. Thus, each variable represents a different "pool" and phase of water (solid, liquid, or gas) that may be seasonally active or present during different seasons.

Soil moisture pivot points and pivot points for other water balance variables like actual evapotranspiration that integrate the effect of temperature and precipitation are included in the appendix figures and tables (see Appendix A; Tables S2 and S4 in NPS 2025).

3.6.2 Spatial patterns of drought tolerance

The map of precipitation pivot points shows that the amount of moisture required to increase production above that of the previous year is linked to vegetation type and also to variation between polygons of the same type (Figure 11). The pattern of divergent pivot points between adjacent polygons in the northern portion of the park, all within the Annual Exotic Grassland alliance group, demonstrates variation in drought tolerance. This variation may result from plant density and composition, which influence water availability according to plant water needs (Stephenson 1998).

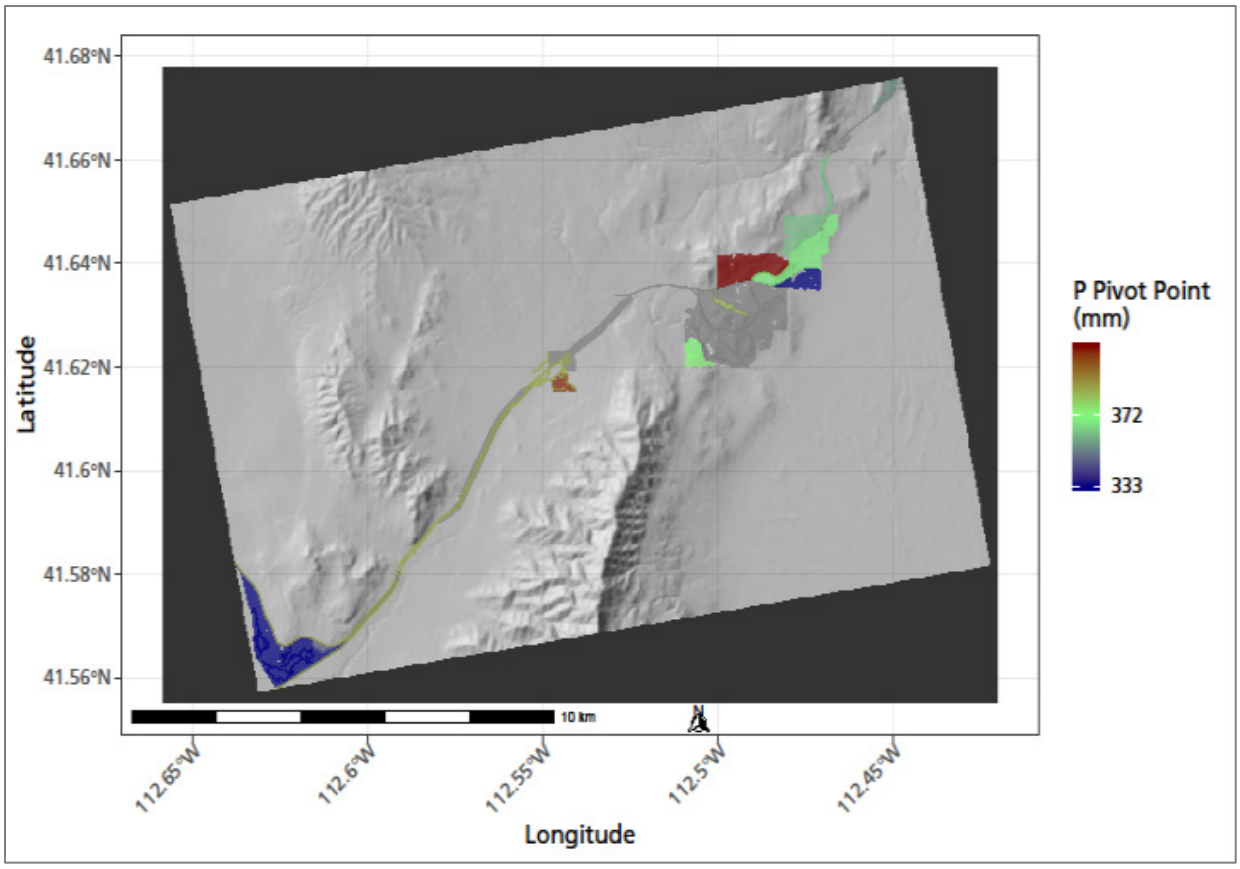


Figure 11. Precipitation pivot points for polygons with a significant relationship (p-value < 0.05) between water-year annual precipitation and change in annual vegetation production, assessed as the interannual difference in iSAVI. The mean precipitation pivot-point values shown here represent spatial patterns in the critical water needs of vegetation.

NPS / DAVID THOMA

3.6.3 Pivot points for other climate variables

Pivot points for other climate and water-balance variables generally reflected the average climate conditions where alliance groups were found (Figure 12; Appendix A). However, the range in pivot

points within alliance groups, and the variation in species assemblages within and between polygons of each alliance group, reflected some variation beyond a pattern purely determined by alliance group name. In semiarid environments like some areas in Golden Spike NHP, pivot points for variables AET, P, SOIL, RAIN, and W are generally lower than the pivot point for D, an indicator of drought. The reason for the lower results is vegetation in semiarid environments is adapted to handle relatively low water availability and high drought stress.

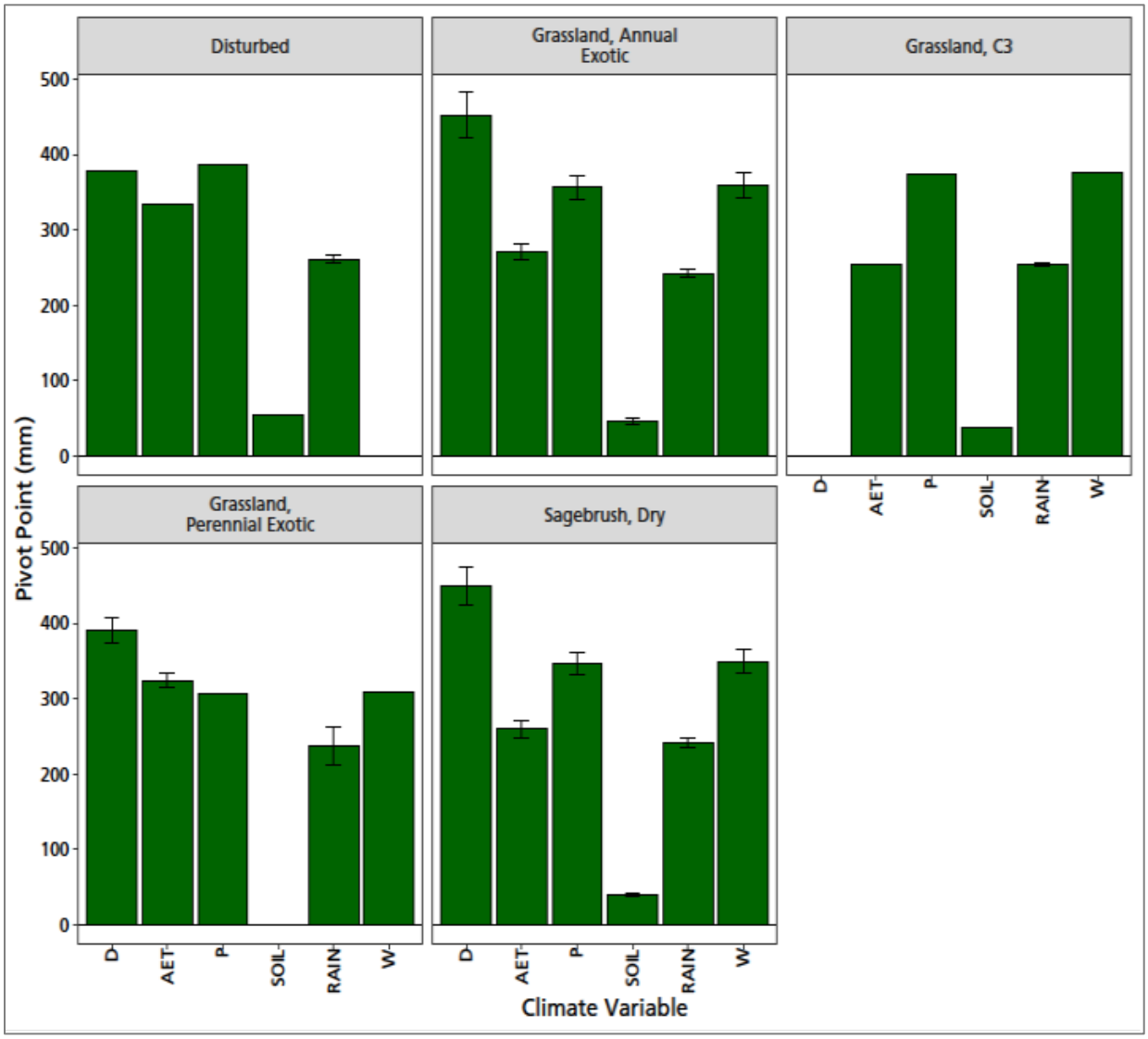


Figure 12. Significant (p-value < 0.05) water-related pivot points by alliance group. See Tables S-2 and S-4 in NPS (2025) for the pivot point values. The magnitude of each pivot point reflects generally average conditions for polygons in each alliance group. The mean pivot-point values are the critical values where annual production switches from below to above average (relative to previous year) for the different alliance groups. D = water deficit (mm), AET = actual evapotranspiration (mm), P = precipitation (mm), SOIL = average soil moisture (mm), RAIN = precipitation as rain (mm), W = snowmelt plus rain (mm). *NPS / DAVID THOMA*

All results shown here are statistically significant. For this reason, any of these alliance group-level pivot points can be compared against historic, present, or future projected growing-season climate conditions to determine if those conditions are likely to result in below- or above-average vegetation production.

Pivot points for each climate variable by polygon are provided in Table S-2 of NPS (2025) and by alliance group in Table S-4. These can be used with data on climate exposure to identify conditions conducive to above- or below-average growth.

3.7 Vegetation response

3.7.1 Vegetation response and climate sensitivity

When they interact with climate, plant traits determine which species grow under different conditions of water availability. The result is a spatial organization of alliance groups that reflect local climate and the sensitivity of vegetation to climate (Figure 13). The interactions between plant traits, site characteristics, and climate-determined patterns of vegetation distribution in the past will determine how vegetation in Golden Spike NHP will be shaped by climate in the future.

Vegetation response is a formal component of vegetation vulnerability assessments used in Climate-Smart Conservation (Stein et al. 2014). The importance of response is related to the need to understand which vegetation groups may respond sooner or more strongly to a given amount of climate exposure. While a unit change in iSAVI is not quantitatively linked to vegetation cover or biomass in this analysis, it is representative of change in both of those attributes. In this way, the iSAVI response indicates where change is likely to happen first and fastest as the climate shifts.

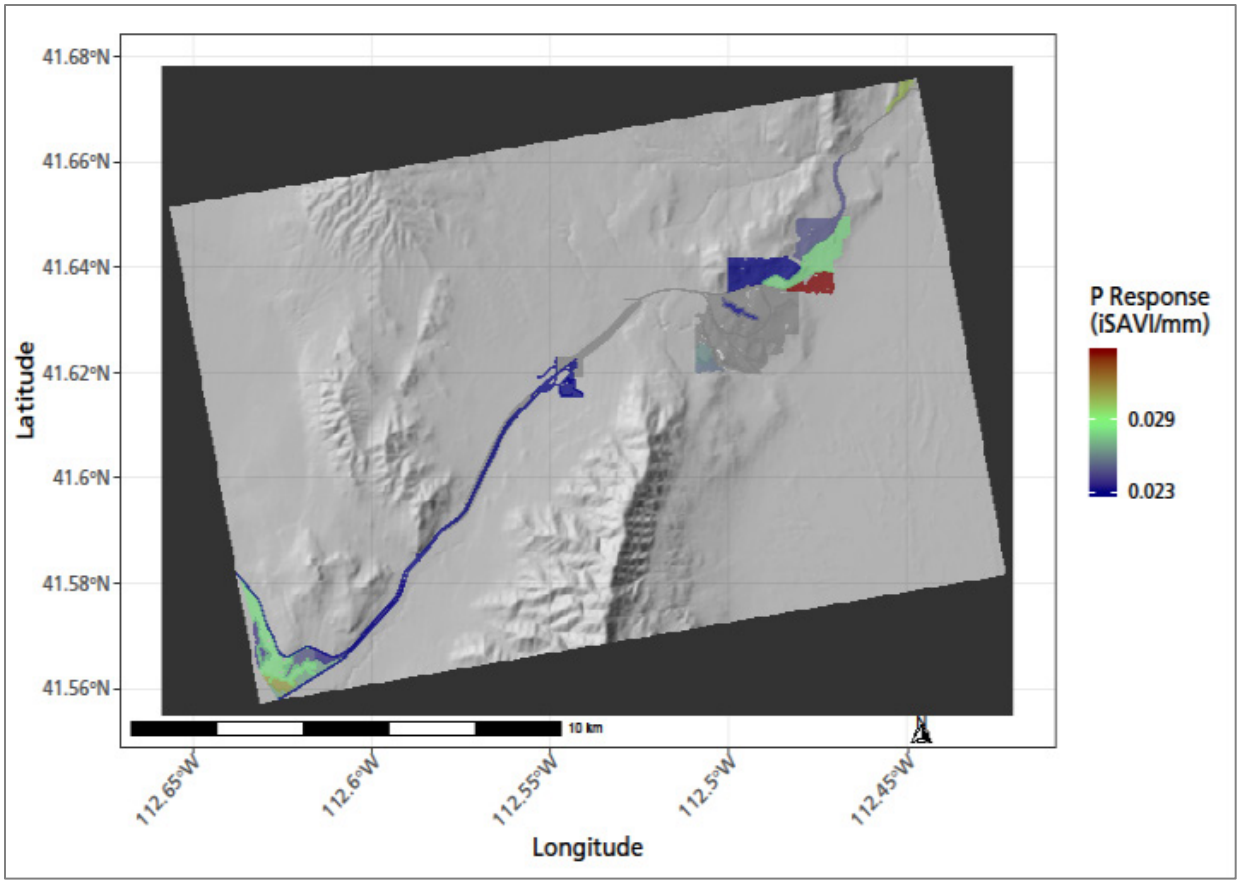


Figure 13. Sensitivity of growing-season vegetation production to annual water-year precipitation. This figure shows which vegetation types will experience change first. Groups with highest response rates are most likely to see change happen first and fastest as the climate shifts. Response is the slope of the linear-regression relationship between annual precipitation and iSAVI change from the previous year. It is the change in iSAVI expected per millimeter of change in annual precipitation. Areas without color were either smaller than the minimum area required for mapping (< 8.3 ha) or did not have a significant relationship with annual precipitation. Areas that were not significantly related to annual precipitation may be related to other climate metrics. Statistics for sensitivity of each polygon to each climate metric, including quality of relationships and regression coefficients, can be found in Table S-2 of NPS (2025). *NPS / DAVID THOMA*

At Golden Spike NHP, the Disturbed alliance group was least responsive to annual precipitation, while other alliance groups were more responsive to variation in annual precipitation (Figure 14). Alliance-group sensitivities to other water-balance variables can be found in Appendix A.

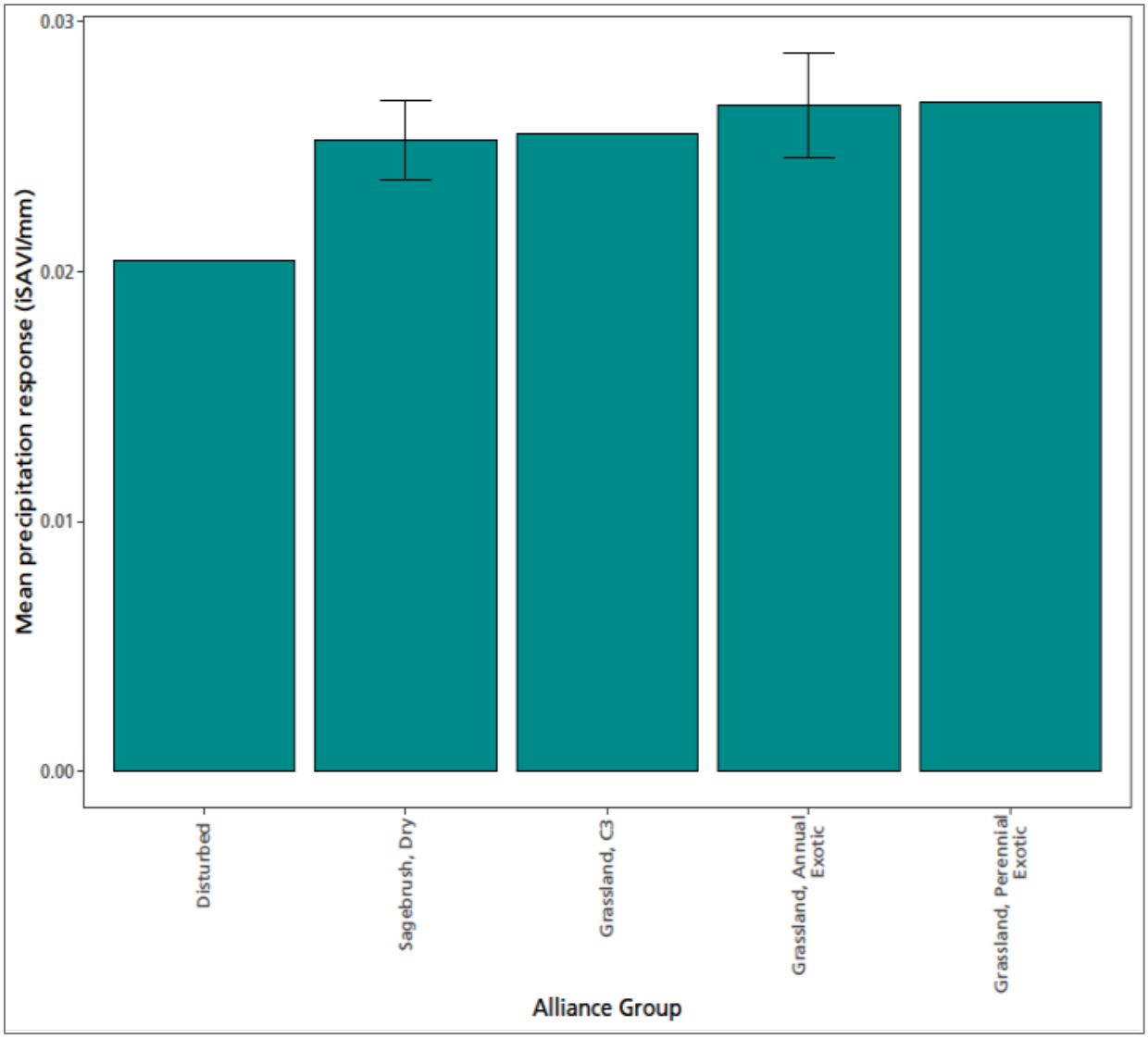


Figure 14. Responses of different vegetation alliance groups to precipitation. Standard error bars indicate range in variability of responses among polygons of an alliance group if more than one polygon of an alliance group had a statistically significant relationship (p-value < 0.05) with precipitation.
NPS / DAVID THOMA

Although the results do not suggest significant differences (except with Disturbed areas) Annual and Perennial Exotic Grasslands had responses higher than other alliance groups which means they may be competitive against other alliance groups when precipitation is abundant. In other words, in years when precipitation is higher than normal, vegetation in the Exotic Grassland alliance groups could become a management concern in or near the park because the rate of response to precipitation input

is greater than that of native vegetation like C3 Grasslands and Dry Sagebrush. Additional response maps can be found in the appendix.[4]

3.7.2 Patterns within alliance groups

While pivot points and responses provide different information, they are linked by plant traits: as precipitation pivot points decrease (i.e., cross the horizontal "no change" line further to the left), response rate increases (Figure 15). Alliance groups or polygons within an alliance group with steeper slopes are considered more responsive to changes in water availability. These groups or polygons increase production with less precipitation, demonstrating that responsiveness to precipitation is greatest where vegetation is most drought tolerant.

[4] Response to soil moisture is greater than sensitivity to precipitation or deficit because incremental changes in soil moisture in this analysis are expressed as a water-year mean, whereas precipitation and deficit are sums (see Table 1). However, the pattern in response to soil moisture is tied to spatial variation in soil properties that play important roles in storing precipitation between events.

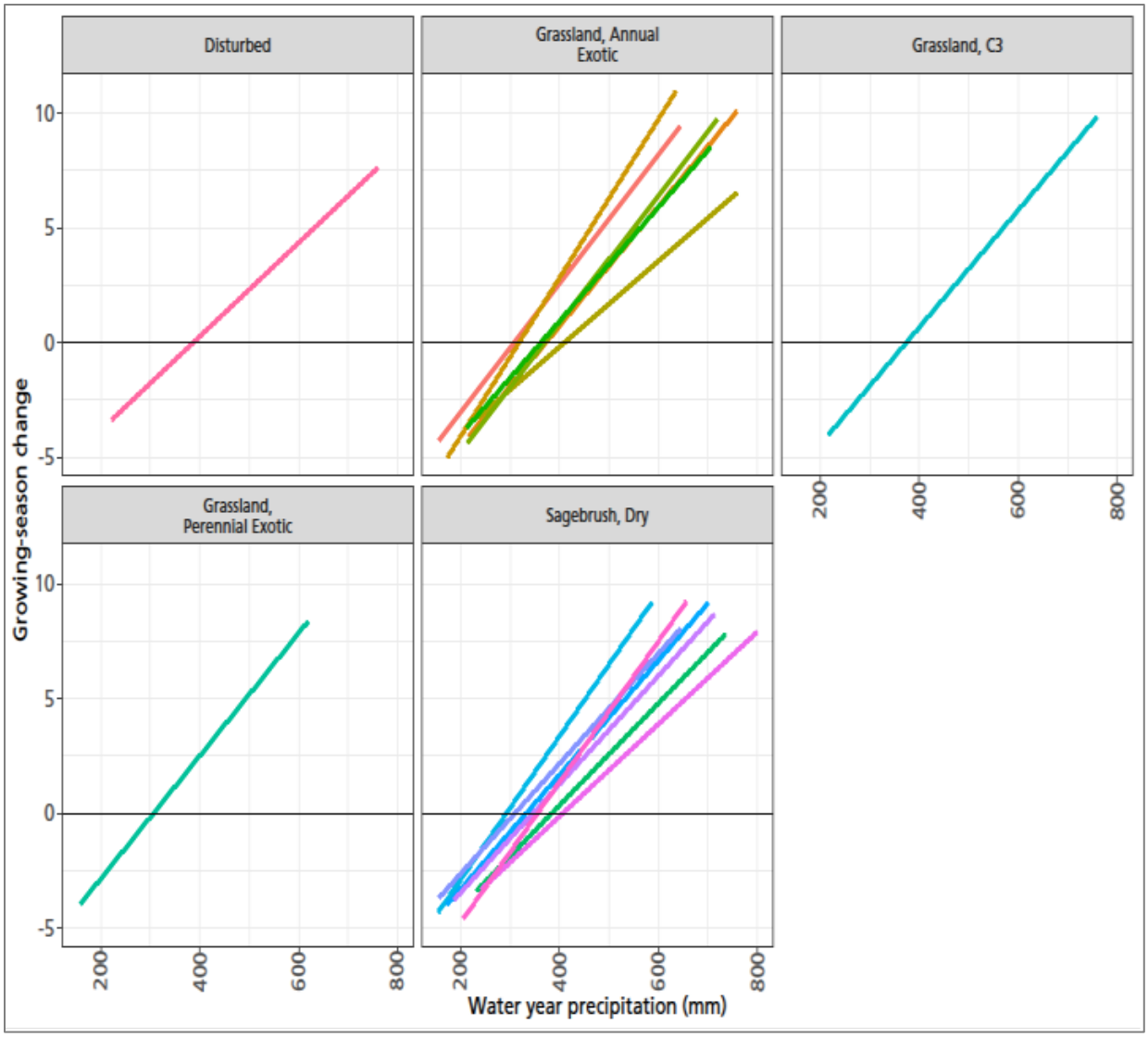


Figure 15. Graphical depiction of the relationship between pivot points and responses in polygons that had a significant relationship (p-value < 0.05) between iSAVI and water-year precipitation (e.g., critical water need vs. rate of growing season iSAVI change per mm precipitation). Polygon-level pivot points and responses are provided in Table S-2 of NPS (2025). Alliance groups with steeper slopes are considered more responsive to changes in water availability. Alliance groups and alliance polygons within alliance groups that cross the horizontal axis further left are more drought resistant. This is because they shift to above-average condition with less precipitation. Only significant relationships are shown. Panels without lines represent alliance groups with no significant relationships between iSAVI and climate variables. Colors help differentiate individual polygons within alliance groups.

NPS / DAVID THOMA

Multiple factors can introduce additional variability in pivot points and responses within alliance groups. These include differences in species assemblages, spacing between plants, and soil properties that affect the retention and distribution of water in the soil profile that is accessible to different growth forms (e.g., plants with shallow or deep roots) (Lauenroth and Bradford 2009; Lauenroth and

Bradford 2012; Schlaepfer et al. 2014). These factors contribute to the range in pivot points and responses, reflecting a range of plant traits responding differently to climate across the park. The patterns of pivot points and responses quantify unique climatic habitats occupied by the different alliance groups in the park, and can serve as a guide to anticipate what, where, when, and why vegetation change may occur. Using information in this report allows tracking of weather conditions during the growing season to indicate vegetation condition at the polygon or alliance-group scale, depending on management interest (NPS 2025, Tables S-2, S-4). The degree of responsiveness was determined by traits that allowed plants to either resist drought or rapidly respond to available water. The result was that vegetation response to climate could be considered coarsely at the alliance-group level, but at higher spatial resolution and often, with higher accuracy, at the polygon level.

3.7.3 Production response to water and non-water variables

Assemblages with higher responses (steeper regression slopes) were more sensitive to climate. Depending on the climate variable, the slope could be positive (as with semiarid environments and water variables, such as precipitation and actual evapotranspiration), or negative (in response to water deficit or potential evapotranspiration, both of which are related to temperature) (Figure 16; also see NPS 2025, Tables S-2 and S-4).

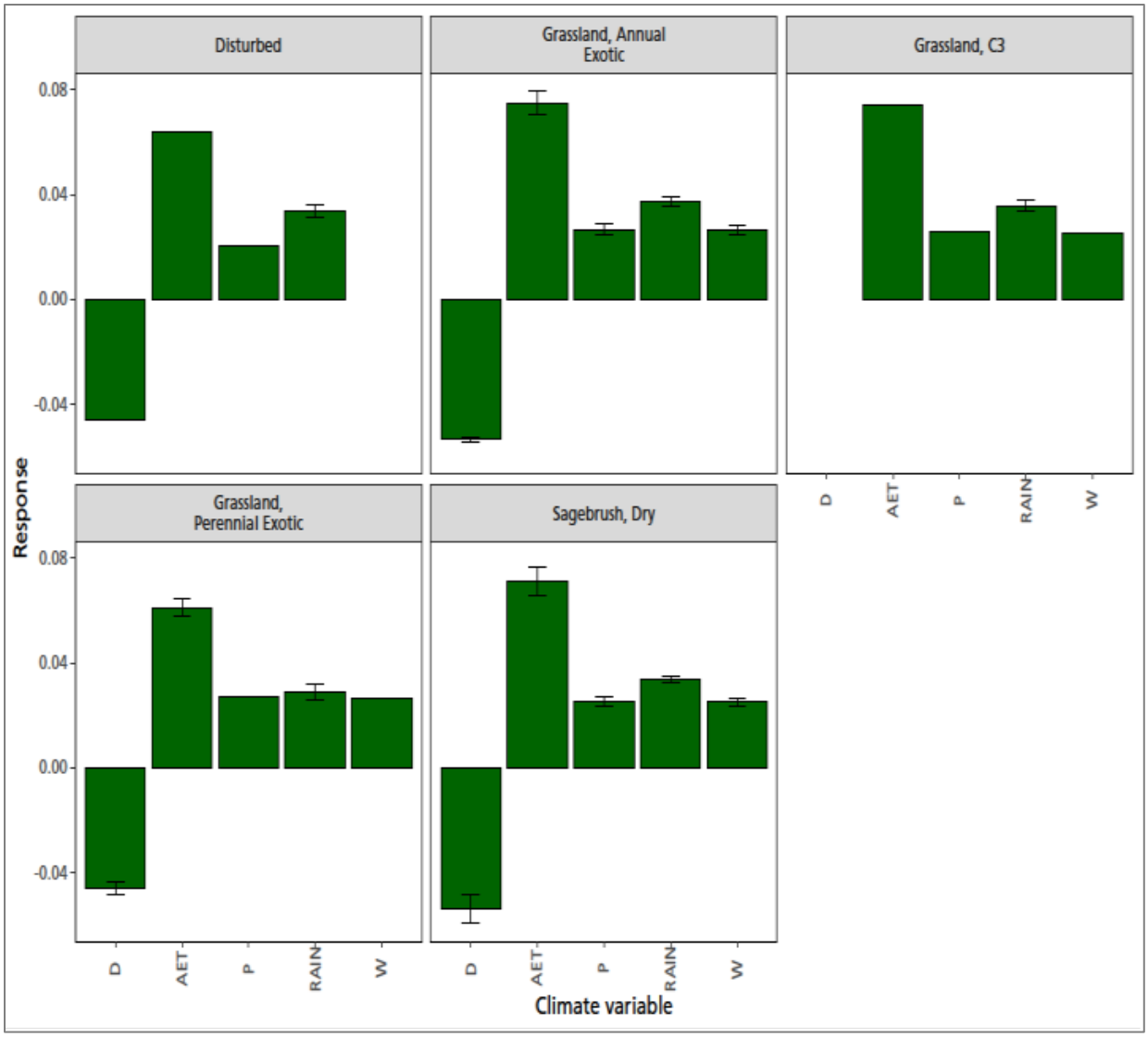


Figure 16. Top models in multi-model comparison of climate correlates with interannual differences in growing-season iSAVI across all alliance groups. Percentages indicate proportion of polygons where each model was competitive. Numbers above bars indicate polygon count. Each polygon may have more than one competitive model; thus, the sum of percentages exceeds 100 across all models. The x-axis labels refer to the *a priori* climate models in Table 3. D = annual deficit; AET = annual evapotranspiration; P = annual precipitation, RAIN = rain, W = snowmelt plus rain. Numbers indicate current and prior years included in each model. 1 = current year; 12 = current and previous year; 123 = current and previous two years.

NPS / DAVID THOMA

3.8 Multivariable indicators of annual vegetation production

Pivot points and responses are ecological measures of annual production, but production is affected by multiple aspects of weather before and during a growing season, as well as conditions in prior growing seasons that set the stage for production potential in the current year (Sala et al. 2012).[5] In the multi-model comparison of climate correlates with interannual differences in growing season iSAVI across all alliance groups, climate indicators of annual production showed that regardless of alliance group, all polygons were influenced by three years of soil moisture. The next most common indicator of production was two years of soil moisture (Figure 17). These patterns generally held within alliance groups (Figure 18), but it can be hard to discern as sample sizes are small in some alliance groups. A list of top-performing models (AICc < 4) by polygon can be found in Table S-5 of NPS (2025).

[5] This is one reason why the annual relationships described above are not as strong as monthly relationships described in some of our earlier work (Thoma et al. 2016).

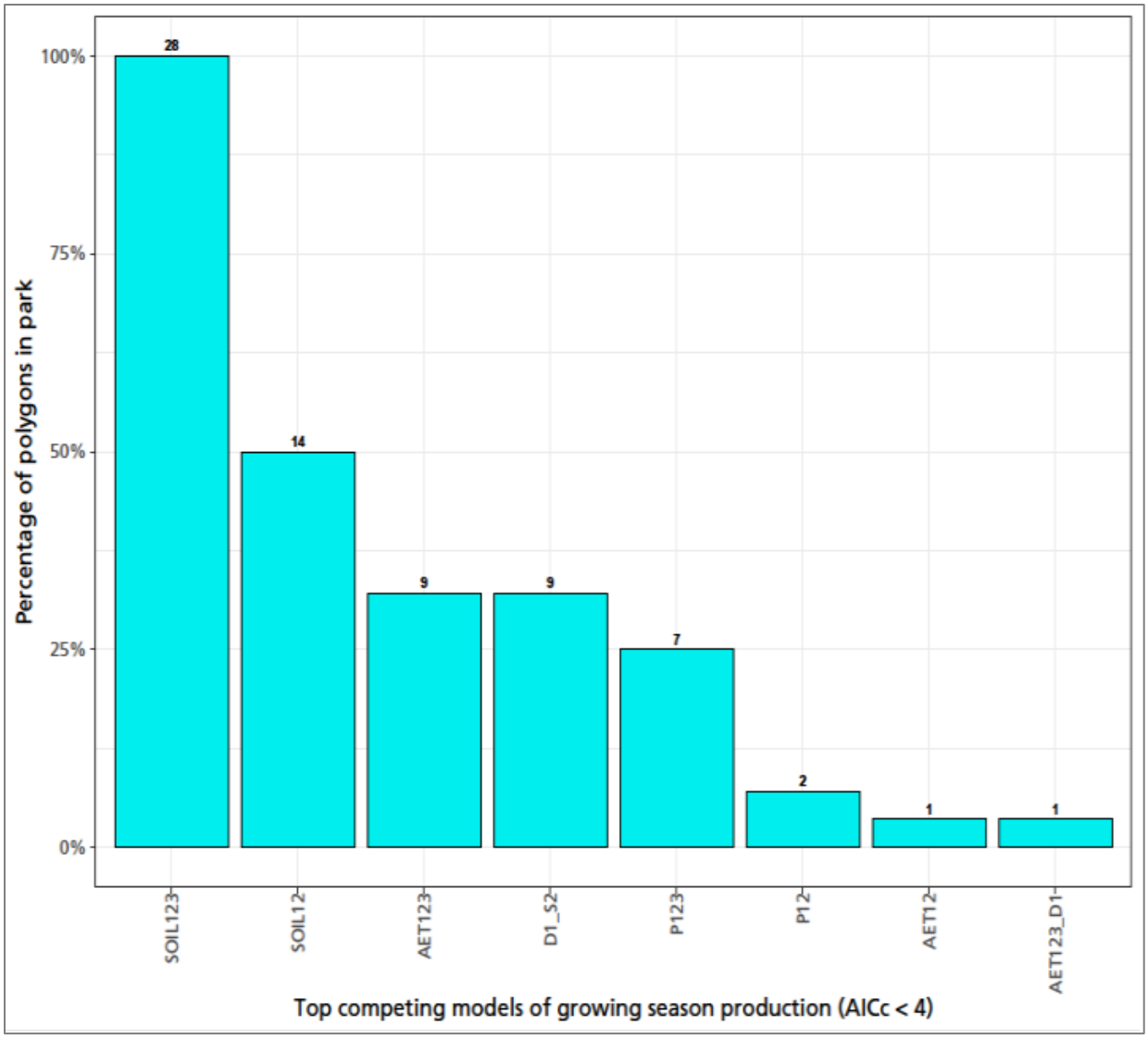


Figure 17. Top models in multi-model comparison of climate correlates with interannual differences in growing-season iSAVI across all alliance groups. Percentages indicate proportion of polygons where each model was competitive. Numbers above bars indicate polygon count. Each polygon may have more than one competitive model; thus, the sum of percentages exceeds 100 across all models. The x-axis labels refer to the *a priori* climate models in Table 3. SOIL = annual average soil moisture; D = annual deficit; AET = annual evapotranspiration; P = annual precipitation. Numbers indicate current and prior years included in each model. 1 = current year; 12 = current and previous year; 123 = current and previous two years.

NPS / DAVID THOMA

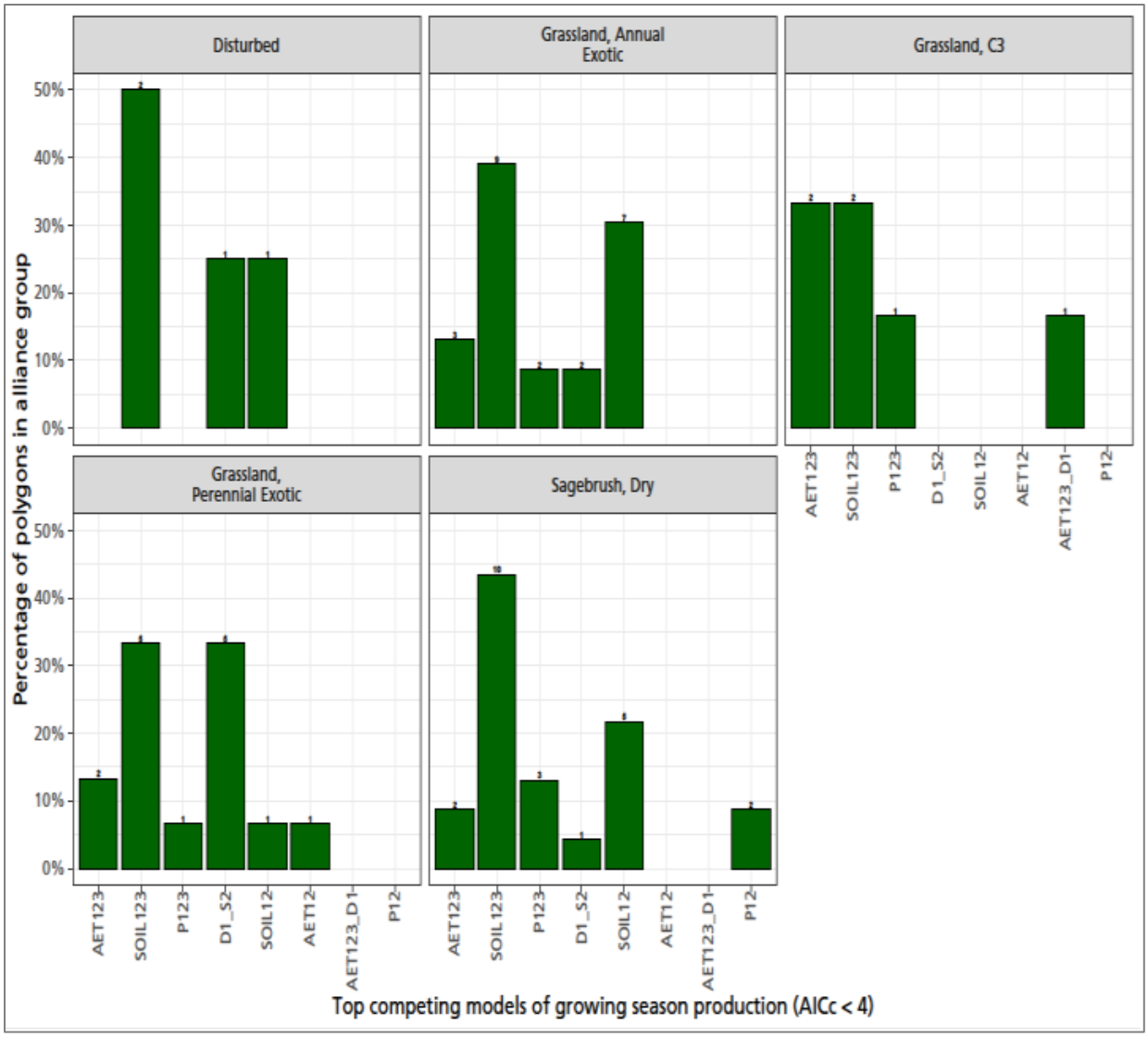


Figure 18. Top models of growing-season production by alliance group in multi-model comparisons of climate correlates with interannual differences in growing season iSAVI. The x-axis labels refer to the *a priori* climate models in Table 3. The y-axis represents the proportion of polygons in each alliance group where each model was competitive. Numbers above bars indicate polygon count. Each polygon may have more than one competitive model; thus, the sum of percentages can exceed 100 across models. SOIL = annual average soil moisture, D = annual deficit, AET = annual evapotranspiration, P = annual precipitation. Numbers are 1 = current year, 12 = current plus previous year, 123 = current plus previous two years.

NPS / DAVID THOMA

Response to multiple years of soil moisture highlights the importance of legacy effects across years in a semiarid environment where water is the growth-limiting factor in most alliance groups in most years (Bisigato et al. 2013). Soil properties that help sustain higher average soil moisture, perhaps through finer soil textures, reduced runoff or deep infiltration, may provide additional benefit.

3.9 Land-surface phenology trends at Golden Spike National Historical Park

By the end of the study across all alliance groups, the growing season was starting 6.2 days earlier and ending 4.5 days later, while the timing of peak growth occurred 15.5 days earlier (Table 6). Although the growing season started earlier and ended later, the average length of the growing season decreased by 10.6 days, likely due to high variability in determination of start and end of season date in polygons that may have been disturbed by land use practices (Table S-7 in NPS 2025, whole-park polygon average). For this reason, the phenology results should be used with caution, or interpreted with ancillary information about grazing or weed control that may alter landscape phenology determined from remote sensing.

Table 6. Changes in land surface phenology in days averaged by alliance group during the 20-year study. ΔSOS = days change in start of season; ΔEOS = days change in end of season; ΔLOS = days change in length of season; ΔPOP = days change in period of peak growth. Trends for each polygon are in Table S-7 in NPS (2025). Significant trends can be found by filtering Table S-7 on p-value < 0.05.

Alliance group	ΔSOS	ΔEOS	ΔLOS	ΔPOP	Hectares	Polygon count	% area
Grassland, Annual Exotic	0.1	−19.9	−2.8	−18.8	379.8	9	47.3
Sagebrush, Dry	−1.9	31.8	−2.0	−14.7	271.4	10	33.8
Grassland, Perennial Exotic	−12.1	−0.8	−19.2	−19.5	101.3	5	12.6
Disturbed	−9.1	19.4	5.3	−11.0	29.1	2	3.6
Grassland, C3	−8.1	−8.3	−34.5	−13.3	21.3	2	2.7

Earlier start of growth and later end of growth are consistent with rising temperatures and increasing water availability that can extend the growing season. It is also consistent with increasing CO_2 concentrations that increase vegetation production through a process known as CO_2 fertilization (Sorokin et al. 2017) that increases water use efficiency. It is unclear why the length of the growing season shortened given the trends in start and end of season phenology at Golden Spike NHP unless it is entirely due to variability and outliers in the relatively small number (28) of polygons analyzed. The strength of the relationship between production and annual precipitation over the study period (see Figure 8) and in findings from Section 3.7 suggested most of the increase in production in semiarid alliance groups was related to increases in water availability during the study, which may have been augmented by increases in CO_2.

Changes in land-surface phenology result from interactions between temperature, moisture, plant traits that control growth rates, and CO_2 concentrations that affect water-use efficiency. Generally, warming reduces growth rates in semiarid environments, while elevated CO_2 increases water-use efficiency of production for the same amount of water. Thus, warming may initiate an earlier start to the growing season, and elevated CO_2 may increase water-use efficiency, resulting in more production for a given amount of water use. But efficiency is ultimately limited if conditions become sufficiently dry and growth ceases. For this reason, and given projected drying on the Colorado Plateau, increases in efficiency may be small and short-lived in the face of disturbance caused by drought or wildfire (Allen et al. 2015). Tracking changes in phenology in NCPN parks and linking

those changes to seasonal changes in temperature and CO_2 concentrations could help further clarify the vulnerability of semiarid vegetation to multiple aspects of climate change (Sorokin et al. 2017).

3.10 Drivers of green-up

3.10.1 A priori *model selection method*

At the park scale, several climate and water balance variables were important to initiation of growth for 6 of 28 polygons (Figure 19). These variables can be characterized as indicators of water availability or temperatures warm enough for growth and the interactions of water and energy needed for growth. This is consistent with findings from Moore et al. (2015), who also describe the importance of temperature and soil moisture in spring as correlated with the onset of growth. Other competitive models included growing degree days and actual evapotranspiration, which incorporates both water and heat needed for growth (Figure 20).

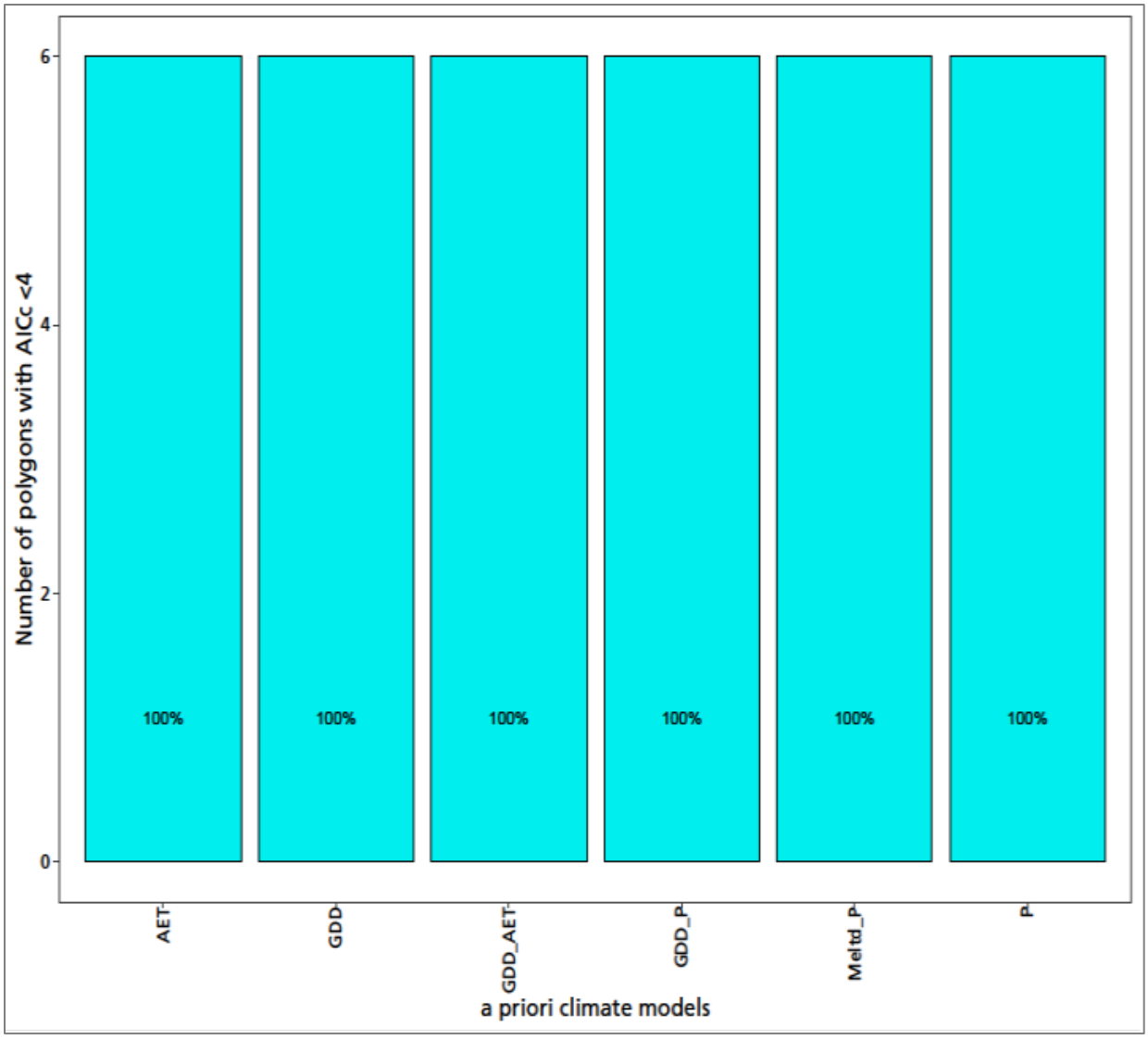


Figure 19. Top models in multi-model comparisons of climate correlates with start of growing season at the whole-park scale. The x-axis labels refer to *a priori* climate models as determinants of green-up or start of season. AET = actual evapotranspiration, GDD = growing degree days, Meltd = day of complete snowmelt, P = precipitation.

NPS / DAVID THOMA

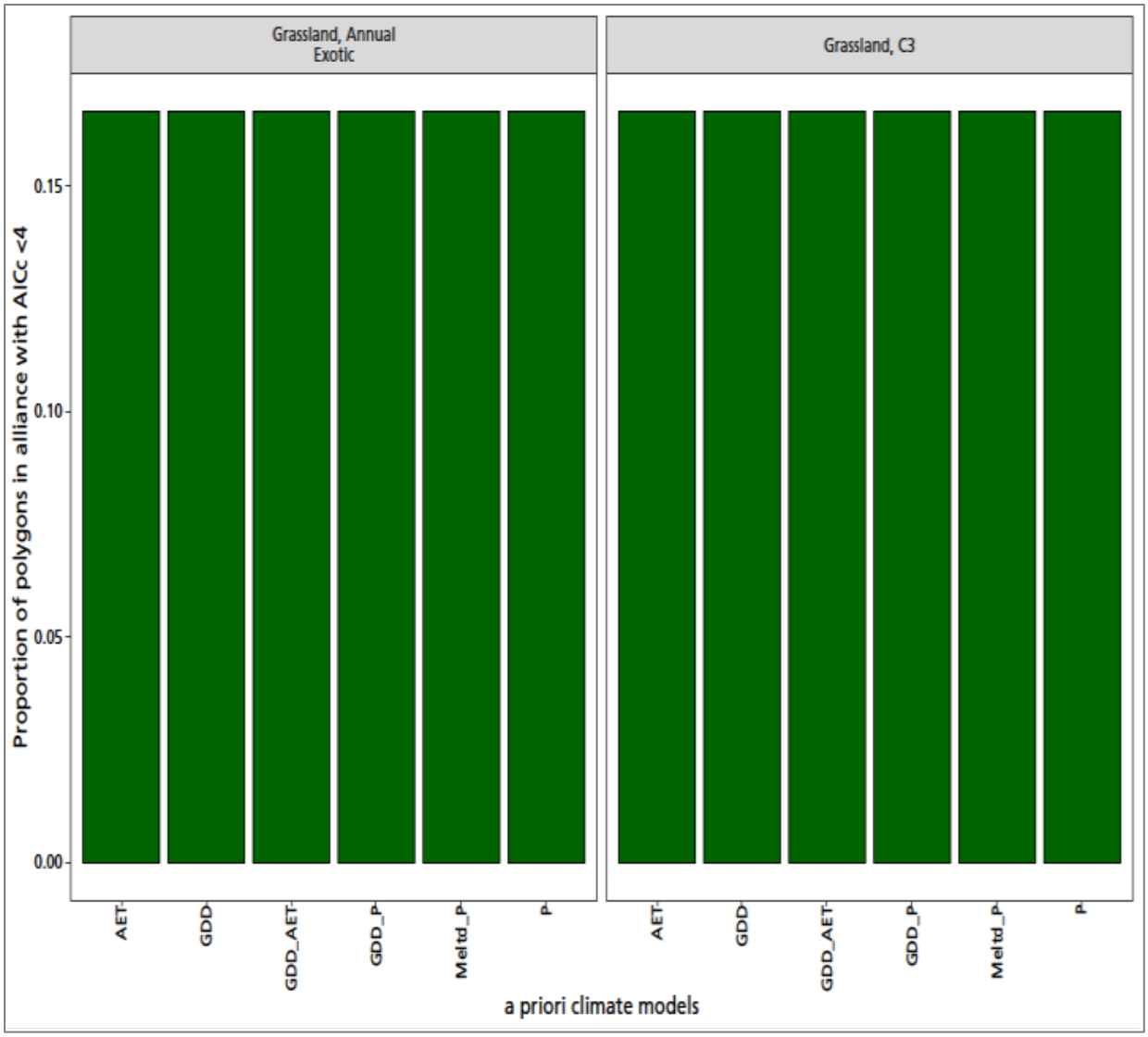


Figure 20. Top models in multi-model comparisons of climate correlates with start of growing season at the alliance-group scale. Only two of five alliance groups had competitive models of start of growing season. The x-axis labels refer to *a priori* climate models as determinants of green-up or start of season. AET = actual evapotranspiration, GDD = growing degree days, Meltd = date of complete snowmelt, P = precipitation.

NPS / DAVID THOMA

Several climate and water balance variables were competitive estimators of start of the growing season. Actual evapotranspiration is an estimate of water used by plants when soil water is available and temperatures are warm enough for growth. Growing degree days are likely important because spring soil moisture is typically at its highest level of the year after the winter recharge period, and warming temperatures are necessary to break dormancy. The importance of precipitation during the calendar year may indicate that the soil water-holding capacity requires spring precipitation to fill to capacity in some years. Otherwise, insufficient precipitation may be a growth-limiting factor for initiating growth. This can occur when dry fall and winter periods result in low moisture levels in

spring that could become a co-limiting factor alongside temperature in spring following dry winters. An alternative explanation is that precipitation in the form of snow may prevent initiation of growth until it melts (see next section).

3.10.2 Random-forest method

Variable importance plots showed the best predictors of start-of-season were precipitation, growing degree days, and the date of snowpack melt (Figure 21). These findings were like those in the multi-variable regression models, where the interaction between temperature and precipitation was important. The addition of the day of snow melt in the random forest model suggests that snow is important for determining initiation of growth, but perhaps not in all years.

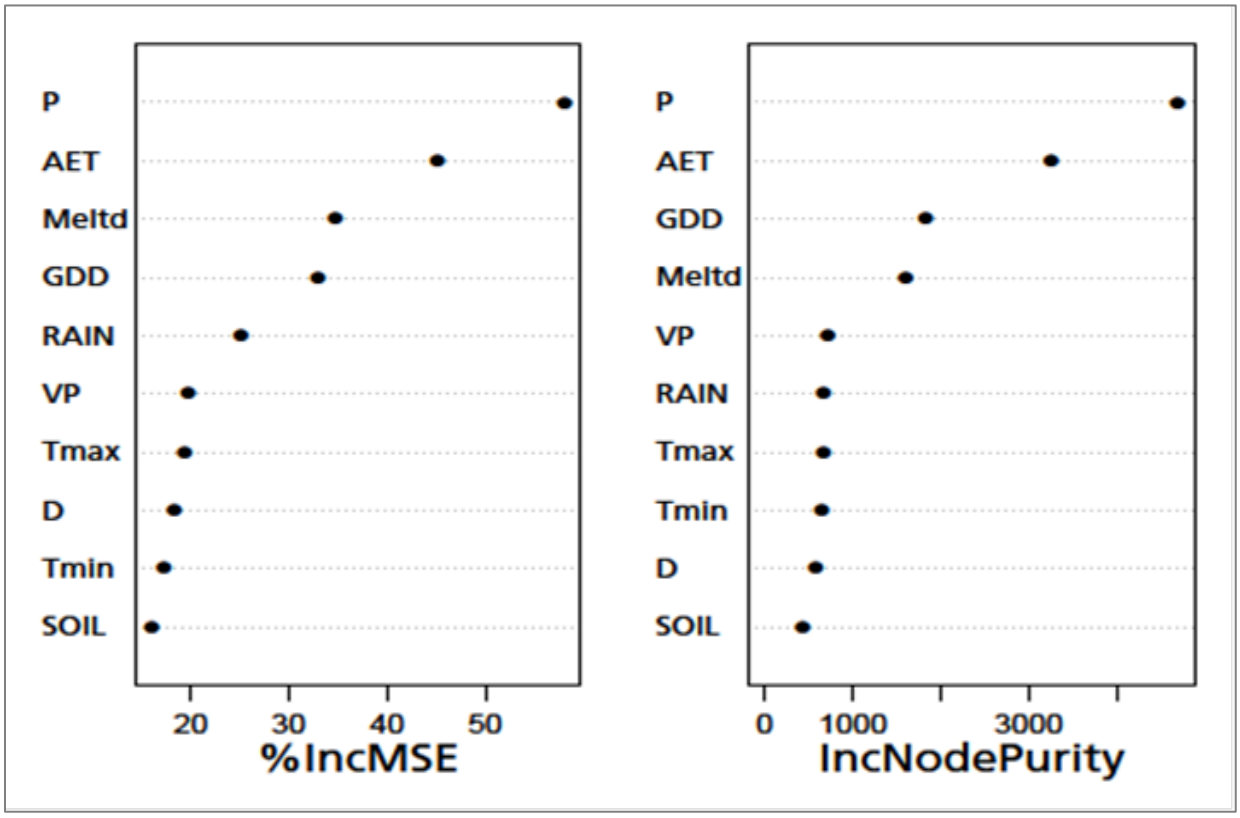


Figure 21. Variable importance in the random-forest model of climate drivers of the start of growing season. Percent increase in mean square error (%IncMSE) is a measure of model performance with each variable. Increase in node purity (IncNodePurity) is the difference in residual sum of squares in regression with or without each variable.

NPS / DAVID THOMA

Findings from the two modeling methods suggested a combination of temperature and moisture is an important indicator of SOS, as is expected in cold semiarid climates. The loss of snow cover that exposes vegetation to warming and solar radiation in spring makes intuitive sense as a driver for the start of growth where snow accumulates over winter, but the effect of spring precipitation is less intuitive unless the soil moisture was not sufficiently replenished over winter to meet plant needs.

The random-forest model obtained from the training dataset was used to model SOS in the validation dataset to determine predictive performance. It predicted SOS date at the park scale with a mean absolute error of ± 3.5 days (Figure 22). When separated by alliance group, the model performed equally well (Figure 23).[6]

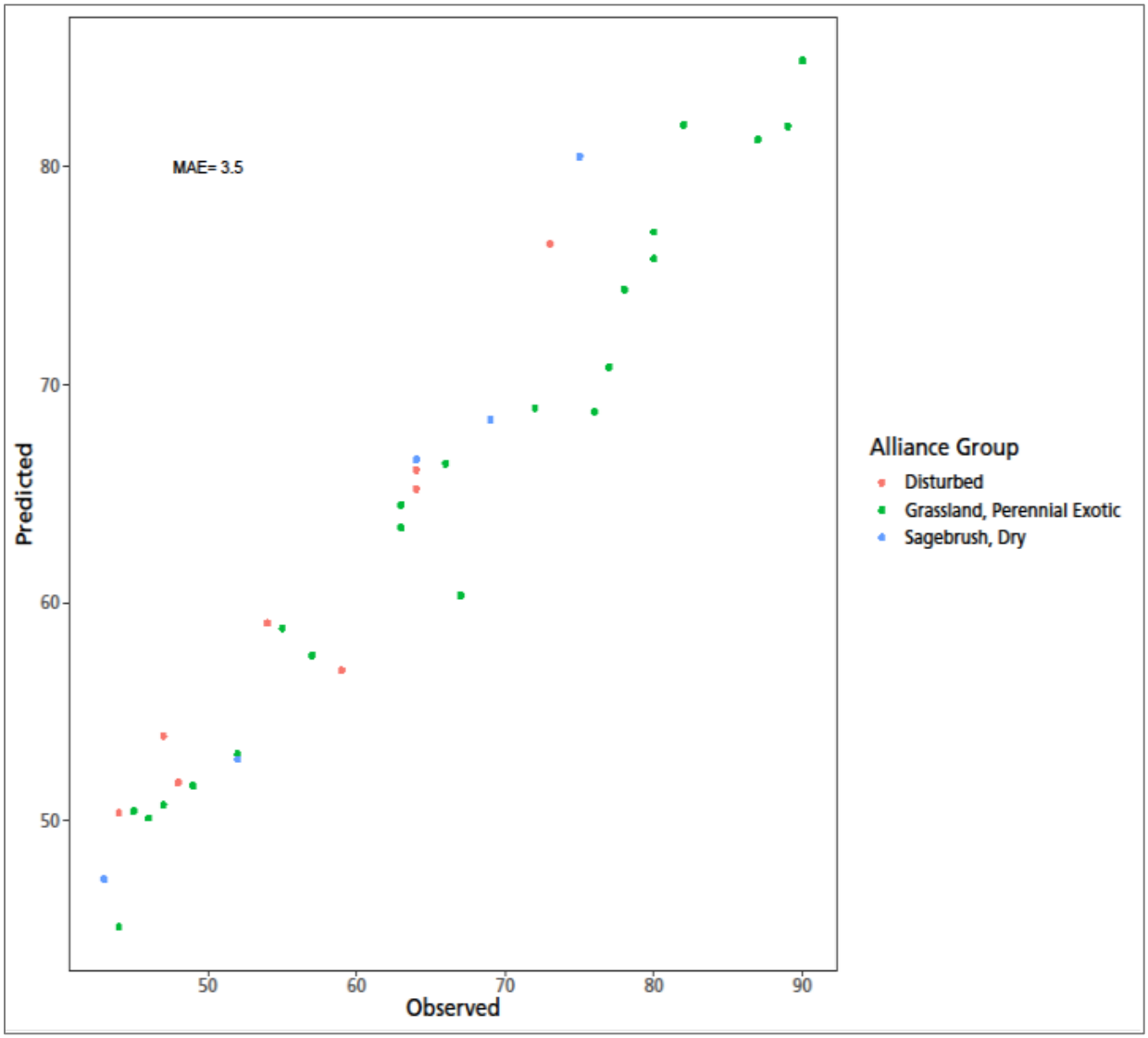


Figure 22. Predicted start-of-season date versus observed start-of-season date in the holdout dataset used for validation of the random-forests model for all polygons in Golden Spike NHP. MAE is mean absolute error of prediction in days. Polygons with annual peaks (POP) occurring between November 1 and April 1 were removed prior to this analysis to minimize effects of vegetation shadows that confound determination of phenology (Norris and Walker 2020).
NPS / DAVID THOMA

[6] The analysis was conducted at the park scale, rather than by polygon, to increase sample size for the random forest modeling process.

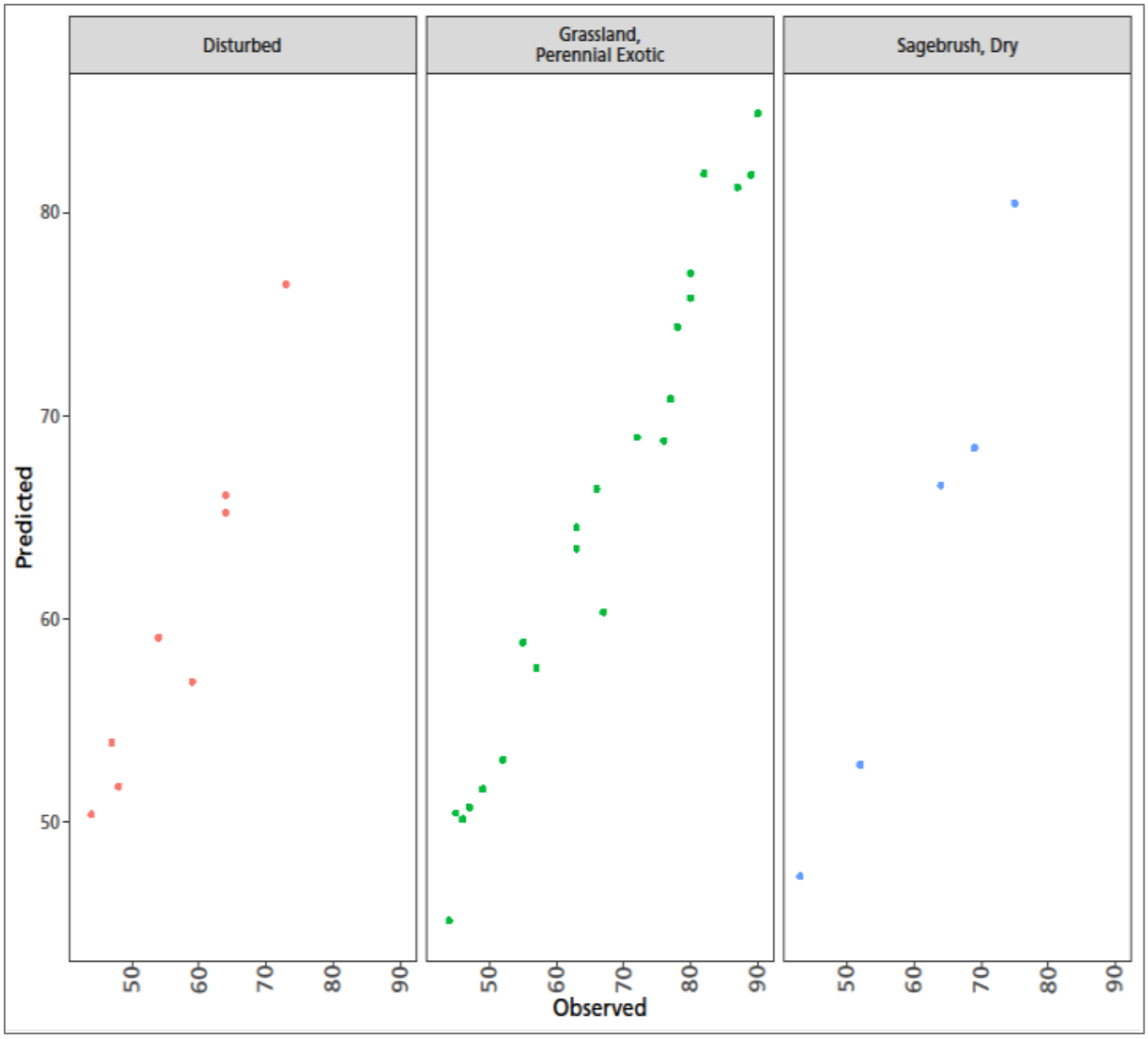


Figure 23. Predicted start-of-season date versus observed start-of-season date in the holdout dataset used for validation of the random-forests model for alliance groups. Polygons with annual peaks (POP) occurring between November 1 and April 1 were removed from this analysis. Outliers are likely due to difficulty in discriminating SOS when SAVI changes monotonically during a growing season in low productivity years.

NPS / DAVID THOMA

Inspection of SOS dates prior to April 1 in Figures 22 and 23 suggests they may have resulted from low amplitude and monotonic increase (straight line with minimal amplitude fluctuation) in SAVI in some years. This combination makes it difficult to identify meaningful SOS dates using the derivative method that relies on a change in the acceleration of growth rate in spring to determine when growth starts. Even though polygon/year combinations with winter SAVI peaks were screened out of the analysis (per Norris and Walker 2020), it is not clear how SOS may be affected by the shadowing noted in sagebrush habitats by Norris and Walker, in part because the shadowing effect is partially dependent on vegetation structure and spacing, which vary on a continuum across the

landscape. For this reason, modeled SOS dates should be considered with skepticism in the alliance groups where SOS is predicted to occur prior to April 1.

Despite these potential shortcomings, the validation demonstrates a strong predictive model of SOS using climate data for most of the Golden Spike NHP landscape. This means climate projections could be used to model SOS dates in the future. This could be helpful in assessing potential vulnerabilities caused by phenological mismatch between pollinators and flowering species, as well as potential impacts to migrating birds and mammals, such as deer. Mule deer in some western states "surf the green wave" of vegetation as it greens up progressively across gradients of latitude and elevation (Aikens et al. 2017; Merkle et al. 2016; van Wijk et al. 2012). Presently, it is unknown if animal species in NCPN parks time their movements with SOS or the green wave thereafter, but this information could be used to help assess if animals are keyed into this land-surface process.

3.11 Climate patterns

Annual temperature, precipitation, and estimates of AET, climatic water deficit, and soil moisture derived from the water-balance model for 1980–2019 exhibited high interannual variability (Figure 24; Appendix A). This variation caused large interannual changes in annual vegetation production. Since 1980, precipitation has declined in most alliance groups.

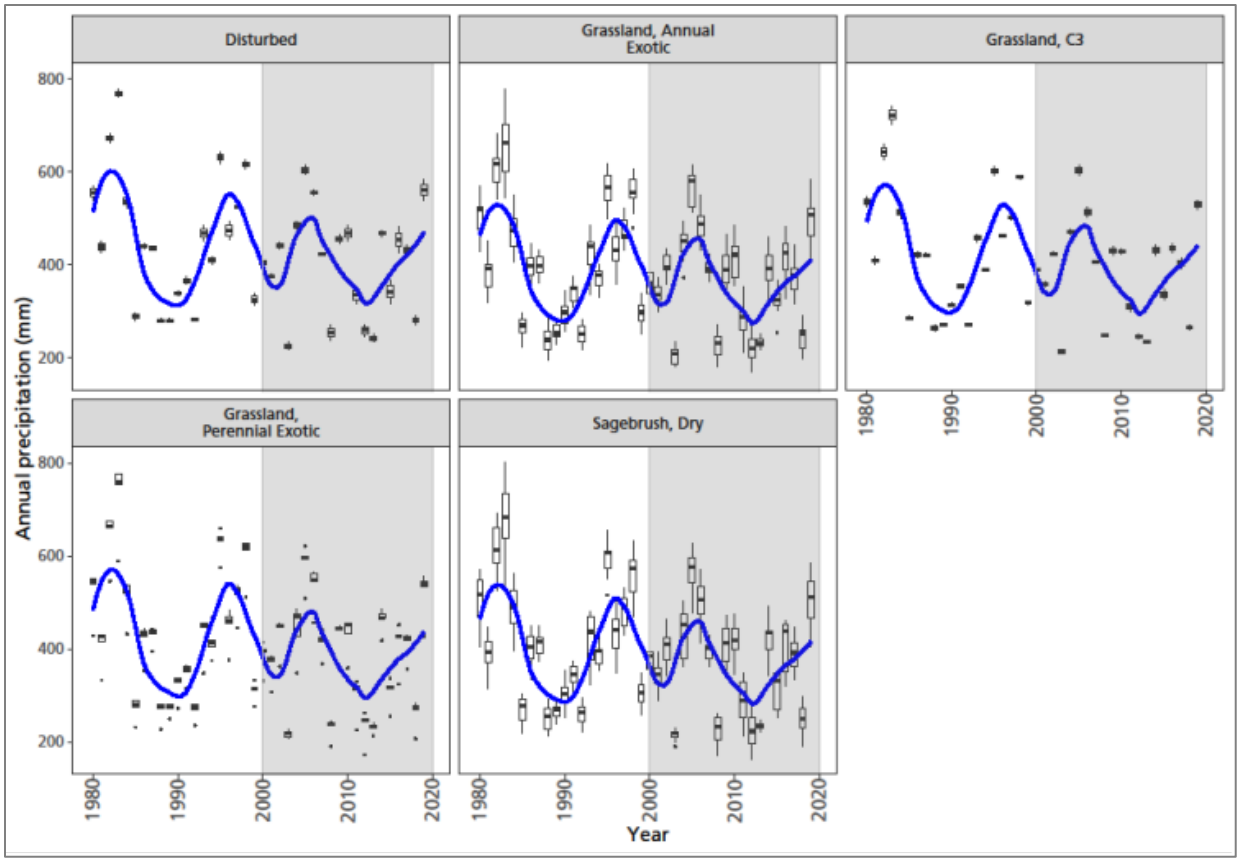


Figure 24. Long-term temporal patterns in precipitation in vegetation alliance groups. Box plots demonstrate the range of variation by year. The line is a loess smooth with a 25% span to illustrate multi-year patterns. Gray shaded area includes the period between 2000 and 2019, investigated for relationships between production and climate when satellite imagery and climate data were both available. Study-period trends and associated statistics for the other water-balance variables are presented in Appendix A.

NPS / DAVID THOMA

In contrast to the longer period beginning in 1980, with obvious downward trends in precipitation, during 2000–2019 there was a slight positive trend in three of five alliance groups, though none were statistically significant (p-value < 0.05) during the study (Figure 25). Average annual temperature declined, although not significantly, during the study period (Appendix A). The slight increase in precipitation and decrease in temperature resulted in a corresponding increase in AET of about 1 millimeter per year in four of five alliance groups, although the increase was not significant in any alliance group. The effect of these seemingly small changes was important, as illustrated by the significant upward trends in production in some of the alliance groups shown in Section 3.3.

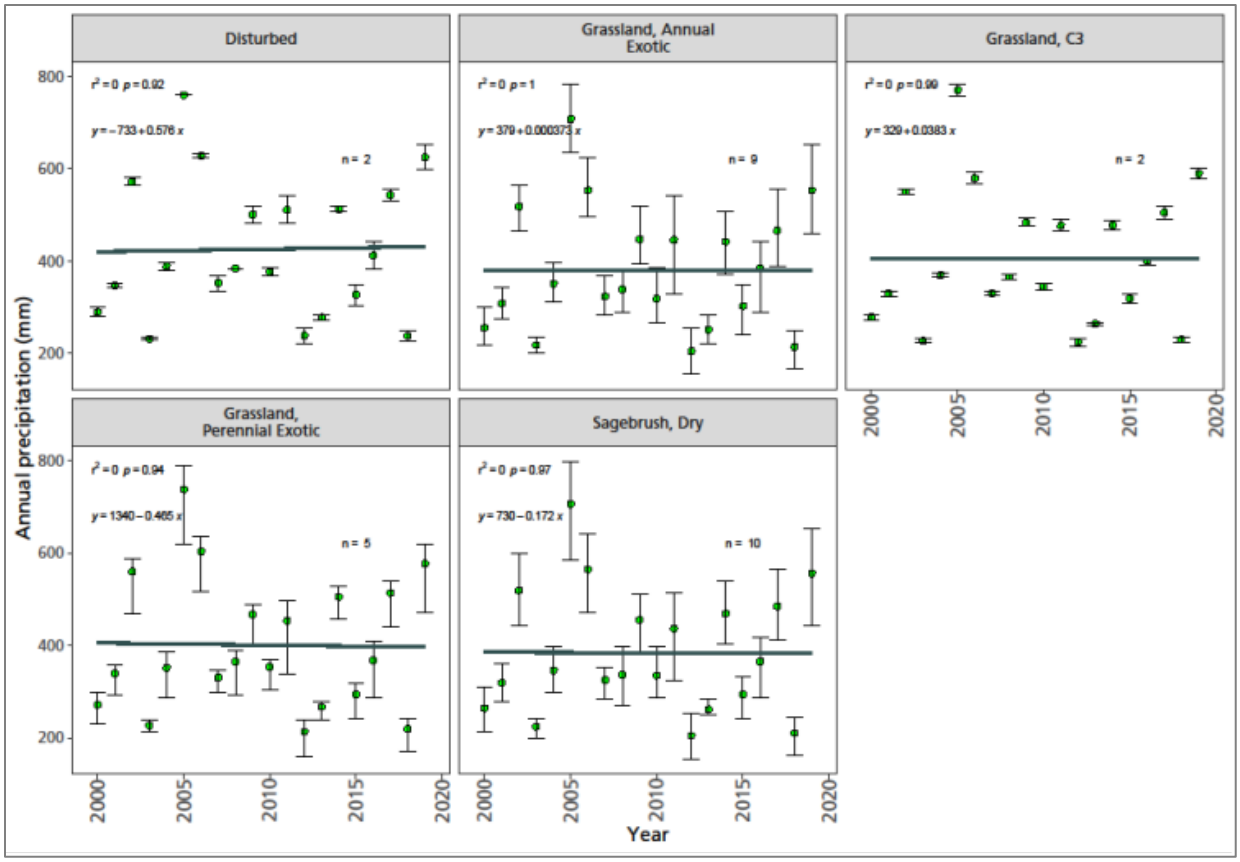


Figure 25. Annual precipitation trend over time, 2000–2019. Error bars are standard error.
NPS / DAVID THOMA

In other NCPN park units, an interesting decadal oscillation in precipitation was evident: peaks in the middle of each decade since 1980 translated to similar peaks in other water-balance variables. The same pattern was apparent in soil moisture, AET, and water deficit (Appendix A), although for deficit the peaks (maximum drought stress) coincided with the times of least precipitation (Appendix A). This pattern was evident at Golden Spike in peaks that occurred in 2005, 2017 and 2019. If the periodicity of these cycles continues in the future, it could serve as a useful guide for timing restoration efforts that require substantial planning, long-term investments, and multiple years of minimal drought stress for germination and establishment. It could also be useful in timing prescribed fires to achieve intended benefit without overly stressing vegetation persisting through a dry cycle.

4 Tools to Inform Near-Term Management

Tracking weather conditions that lead up to or surpass pivot points during the growing season is a useful climate-based tool for assessing vegetation condition—but it provides an indirect assessment. Additional tools can provide real-time assessments of vegetation condition by identifying both trends in vegetation greenness and the vegetation anomaly (a comparison of current growing conditions versus past conditions). With these tools, users can iteratively identify the spatial pattern and strength of trends and where disturbance or unusual events are happening in near-real time.[7]

Interpreting the link between those patterns and climate requires contemporaneous climate data. Gridded climate data used in this report were created from weather-station data, typically in the year following a full year of data collected at weather stations. Weather-station data are better suited to investigations of real-time change in conditions, especially extreme events that garner interest as they happen or soon after—as was the case when park managers noted juniper mortality in 2018 and 2019.

The NCPN supports ClimateAnalyzer.org, which makes accessing weather-station data intuitive and easy. Data from the park weather station and other sources can be used to determine how weather and vegetation condition vary together in near real-time. This could be the basis for real-time condition assessments used in the tactical decisions needed to achieve long-range management goals. Care must be taken when analyzing trends from weather-station data due to missing values and outliers. Nevertheless, over the period analyzed in this report, the upward trend in station precipitation and no-trend in average temperature were consistent with the trends found using Daymet, the gridded climate data used in analysis for this report.

[7] More information on these tools can be obtained from the author of this report.

5 Conclusions

Since 2000, a very dry period, growing-season primary production has increased in all alliance groups in Golden Spike NHP. The increase coincided with a slight increase in precipitation and a slight decrease in temperature over the same period. However, over this period, there were dry years and dry periods extending for several years resulting in substantial declines in vegetation cover which largely rebounded by the end of the study.

The variation in vegetation condition across wet and dry years was evaluated to identify which alliance groups were most tolerant of low annual precipitation (Perennial Exotic Grassland), and which were least sensitive to variation in precipitation (Disturbed areas). The climate variable most strongly correlated with vegetation production was three years of soil moisture. Over the study period, the start of the growing season shifted earlier and the end of growing season later. However, perhaps due to variability or disturbance (fire, weed control or other land use), changes in the length of the growing season should be interpreted carefully. Precipitation, actual evapotranspiration, growing degree days, and day of snowmelt were the primary determinants of green-up timing.

The variation in weather conditions and corresponding vegetation response provide a window into the past that will inform understanding and management of vegetation that has always, and will continue to, respond to climate at Golden Spike NHP. Much of the information in this report will soon be outdated. Even so, some of the findings described here have long-term value and are unlikely to change until vegetation composition changes in the future, such as pivot points and sensitivity of vegetation to weather and climate—because drought tolerance and response to weather are factors inherent to the natural history traits of vegetation and where it grows. At the same time, climate is changing rapidly, and extreme weather events are becoming more frequent. The tools developed for these analyses can help National Park Service managers anticipate and plan for changes in climate—and manage change as it happens. This report demonstrates how combining satellite observations of vegetation condition with climate data can help determine the right time and place for near-term action to help achieve long-range management goals for stewarding park resources through continuous change.

6 Literature Cited

Aikens, E. O., M. J. Kauffman, J. A. Merkle, S. P. H. Dwinnell, G. L. Fralick, and K. L. Monteith. 2017. The greenscape shapes surfing of resource waves in a large migratory herbivore. Ecology Letters. https://doi.org/10.1111/ele.12772

Allen, C. D., D. D. Breshears, and N. G. McDowell. 2015. On underestimation of global vulnerability to tree mortality and forest die-off from hotter drought in the Anthropocene. Ecosphere 6. https://doi.org/10.1890/ES15-00203.1

Barger, N. N., S. R. Archer, J. L. Campbell, C. Huang, J. A. Morton, and A. K. Knapp. 2011. Woody plant proliferation in North American drylands: a synthesis of impacts on ecosystem carbon balance. Journal of Geophysical Research: Biogeosciences 116: 1–17. https://doi.org/10.1029/2010JG001506

Barnes, M. L., M. S. Moran, R. L. Scott, T. E. Kolb, G. E. Ponce-Campos, D. L. P. Moore, M. A. Ross, B. Mitra, and S. Dore. 2016. Vegetation productivity responds to sub-annual climate conditions across semi-arid biomes. Ecosphere 7: 1–20. https://doi.org/10.1002/ecs2.1339

Bisigato, A. J., L. Hardtke, and H. F. del Valle. 2013. Soil as a capacitor: Considering soil water content improves temporal models of productivity. Journal of Arid Environments 98: 88–92. https://doi.org/10.1016/j.jaridenv.2013.08.004

Bradford, J. B., D. R. Schlaepfer, and W. K. Lauenroth. 2014. Ecohydrology of adjacent sagebrush and lodgepole pine ecosystems: the consequences of climate change and disturbance. Ecosystems 17: 590–605. https://doi.org/10.1007/s10021-013-9745-1

Breiman, L. 2001. Random forests. Machine Learning 45: 5–32. https://doi.org/10.1201/9780367816377-11

Bunting, E. L., S. M. Munson, and J. B. Bradford. 2019. Assessing plant production responses to climate across water-limited regions using Google Earth Engine. Remote Sensing of Environment 233: 111379. https://doi.org/10.1016/j.rse.2019.111379

Coles, J., A. Wight, J. Von Loh, K. Schulz, and A. Evenden. 2011. Vegetation classification and mapping project report, Golden Spike National Historic Site. Natural Resource Technical Report. NPS/NCPN/NRTR—2011/508. National Park Service, Natural Resource Stewardship and Science. Fort Collins, Colorado https://irma.nps.gov/DataStore/Reference/Profile/2180896

de Beurs, K. M., and G. M. Henebry. 2010. Spatio-temporal statistical methods for modelling land surface phenology. In Phenological research: Methods for environmental and climate change analysis, edited by I. L. Hudson and M. R. Keatley, 177–208. Springer Science+Business Media BV. https://doi.org/10.1007/978-90-481-3335-2

Didan, K., A. B. Munoz, R. Solano, and A. Huete. 2015. MODIS vegetation index user's guide (Collection 6). University of Arizona, Tucson, AZ.

Dunn, H. A., and K. M. de Beurs. 2011. Land surface phenology of North American mountain environments using moderate resolution imaging spectroradiometer data. Remote Sensing of Environment 115(5): 1220–1233. https://doi.org/10.1016/j.rse.2011.01.005

Federal Geographic Data Committee (FGDC). 2008. National Vegetation Classification Standard. Version 2. U.S. Geological Survey, Reston, VA. http://usnvc.org/wp-content/uploads/2011/02/NVCS_V2_FINAL_2008-02.pdf

Forkel M. 2015. greenbrown - land surface phenology and trend analysis. https://greenbrown.r-forge.r-project.org/

Forkel, M., N. Carvalhais, J. Verbesselt, M. Mahecha, C. S. R. Neigh, and M. D. Reichstein. 2013. Trend change detection in NDVI Timeseries: effects of inter-annual variability and methodology. Remote Sensing 5(5): 2113–2144. https://doi.org/10.3390/rs5052113

Fu, Y., H. Zhang, W. Dong, and W. Yuan. 2014. Comparison of phenology models for predicting the onset of growing season over the northern hemisphere. PLoS ONE 9(10): e109544. https://doi.org/10.1371/journal.pone.0109544

Garroutte, E., A. Hansen, and R. Lawrence. 2016. Using NDVI and EVI to map spatiotemporal variation in the biomass and quality of forage for migratory elk in the Greater Yellowstone Ecosystem. Remote Sensing 8(5):404. https://doi.org/10.3390/rs8050404

Gremer, J. R., C. Andrews, J. R. Norris, L. P. Thomas, S. M. Munson, M. C. Duniway, and J. B. Bradford. 2018. Increasing temperature seasonality may overwhelm shifts in soil moisture to favor shrub over grass dominance in Colorado Plateau drylands. Oecologia 188: 1195–1207. https://doi.org/10.1007/s00442-018-4282-4

Grossiord, C., T. N. Buckley, L. A. Cernusak, K. A. Novick, B. Poulter, R. T. W. Siegwolf, J. S. Sperry, and N. G. McDowell. 2020. Plant responses to rising vapor-pressure deficit. New Phytologist 226: 1550–1566. https://doi.org/10.1111/nph.16485

Huete, A. R. 1988. A soil-adjusted vegetation index (SAVI). Remote Sensing of Environment 25(3): 295–309. https://doi.org/10.1016/0034-4257(88)90106-X

Jennings, M. D., D. Faber-Langendoen, O. L. Loucks, R. K. Peet, and D. Roberts. 2009. Standards for associations and alliances of the US National Vegetation Classification. Ecological Monographs 79: 173–199. https://doi.org/10.1890/07-1804.1

Johnson, H. E., D. D. Gustine, T. S. Golden, L. G. Adams, L. S. Parrett, E. A. Lenart, and P. S. Barboza. 2018. NDVI exhibits mixed success in predicting spatiotemporal variation in caribou summer forage quality and quantity. Ecosphere 9(7): e02361. https://doi.org/10.1002/ecs2.2461

Kariyeva, J., and W. J. D. van Leeuwen. 2011. Environmental drivers of NDVI-based vegetation phenology in Central Asia. Remote Sensing 3(2): 203–246. https://doi.org/10.3390/rs3020203

Lauenroth, W. K., and J. B. Bradford. 2009. Ecohydrology of dry regions of the United States: Precipitation pulses and intraseasonal drought. Ecohydrology 2: 173–181. https://doi.org/10.1002/eco.53

Lauenroth, W. K., and J. B. Bradford. 2012. Ecohydrology of dry regions of the United States: water balance consequences of small precipitation events. Ecohydrology 5: 46–53. https://doi.org/10.1002/eco.195

McMaster, G. S., and W. W. Wilhelm. 1997. Growing degree days: one equation, two interpretations. Agricultural and Forest Meteorology 87(4):291–300. https://doi.org/10.1016/S0168-1923(97)00027-0

Mendez-Barroso, L. A., E. R. Vivoni, C. J. Watts, and J. C. Rodriguez. 2009. Seasonal and interannual relations between precipitation, surface soil moisture and vegetation dynamics in the North American monsoon region. Journal of Hydrology 377(1–2): 59–70. https://doi.org/10.1016/j.jhydrol.2009.08.009

Merkle, J. A., K. L. Monteith, E. O. Aikens, M. M. Hayes, K. R. Hersey, A. D. Middleton, B. A. Oates, H. Sawyer, B. M. Scurlock, and M. J. Kauffman. 2016. Large herbivores surf waves of green-up during spring. Proceedings of the Royal Society B: Biological Sciences 283: 1–8. https://doi.org/10.1098/rspb.2016.0456

Moore, L. M., W. K. Lauenroth, D. M. Bell, and D. R. Schlaepfer. 2015. Soil water and temperature explain canopy phenology and onset of spring in a semiarid steppe. Great Plains Research. https://doi.org/10.1353/gpr.2015.0027

Munson, S. M. 2013. Plant responses, climate pivot points, and trade-offs in water-limited ecosystems. Ecosphere 4(9): 1–15. https://doi.org/10.1890/ES13-00132.1

Munson, S. M., M. C. Duniway, and J. K. Johanson. 2016. Rangeland monitoring reveals long-term plant responses to precipitation and grazing at the landscape scale. Rangeland Ecological Management 69(1): 76–83.

Munson, S. M., R. H. Webb, J. Belnap, J. A. Hubbard, D. E. Swann, and S. Rutman. 2011. Forecasting climate change impacts to plant community composition in the Sonoran Desert region. Global Change Biology 18(3): 1083–1095. https://doi.org/10.1111/j.1365-2486.2011.02598.x

Munson, S. M., R. H. Webb, D. C. Housman, K. E. Veblen, K. E. Nussear, E. A. Beever, K. B. Hartney, M. N. Miriti, S. L. Phillips, R. E. Fulton, and N. G. Tallent. 2015. Long-term plant responses to climate are moderated by biophysical attributes in a North American desert. Journal of Ecology 103(3): 657–668. https://doi.org/10.1111/1365-2745.12381

National Park Service (NPS), Northern Colorado Plateau Network (NCPN). 2025. Supplemental tables for report on landscape phenology, vegetation condition, and relations with climate at Golden Spike National Historical Park, 2000–2019. National Park Service. https://irma.nps.gov/DataStore/Reference/Profile/2311149

Natural Resources Conservation Service (NRCS). 2015. Web Soil Survey. U.S. Department of Agriculture. http://websoilsurvey.nrcs.usda.gov

Norris, J. R., and J. J. Walker. 2020. Solar and sensor geometry, not vegetation response, drive satellite NDVI phenology in widespread ecosystems of the western United States. Remote Sensing of Environment 249: 112013. https://doi.org/10.1016/j.rse.2020.112013

Noy-Meir, I. 1973. Desert Ecosystems: environment and producers. Annual Review of Ecology and Systematics 4: 25–51. https://doi.org/10.1146/annurev.es.04.110173.000325

Oudin, L., F. Hervieu, C M, C. Perrin, V. Andréassian, F. Anctil, and C. Loumagne. 2005. Which potential evapotranspiration input for a lumped rainfall-runoff model? Part 2 - Towards a simple and efficient potential evapotranspiration model for rainfall-runoff modelling. Journal of Hydrology 303(1–4): 290–306. https://doi.org/10.1016/j.jhydrol.2004.08.026

Paruelo, J. M., M. Oesterheld, C. M. Di Bella, M. Arzadum, J. Lafontaine, M. Cahuepé, and C. M. Rebella. 2000. Estimation of primary production of subhumid rangelands from remote sensing data. Applied Vegetation Science 3(2): 189–195. https://doi.org/10.2307/1478997

Qi, J., A. Chehbouni, A. R. Huete, Y. H. Kerr, and S. Sorooshian. 1994. A modified soil adjusted vegetation index. Remote Sensing of Environment 48(2): 119–126. https://doi.org/10.1016/0034-4257(94)90134-1

Reed, B. C., J. F. Brown, D. VanderZee, T. R. Loveland, J. W. Merchant, and D. O. Ohlen. 1994. Measuring phenological variability from satellite imagery. Journal of Vegetation Science 5(5): 703–714. https://doi.org/10.2307/3235884

Sala, O. E., L. A. Gherardi, L. Reichmann, E. Jobbágy, and D. Peters. 2012. Legacies of precipitation fluctuations on primary production: theory and data synthesis. Philosophical Transactions of the Royal Society B: Biological Sciences 367(1606): 3135–3144. https://doi.org/10.1098/rstb.2011.0347

Schlaepfer, Daniel R., William K. Lauenroth, and John B. Bradford. 2014. Modeling regeneration responses of big sagebrush (*Artemisia tridentata*) to abiotic conditions. Ecological Modelling 286. https://doi.org/10.1016/j.ecolmodel.2014.04.021

Seager, R., A. Hooks, A. P. Williams, B. Cook, J. Nakamura, and N. Henderson. 2015. Climatology, variability, and trends in the U.S. vapor-pressure deficit, an important fire-related meteorological quantity. Journal of Applied Meteorology and Climatology 54(6): 1121–1141. https://doi.org/10.1175/JAMC-D-14-0321.1

Sorokin, Y., T. J. Zelikova, D. Blumenthal, D. G. Williams, and E. Pendall. 2017. Seasonally contrasting responses of evapotranspiration to warming and elevated CO_2 in a semi-arid grassland. Ecohydrology 10(7): e1880. https://doi.org/10.1002/eco.1880

St. Peter, J. R. 2015. A model for determining drivers of phenology in western United States rangelands. Master's thesis, University of Montana. Graduate Student Theses, Dissertations, and Professional Papers, no. 4444.

Stein, B. A., P. Glick, N. Edelson, and A. Staudg. 2014. Climate-smart conservation: putting adaption principles into practice. National Wildlife Federation, Washington, D.C.

Stephenson, N. L. 1990. Climatic control of vegetation distribution: the role of the water balance. The American Naturalist 135(5): 649–670. https://doi.org/10.1086/285067

Stephenson, N. L. 1998. Actual evapotranspiration and deficit: Biologically meaningful correlates of vegetation distribution across spatial scales. Journal of Biogeography 25(5): 855–870. https://doi.org/10.1046/j.1365-2699.1998.00233.x

Thoma, D., J. Norris, and P. Lauck. 2017. Satellite-based vegetation phenology and condition, and snow cover extent monitoring protocol for the Northern and Southern Colorado Plateau networks. Natural Resource Report NPS/SCPN/NRR–2017/1533. National Park Service, Fort Collins, CO. https://irma.nps.gov/DataStore/Reference/Profile/2246068

Thoma, D. P., D. W. Bailey, D. S. Long, G. A. Nielsen, M. P. Henry, M. C. Breneman, and C. Montagne. 2002. Short-term monitoring of rangeland forage conditions with AVHRR imagery. Journal of Range Management 55(4): 383–389. https://doi.org/10.2307/4003475

Thoma, D. P., M. T. Tercek, E. W. Schweiger, S. M. Munson, J. E. Gross, and S. T. Olliff. 2020. Water balance as an indicator of natural resource condition: case studies from Great Sand Dunes National Park and Preserve. Global Ecology and Conservation 24: e01300. https://doi.org/10.1016/j.gecco.2020.e01300

Thoma, D. P., S. M. Munson, and D. L. Witwicki. 2019. Landscape pivot points and responses to water balance in national parks of the southwest U.S. Journal of Applied Ecology 56(1): 157–167. https://doi.org/10.1111/1365-2664.13250

Thoma, D. P., S. M. Munson, K. M. Irvine, D. L. Witwicki, E. L. Bunting, and J. Paruelo. 2016. Semi-arid vegetation response to antecedent climate and water balance windows. Applied Vegetation Science 19(3): 413–429. https://doi.org/10.1111/avsc.12232

Thornton, P. E., M. M. Thornton, B. W. Mayer, Y. Wei, R. Devarakonda, R. S. Vose, and R. B. Cook. 2018. Daymet: Daily surface weather data on a 1-km grid for North America, version 3. Oak Ridge, TN: Oak Ridge National Laboratory, Distributed Active Archive Center.

van Wijk, R. E., A. Kölzsch, H. Kruckenberg, B. S. Ebbinge, G. J. D. Müskens, and B. A. Nolet. 2012. Individually tracked geese follow peaks of temperature acceleration during spring migration. Oikos 121(5): 655–664. https://doi.org/10.1111/j.1600-0706.2011.20083.x

Wang, C., J. Chen, Y. Tang, T. A. Black, and K. Zhu. 2018. A novel method for removing snowmelting-induced fluctuation in GIMMS NDVI3g data for vegetation phenology monitoring: A case study in deciduous forests of North America. IEEE Journal of Selected Topics in Applied Earth Observations and Remote Sensing 11(3): 800–807. https://doi.org/10.1109/JSTARS.2017.2778076

Witwicki, D. L., S. M. Munson, and D. P. Thoma. 2016. Effects of climate and water balance across grasslands of varying C3 and C4 grass cover. Ecosphere 7(11): 1–19. https://doi.org/10.1002/ecs2.1577

Workie, T. G., and H. J. Debella. 2018. Climate change and its effects on vegetation phenology across ecoregions of Ethiopia. Global Ecology and Conservation 13:e00366. https://doi.org/10.1016/j.gecco.2017.e00366

Yang, Y., T. Wu, S. Wang, J. Li, and F. Muhanmmad. 2019. The NDVI-CV method for mapping evergreen trees in complex urban areas using reconstructed Landsat 8 time-series data. Forests 10(2): 139. https://doi.org/10.3390/f10020139

7 Appendix A. Supplemental Figures for Landscape Phenology, Vegetation Condition, and Relations with Climate at Golden Spike National Historical Park, 2000–2019

Figures 26 to 68 contain information about the landscape phenology, vegetation condition, and relations with climate that were observed in Golden Spike National Historical Park during the study period from 2000 to 2019.

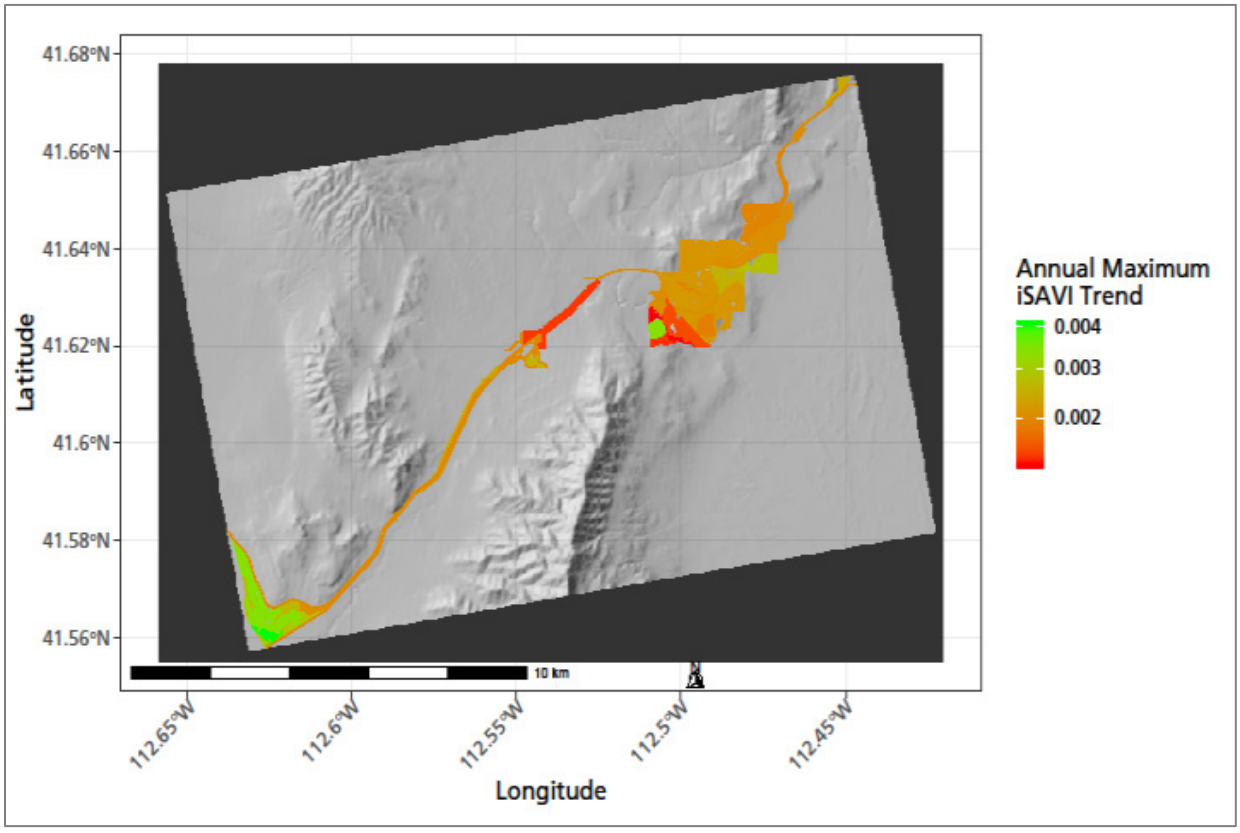


Figure 26. Spatial pattern of trends in maximum annual iSAVI. Trend is average change in iSAVI per year for the period 2000–2019.

NPS / DAVID THOMA

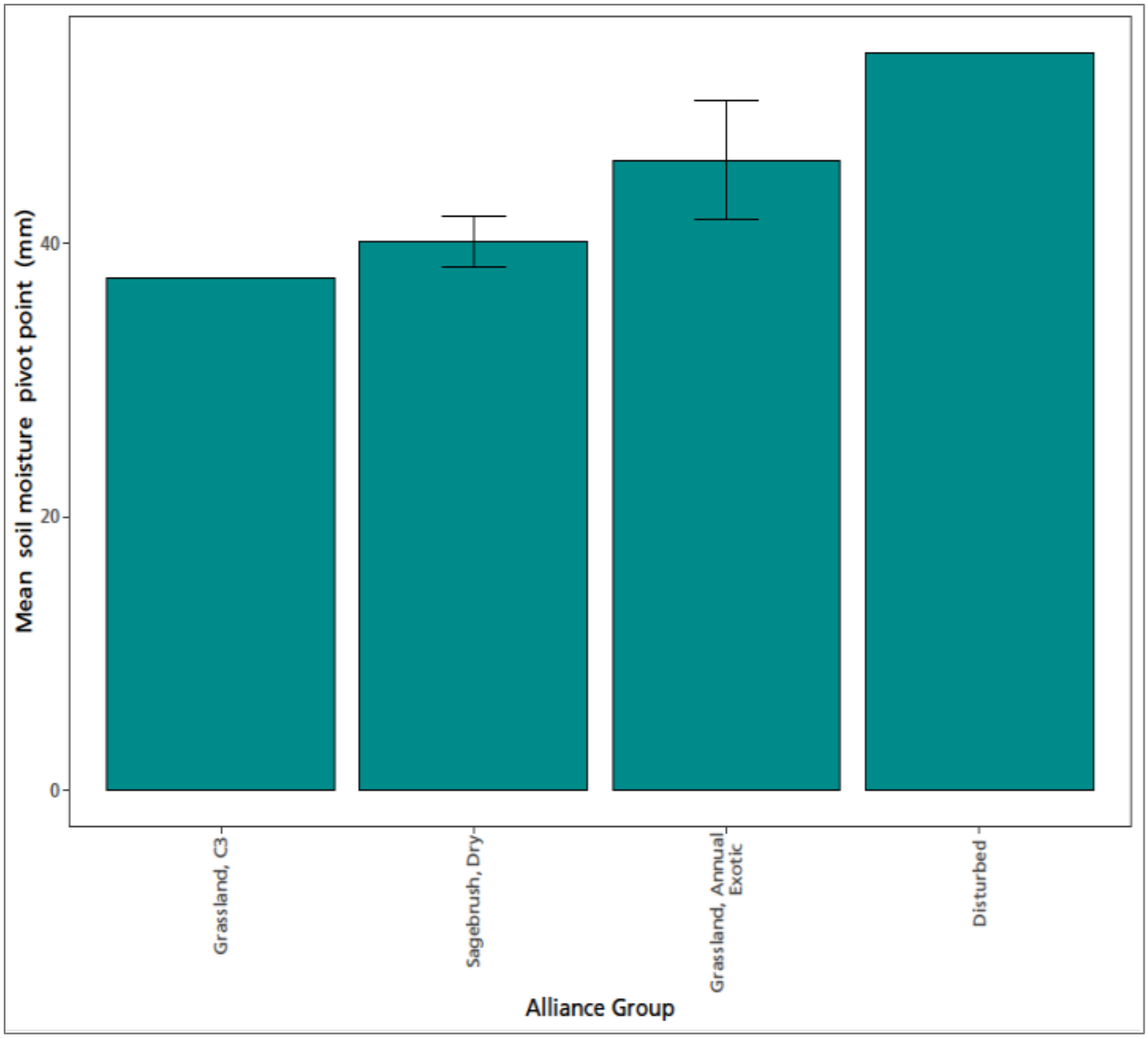


Figure 27. Pivot points for polygons where soil moisture was significantly related to interannual variation in production (p-value < 0.05). Climate data summarized by water year.

NPS / DAVID THOMA

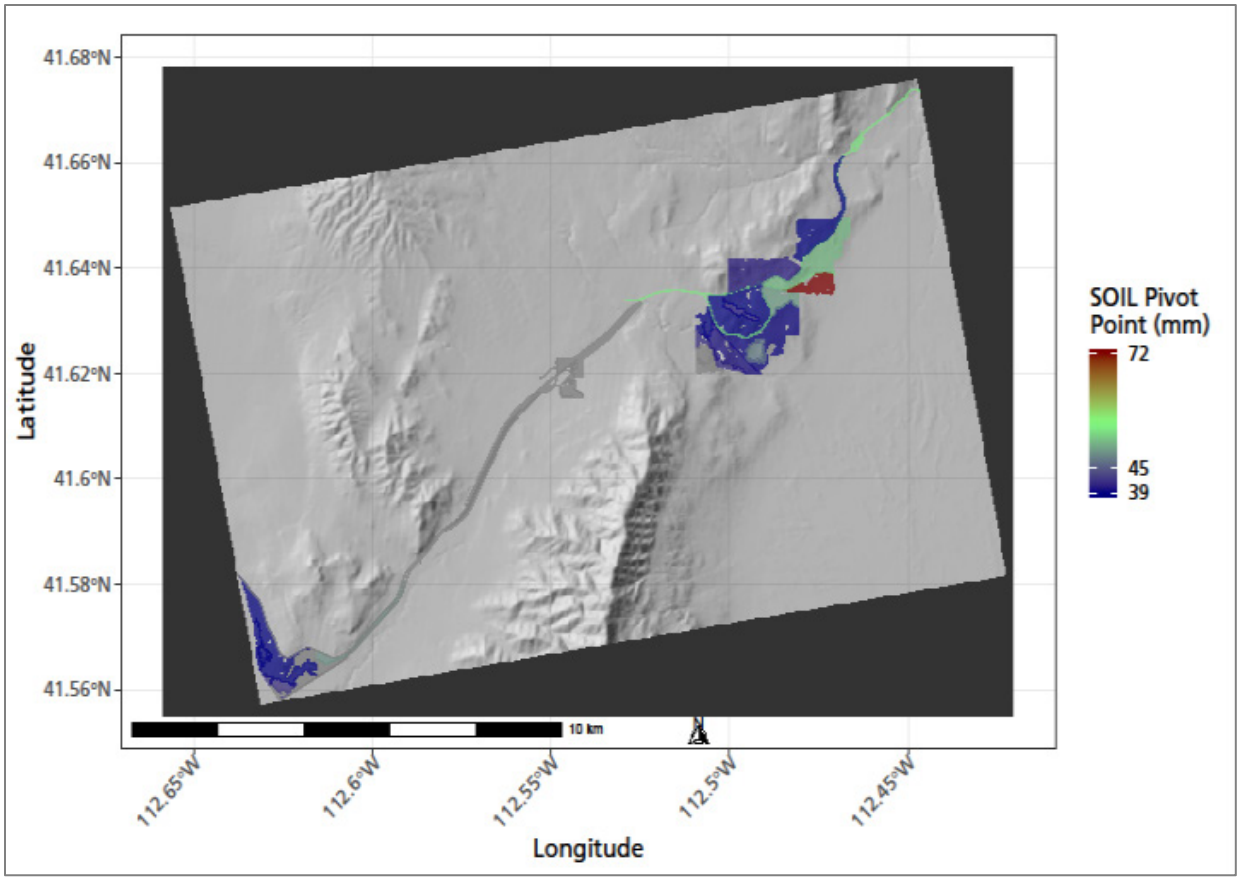


Figure 28. A map of Golden Spike NHP showing the locations of polygons where soil moisture was significantly related to interannual variation in production (p-value < 0.05). Climate data summarized by water year.

NPS / DAVID THOMA

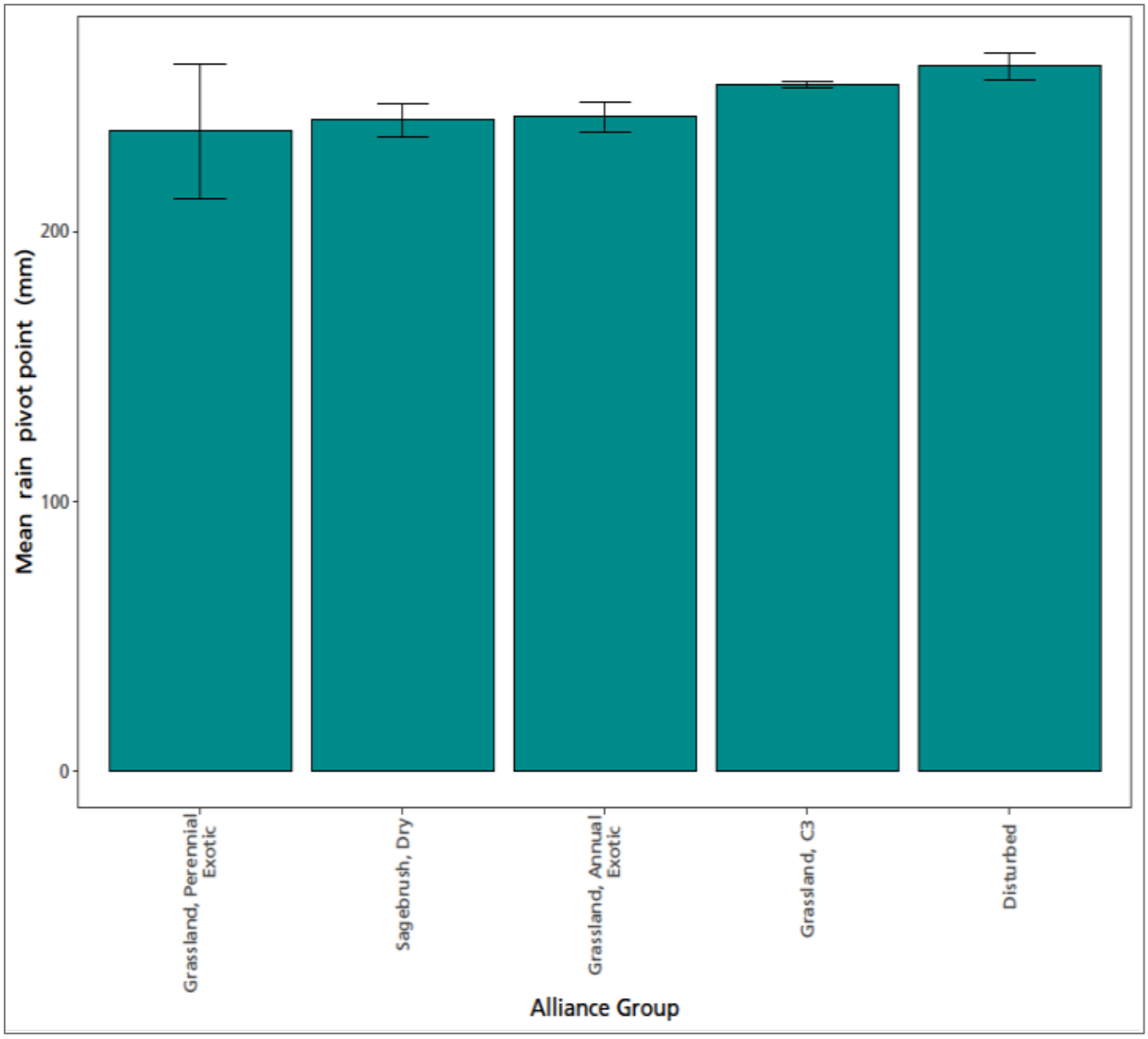


Figure 29. Pivot points for polygons where rain was significantly related to interannual variation in production (p-value < 0.05). Climate data summarized by water year.

NPS / DAVID THOMA

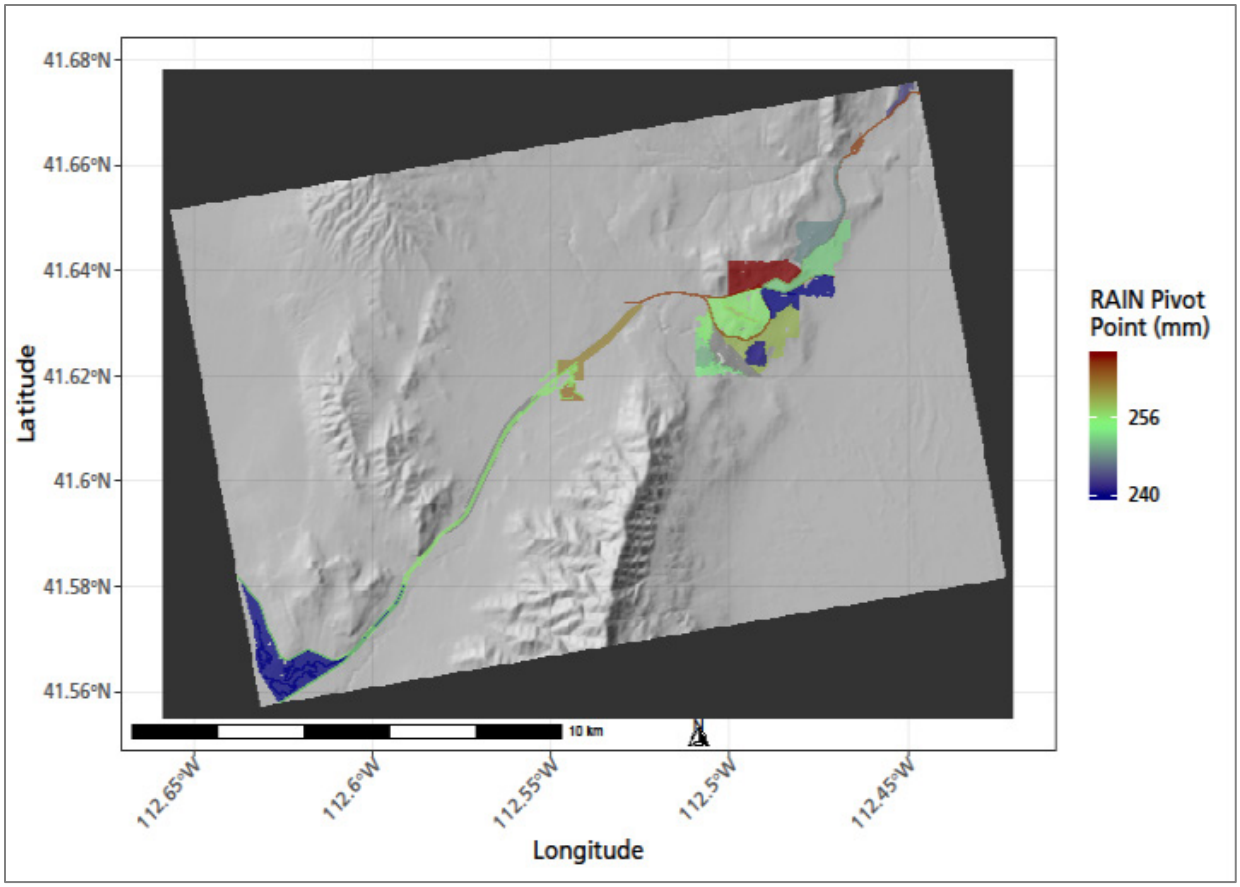


Figure 30. A map showing the locations of polygons where rain was significantly related to interannual variation in production (p-value < 0.05). Climate data summarized by water year.

NPS / DAVID THOMA

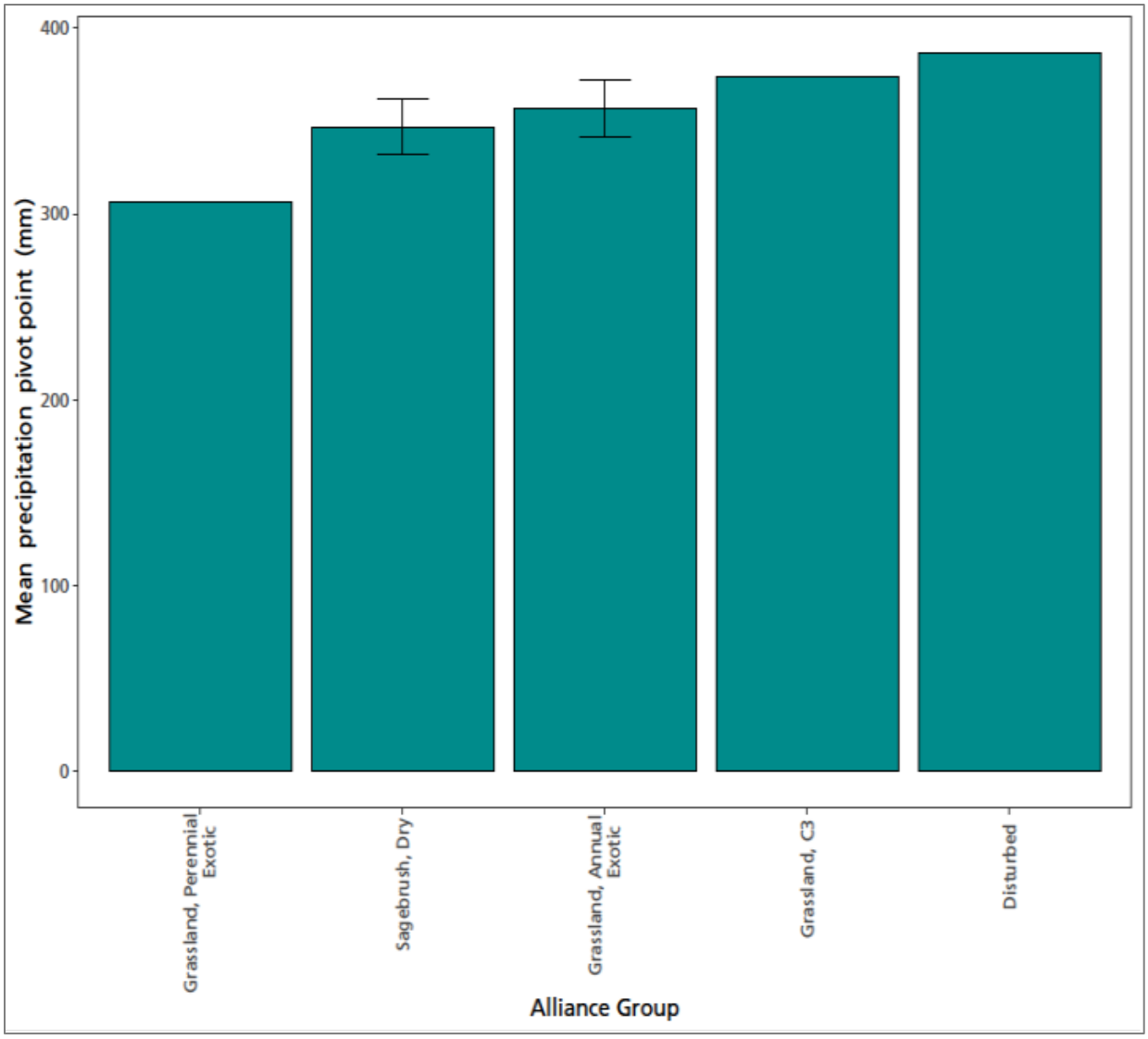


Figure 31. Pivot points for polygons where precipitation was significantly related to interannual variation in production (p-value < 0.05). Climate data summarized by water year.

NPS / DAVID THOMA

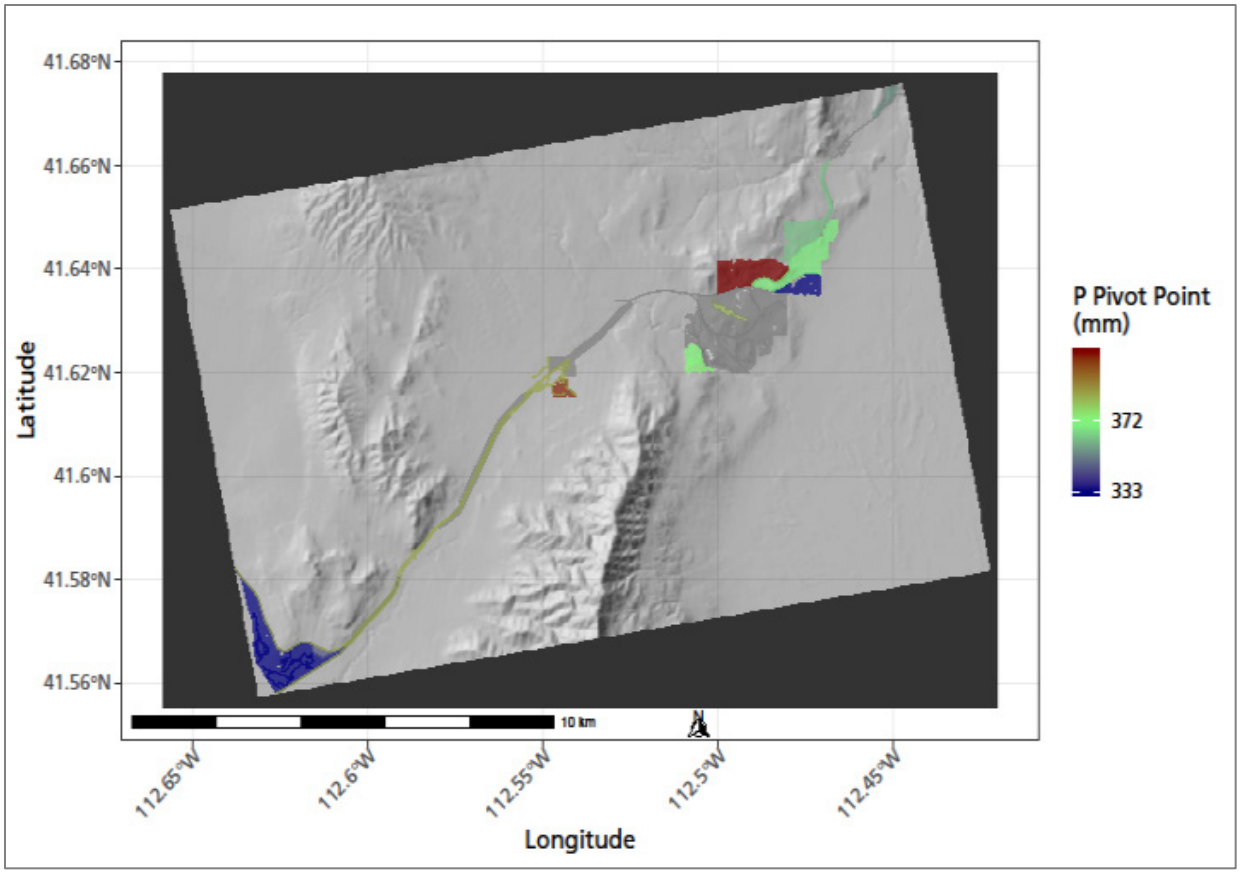


Figure 32. A map showing the locations of polygons where precipitation was significantly related to interannual variation in production (p-value < 0.05). Climate data summarized by water year.

NPS / DAVID THOMA

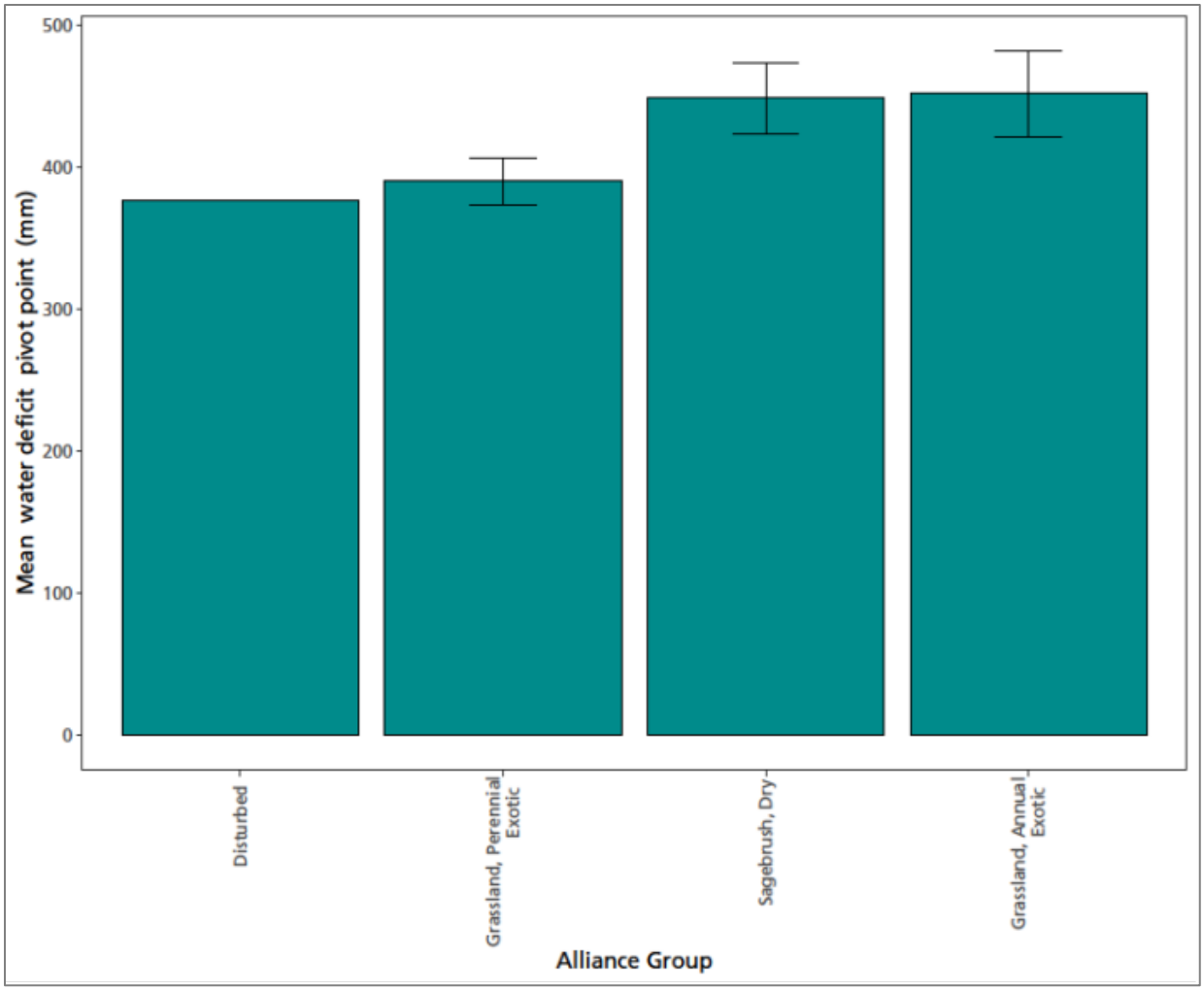


Figure 33. Pivot points for polygons where water deficit was significantly related to interannual variation in production (p-value < 0.05). Climate data summarized by water year.

NPS / DAVID THOMA

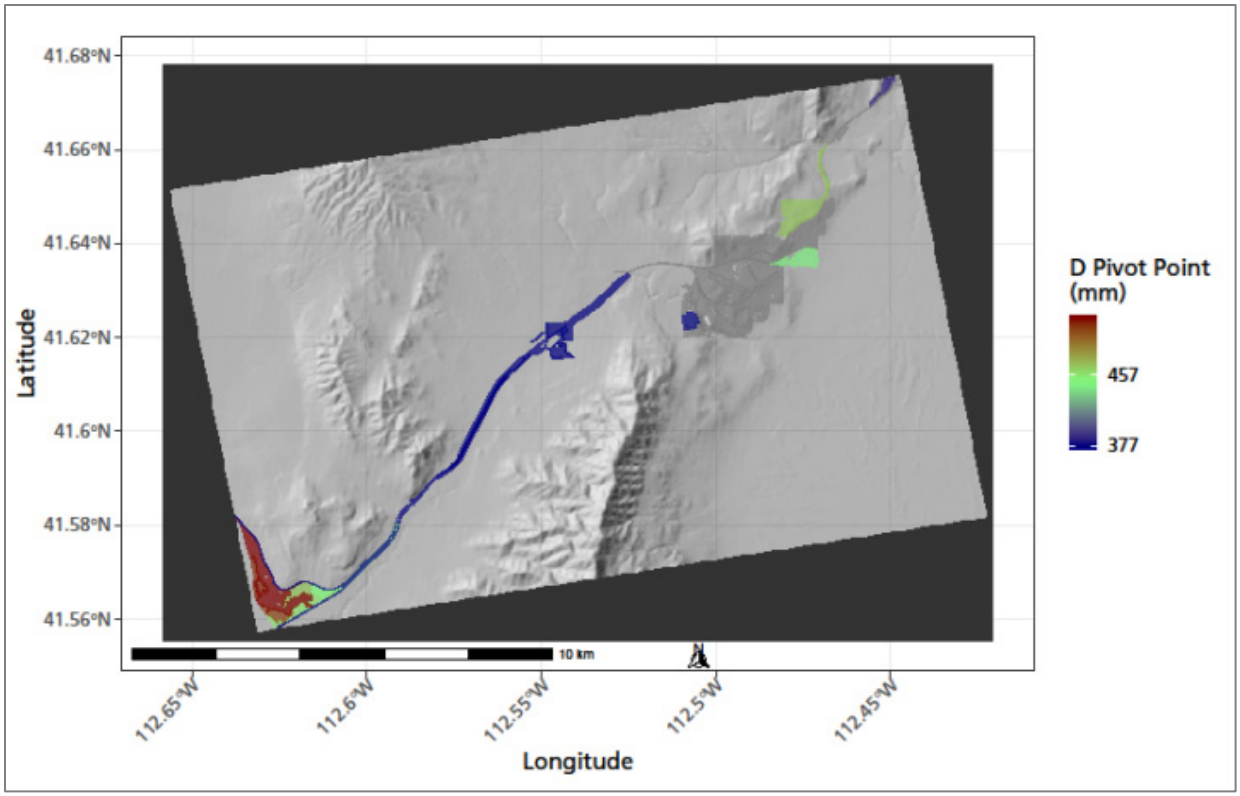


Figure 34. A map showing the locations of polygons where water deficit was significantly related to interannual variation in production (p-value < 0.05). Climate data summarized by water year.
NPS / DAVID THOMA

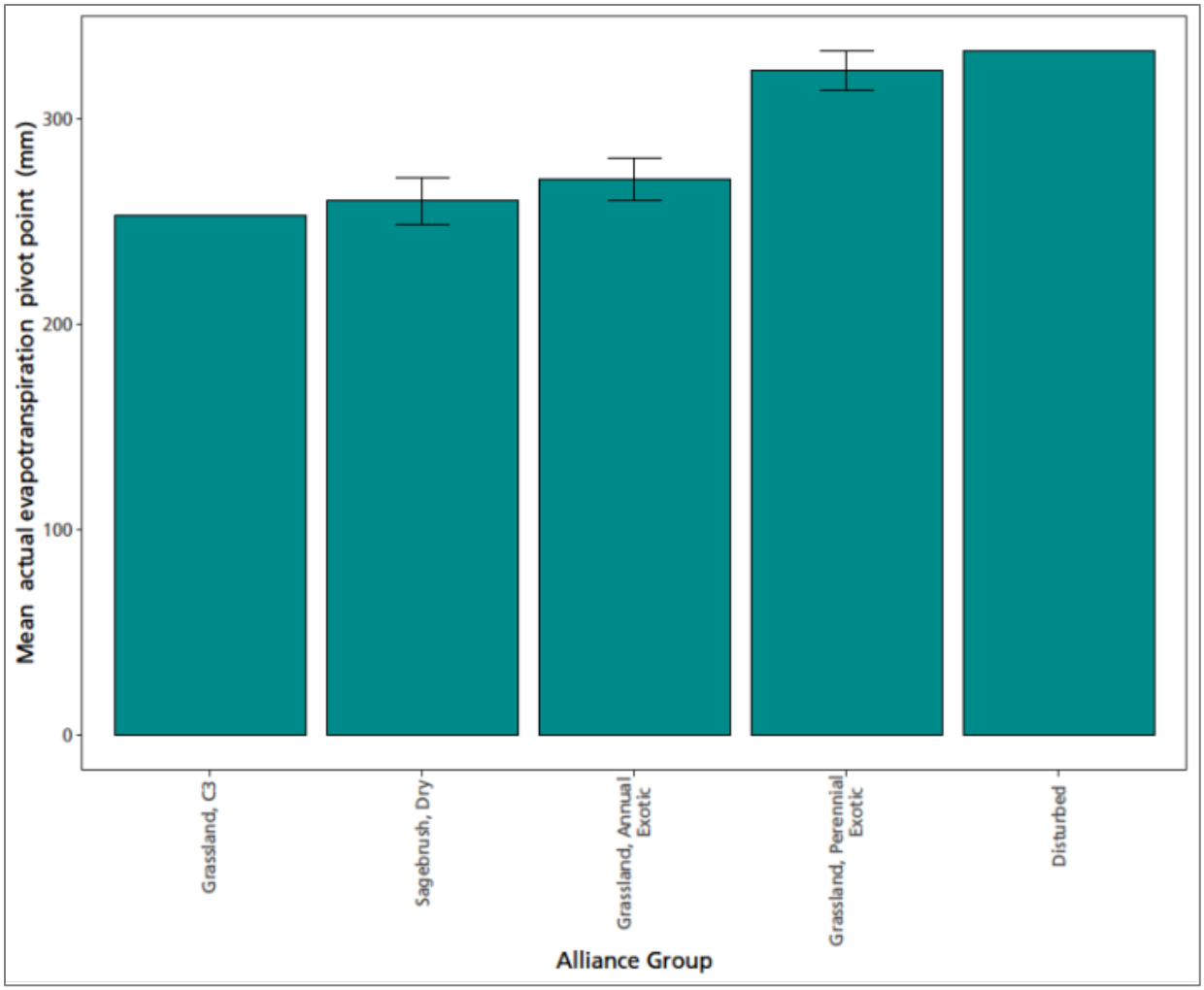


Figure 35. Pivot points for polygons where actual evapotranspiration was significantly related to interannual variation in production (p-value < 0.05). Climate data summarized by water year.
NPS / DAVID THOMA

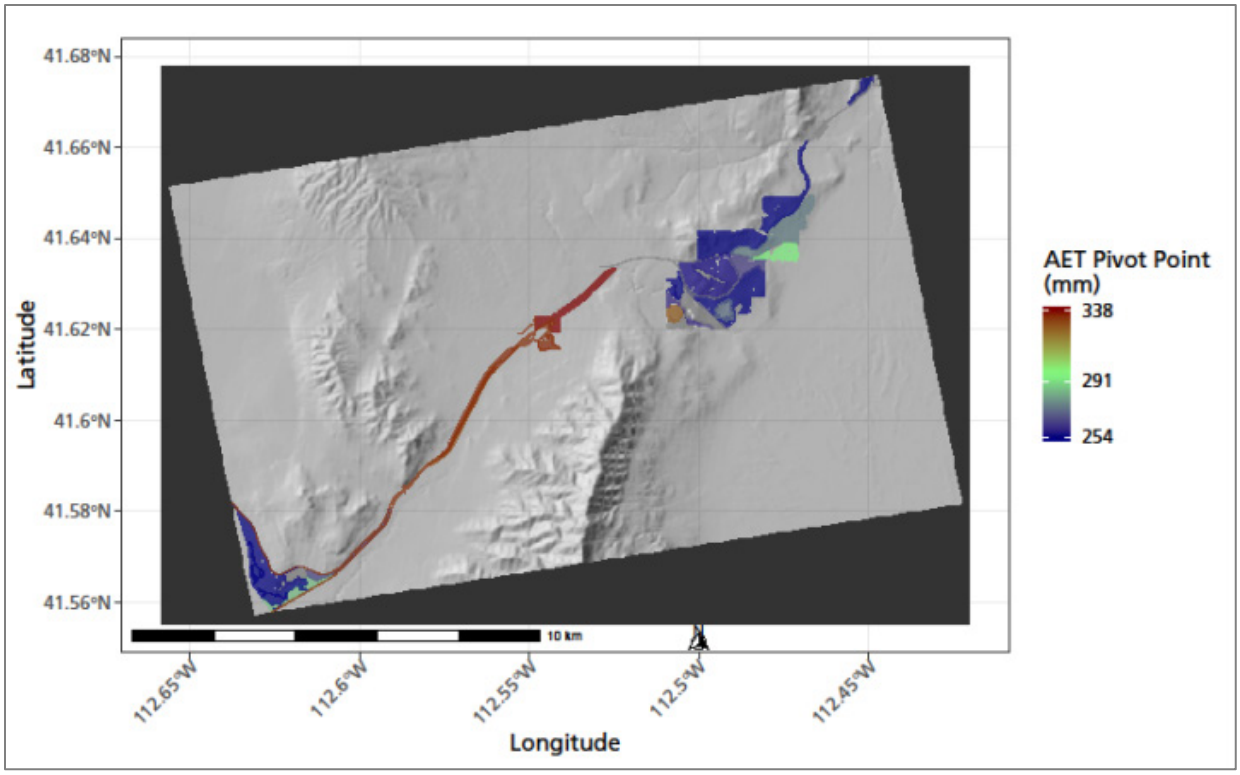


Figure 36. A map showing the locations of polygons where actual evapotranspiration was significantly related to interannual variation in production (p-value < 0.05). Climate data summarized by water year.
NPS / DAVID THOMA

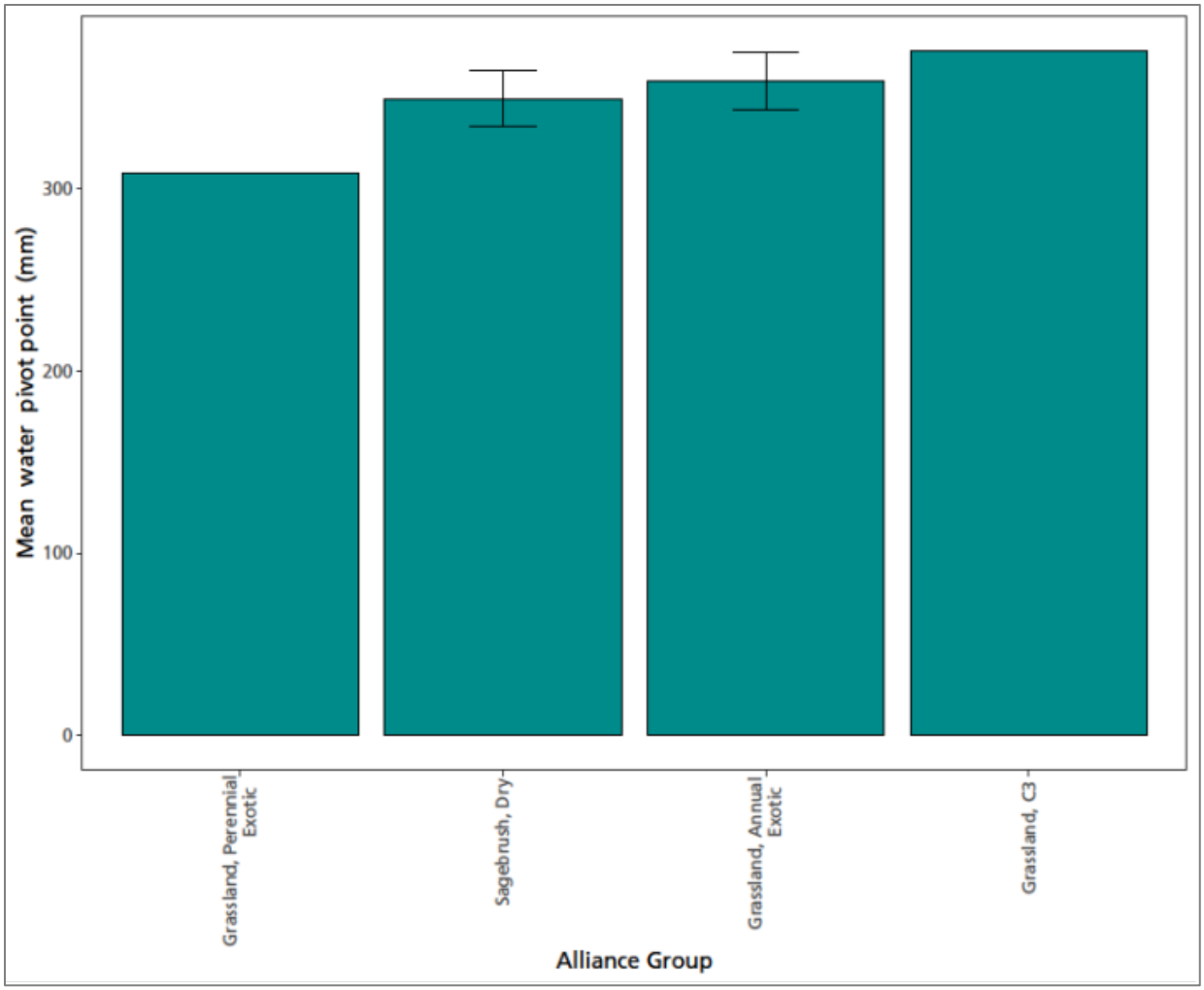


Figure 37. Pivot points for polygons where water was significantly related to interannual variation in production (p-value < 0.05). Climate data summarized by water year.

NPS / DAVID THOMA

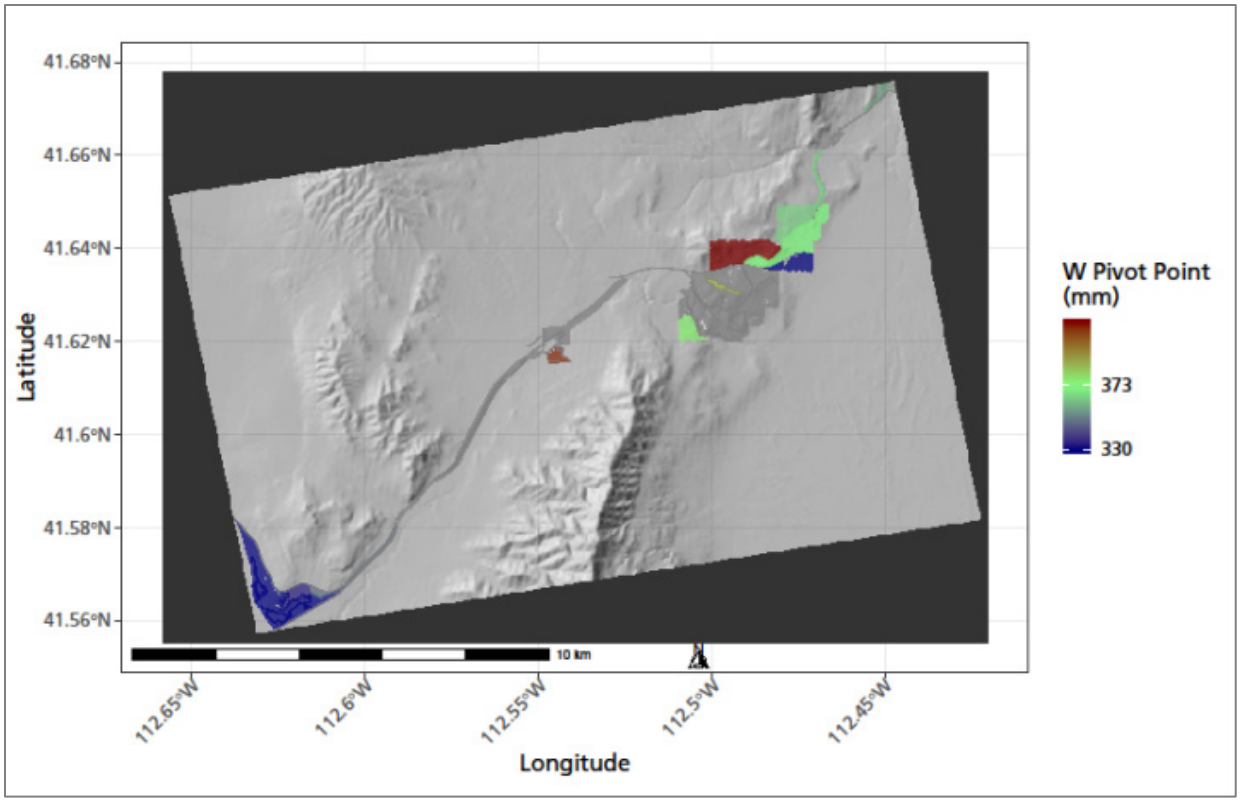


Figure 38. A map showing the locations of polygons where water was significantly related to interannual variation in production (p-value < 0.05). Climate data summarized by water year.

NPS / DAVID THOMA

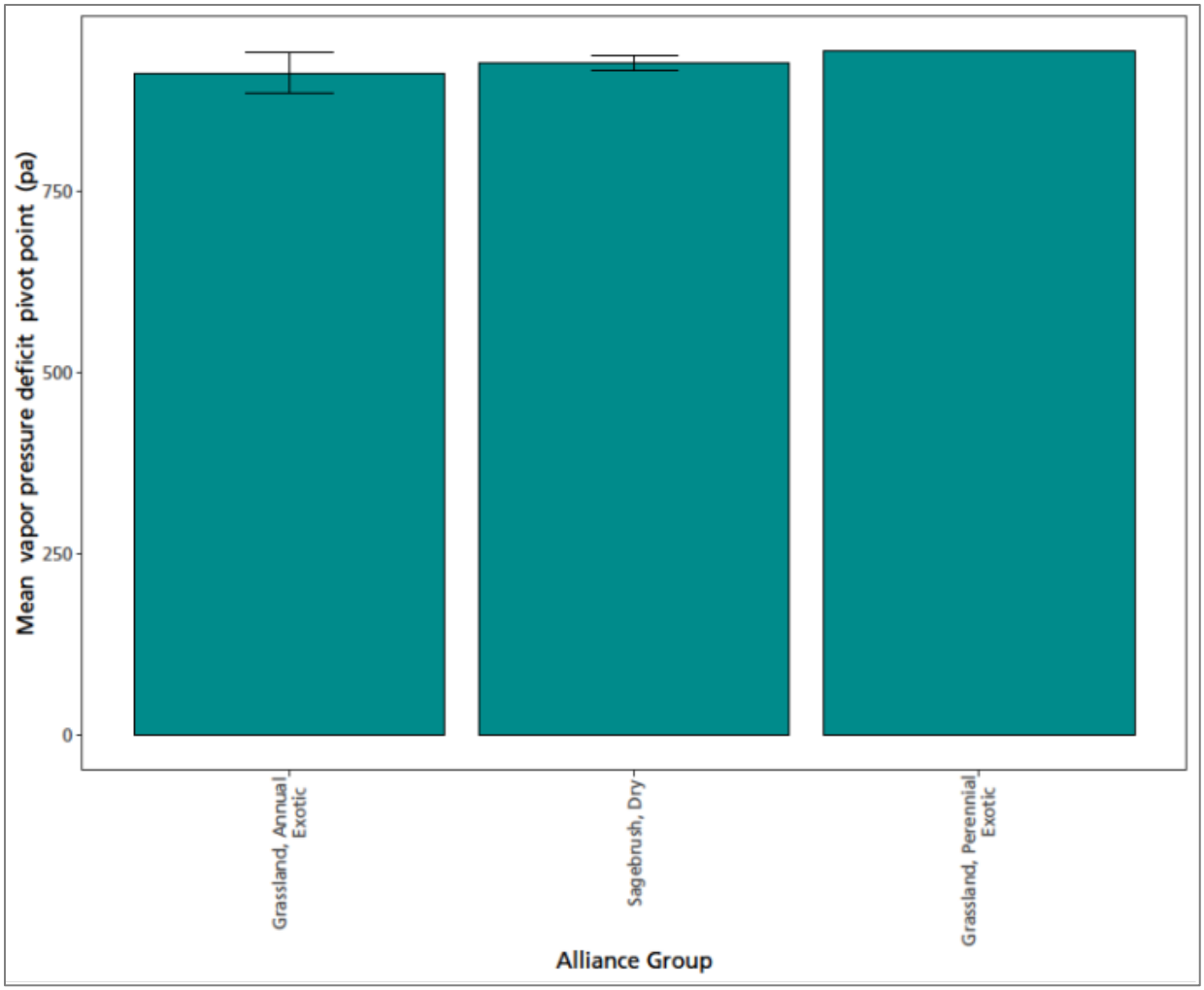


Figure 39. Pivot points for polygons where vapor pressure deficit was significantly related to interannual variation in production (p-value < 0.05). Climate data summarized by water year.

NPS / DAVID THOMA

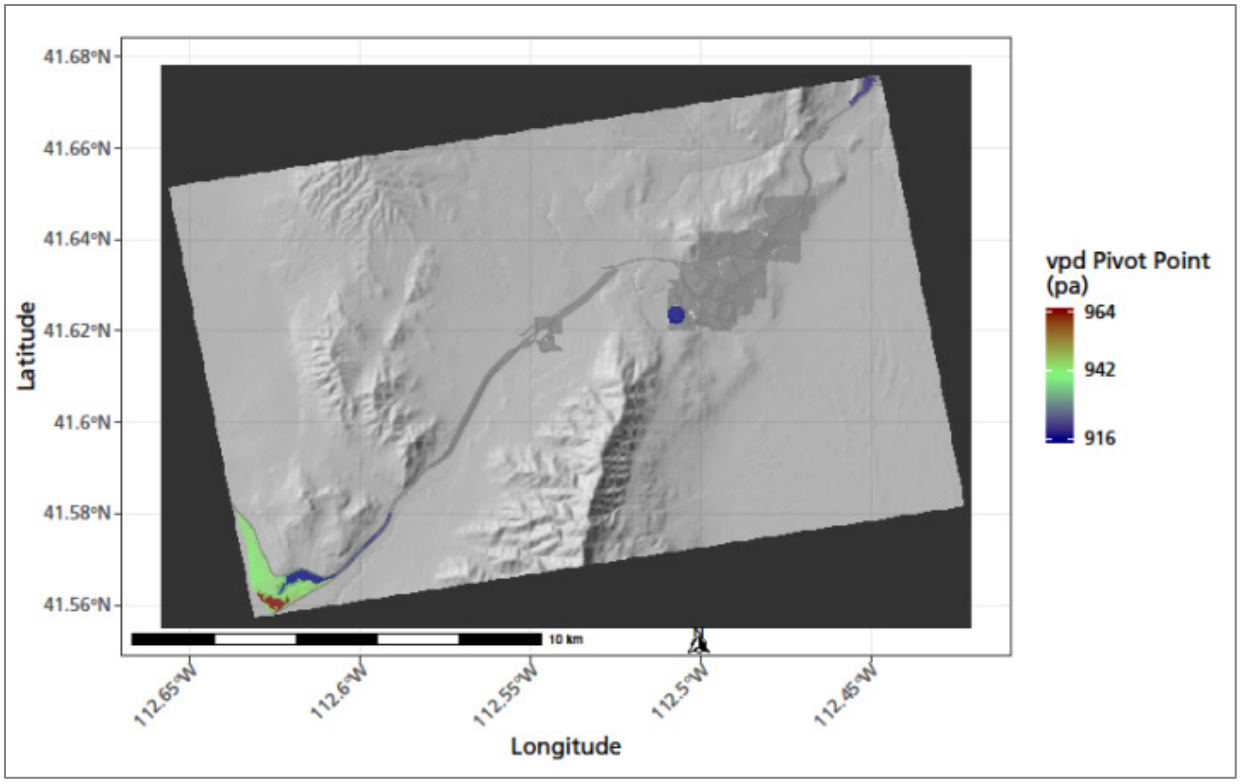


Figure 40. A map showing the locations of polygons where vapor pressure deficit was significantly related to interannual variation in production (p-value < 0.05). Climate data summarized by water year. *NPS / DAVID THOMA*

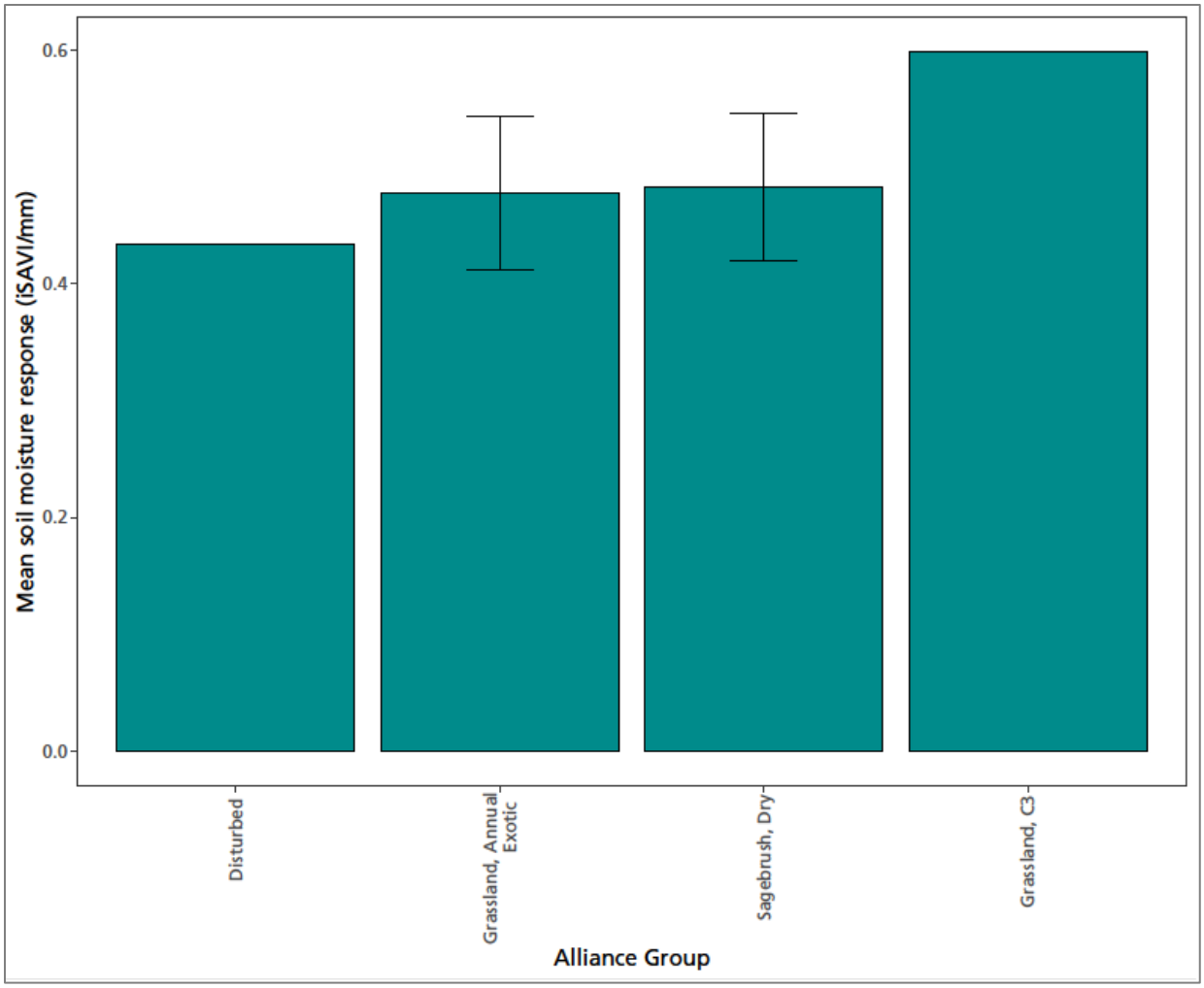


Figure 41. Sensitivity of growing season vegetation production to soil moisture in polygons, where the relationship was significant (p-value < 0.05). Climate data summarized by water year.

NPS / DAVID THOMA

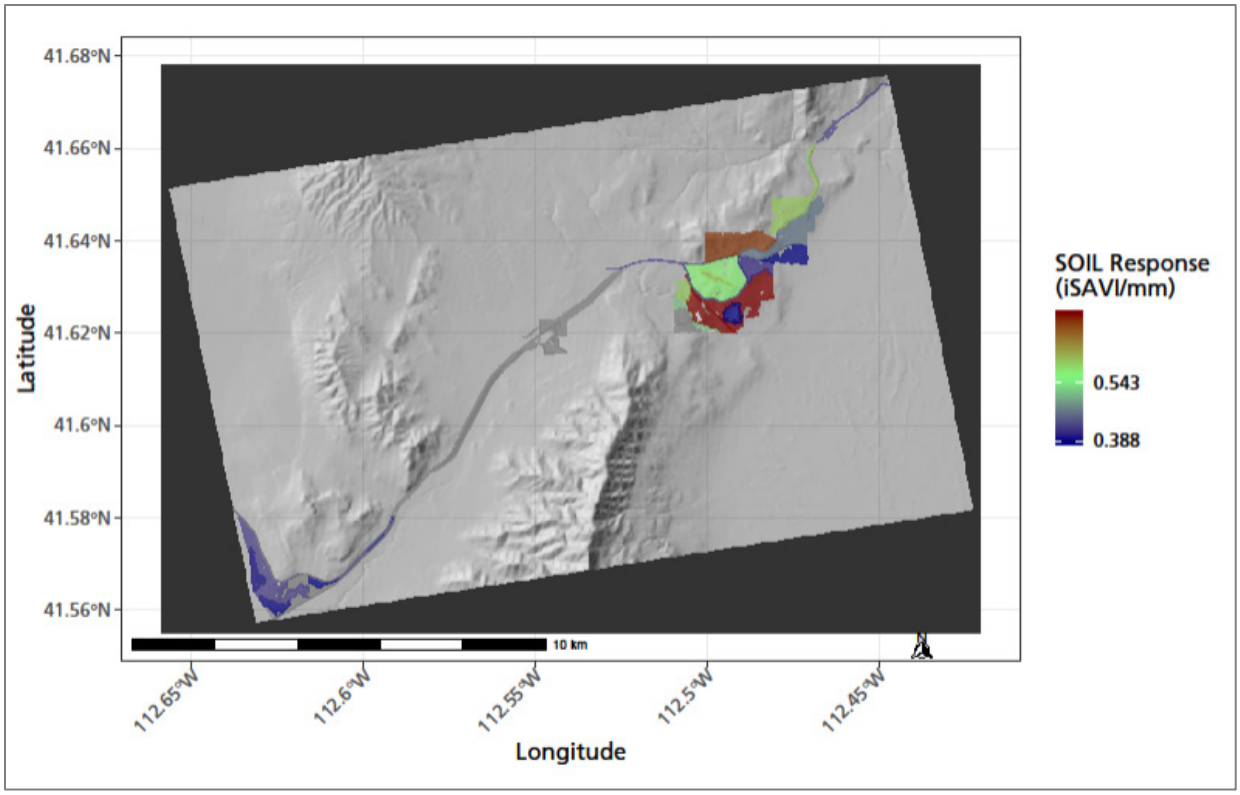


Figure 42. A map showing the sensitivity of growing season vegetation production to soil moisture in polygons, where the relationship was significant (p-value < 0.05). Climate data summarized by water year.

NPS / DAVID THOMA

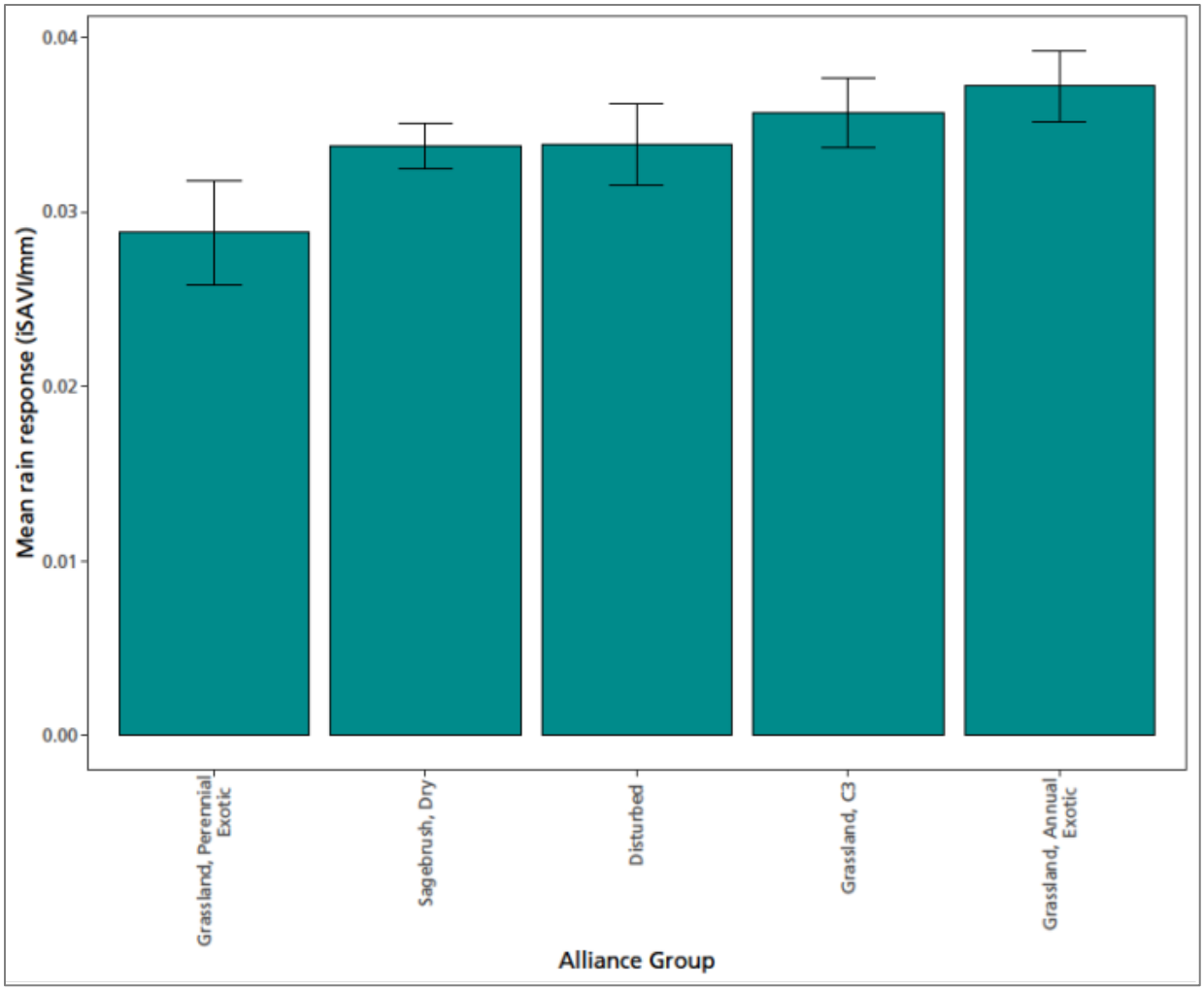


Figure 43. Sensitivity of growing season vegetation production to rain in polygons, where the relationship was significant (p-value < 0.05). Climate data summarized by water year.

NPS / DAVID THOMA

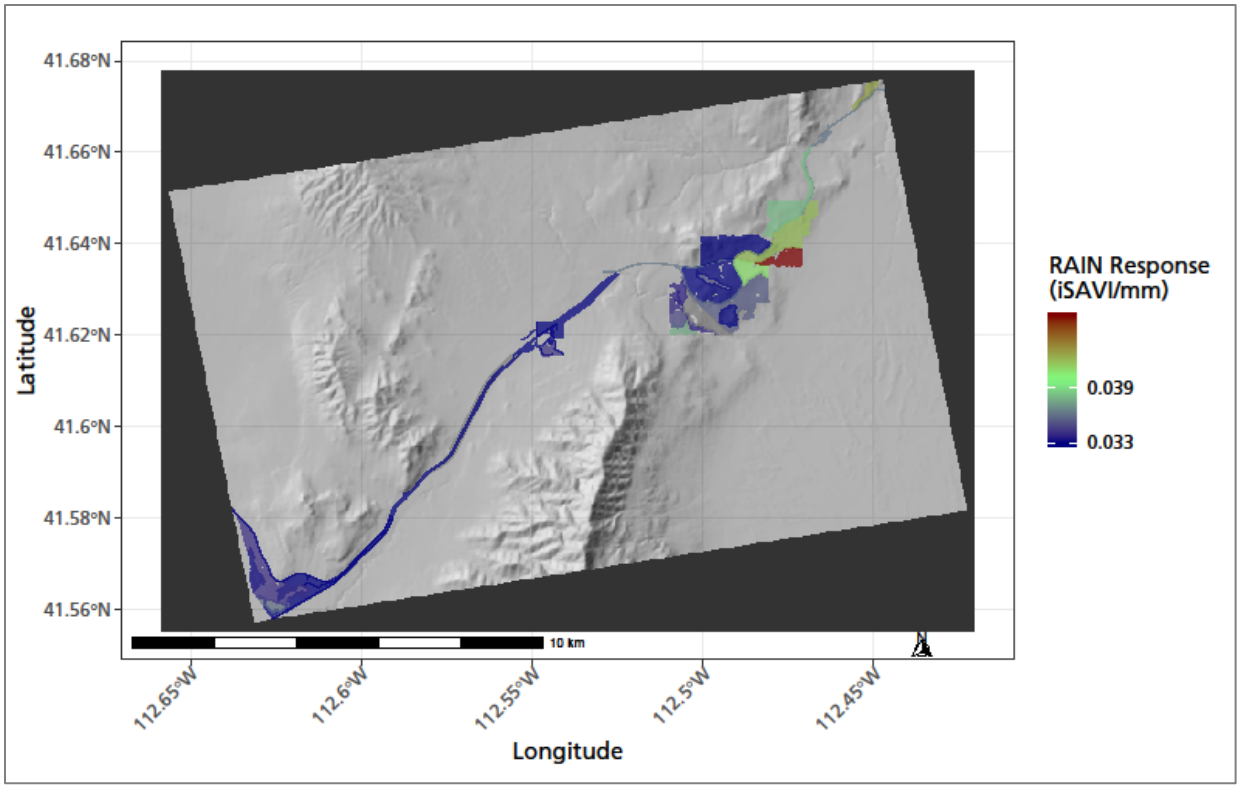


Figure 44. A map showing the sensitivity of growing season vegetation production to rain in polygons where the relationship was significant (p-value < 0.05). Climate data summarized by water year.
NPS / DAVID THOMA

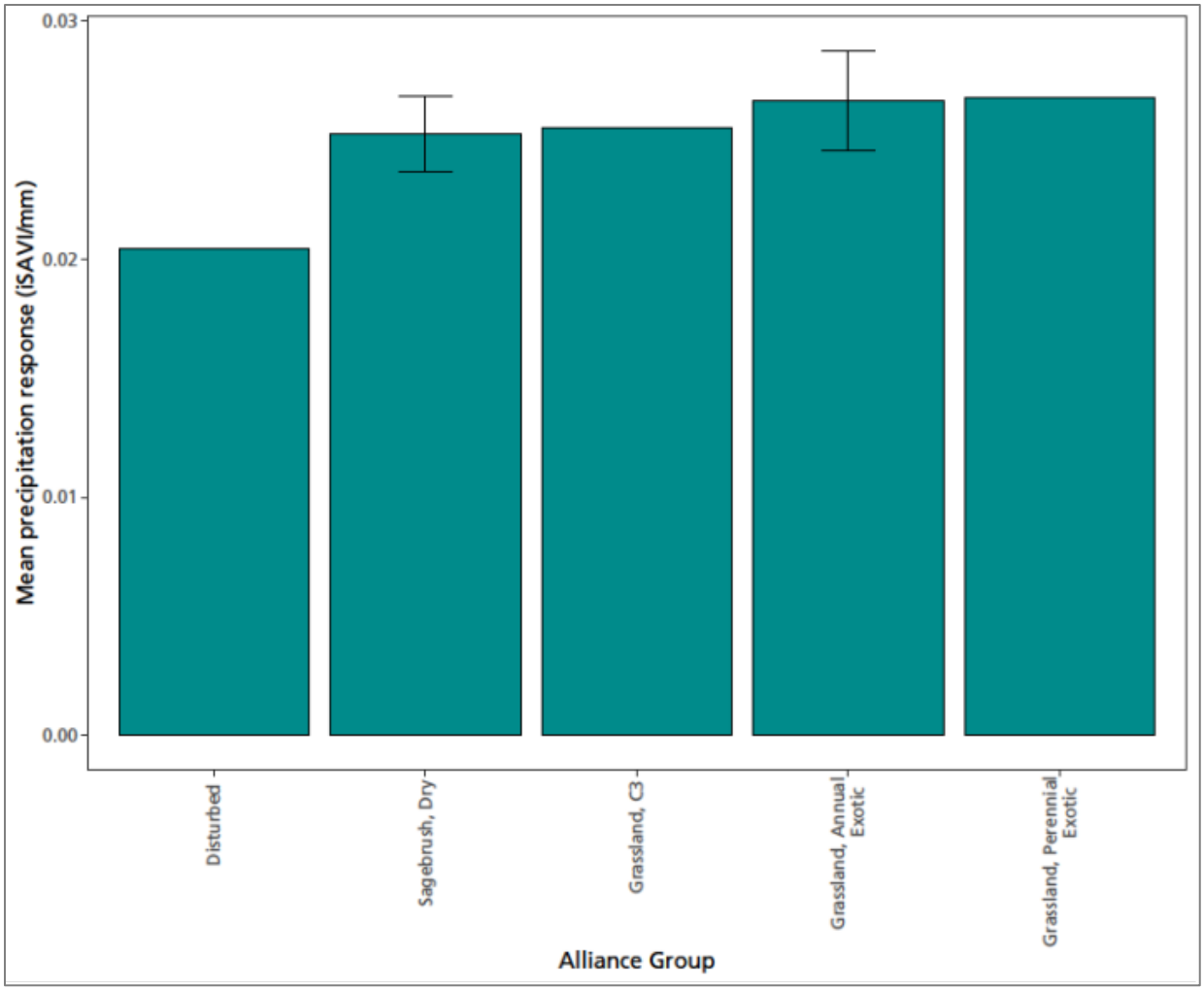


Figure 45. Sensitivity of growing season vegetation production to precipitation in polygons, where the relationship was significant (p-value < 0.05). Climate data summarized by water year.

NPS / DAVID THOMA

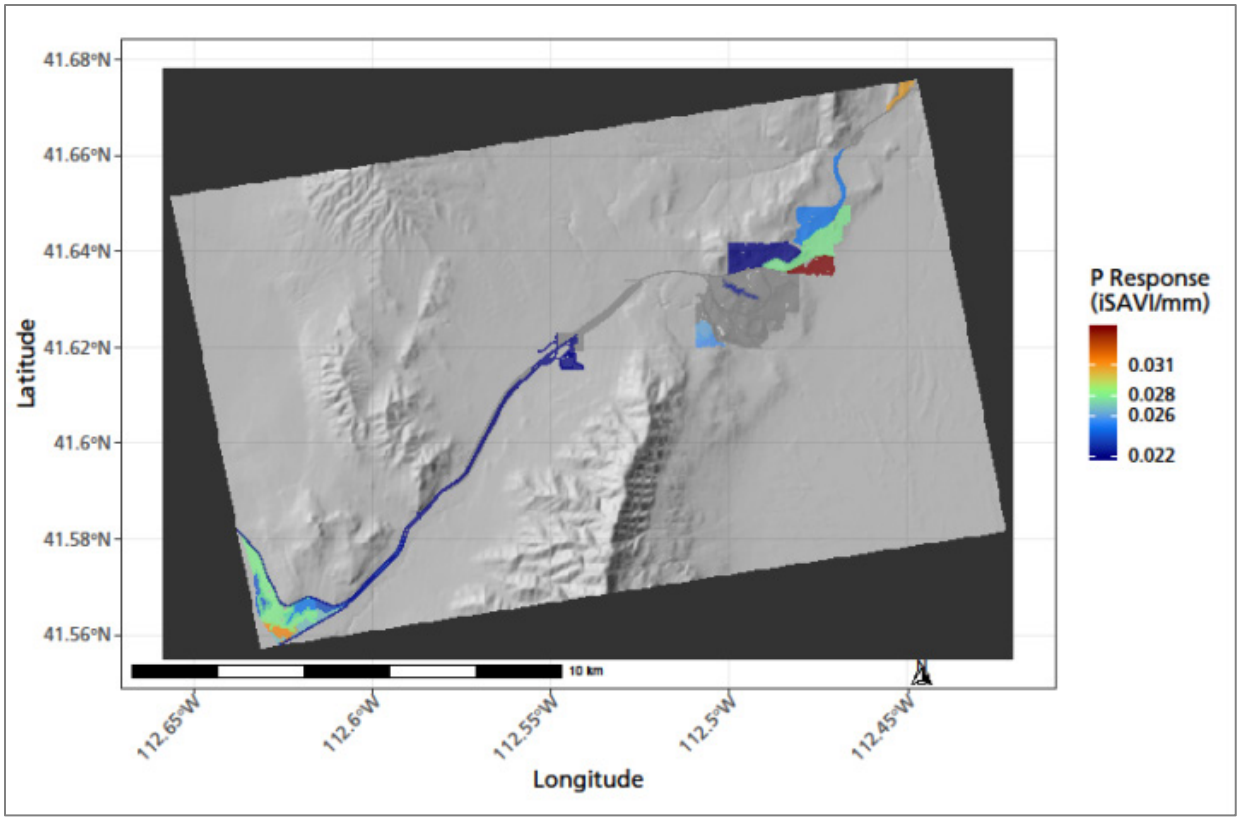


Figure 46. A map showing the sensitivity of growing season vegetation production to precipitation in polygons where the relationship was significant (p-value < 0.05). Climate data summarized by water year. *NPS / DAVID THOMA*

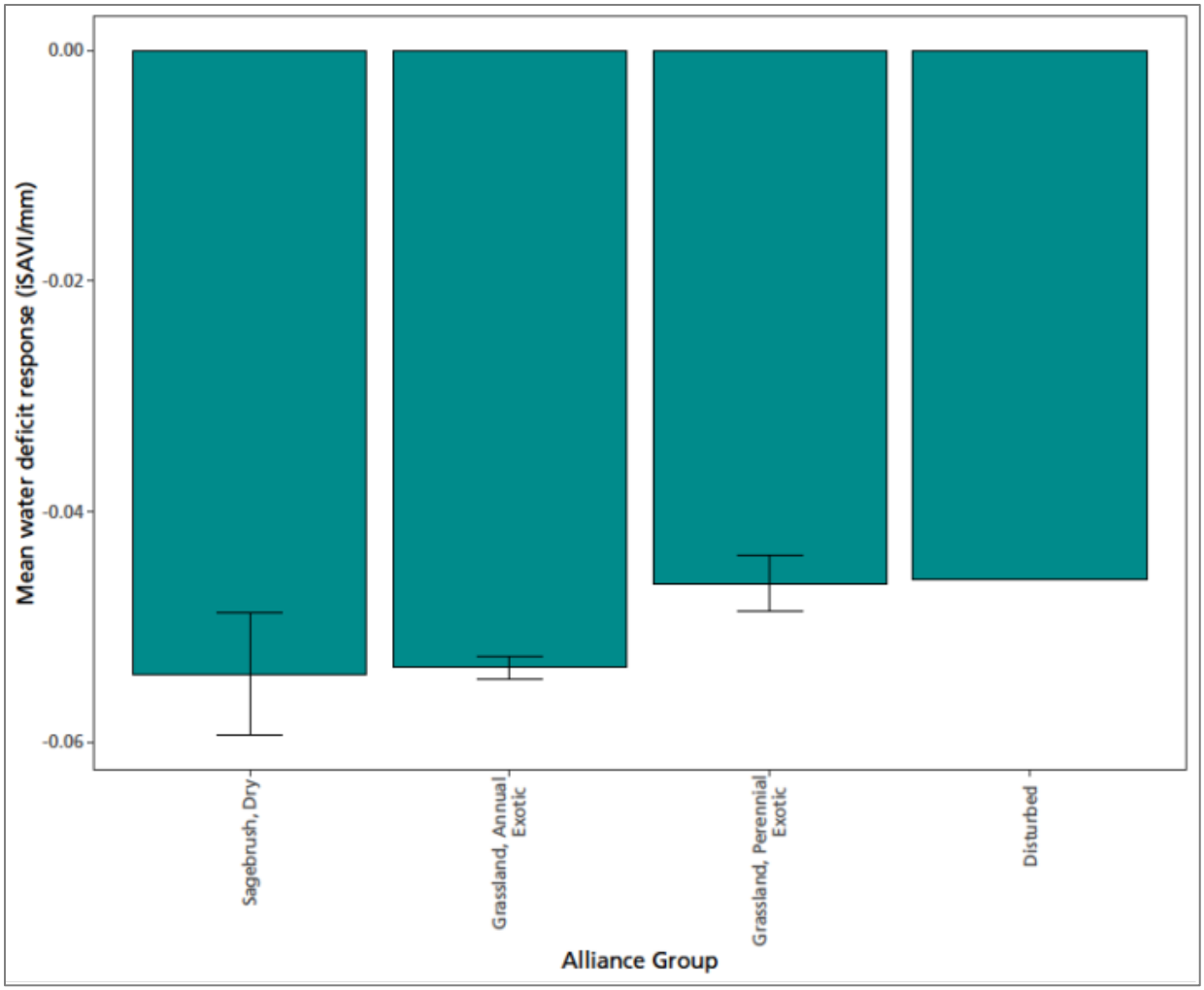


Figure 47. Sensitivity of growing season vegetation production to water deficit in polygons, where the relationship was significant (p-value < 0.05). Climate data summarized by water year.

NPS / DAVID THOMA

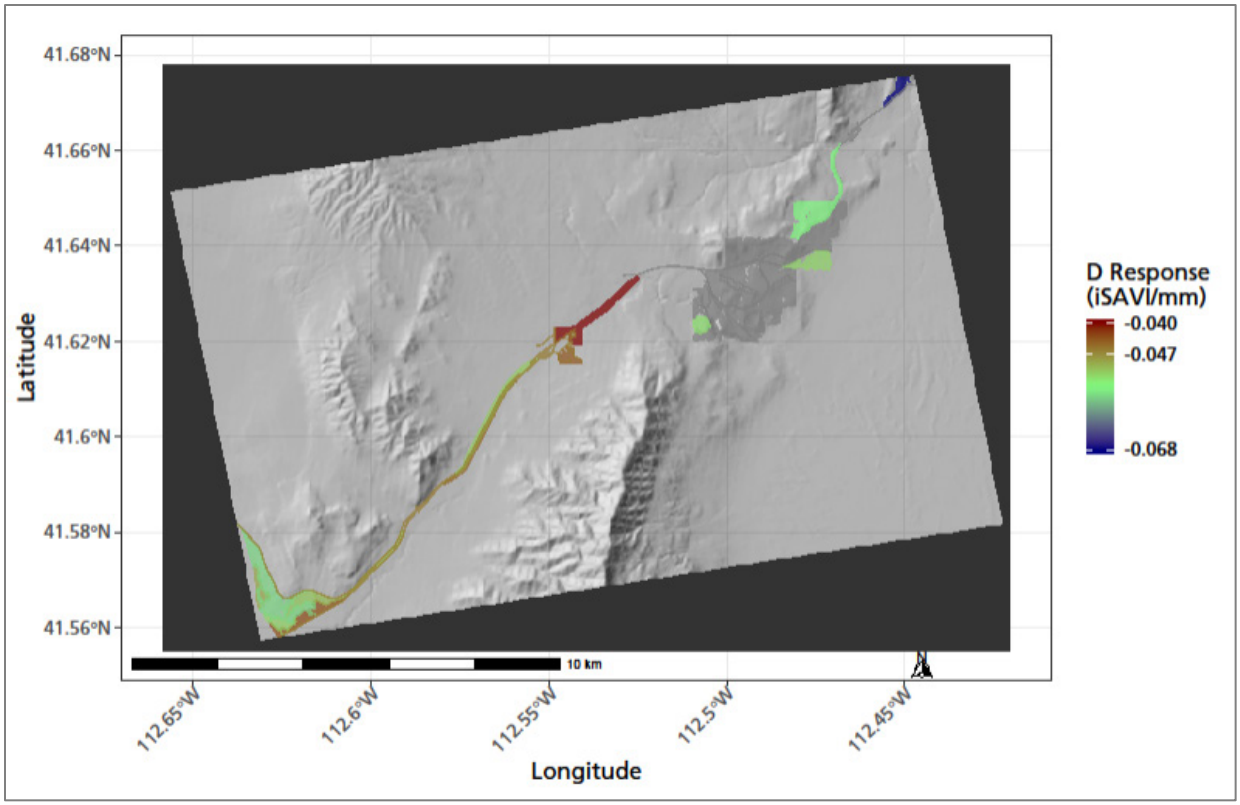


Figure 48. Sensitivity of growing season vegetation production to water deficit, where the relationship was significant (p-value < 0.05). Climate data summarized by water year.

NPS / DAVID THOMA

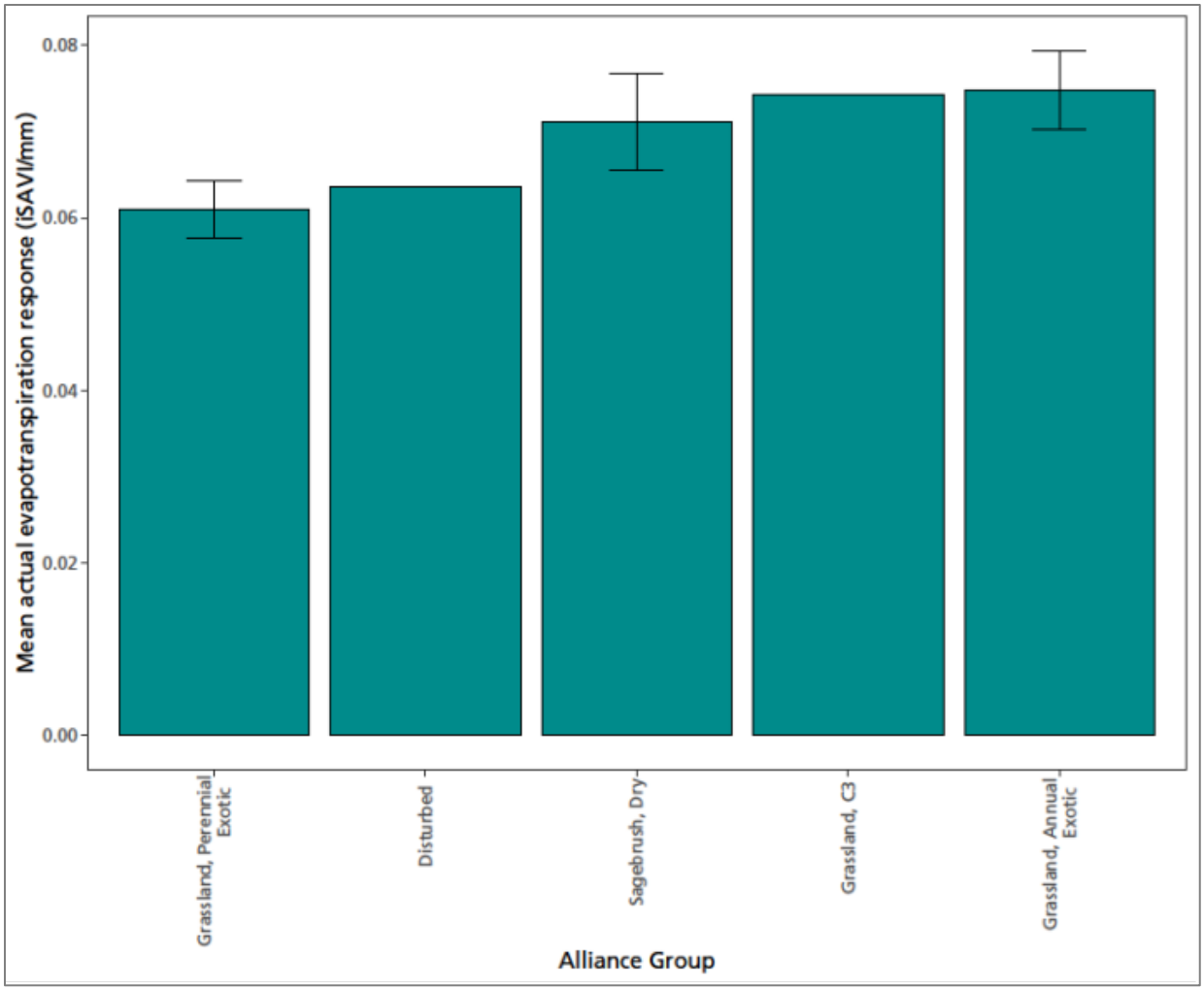


Figure 49. Sensitivity of growing season vegetation production to actual evapotranspiration in polygons, where the relationship was significant (p-value < 0.05). Climate data summarized by water year.
NPS / DAVID THOMA

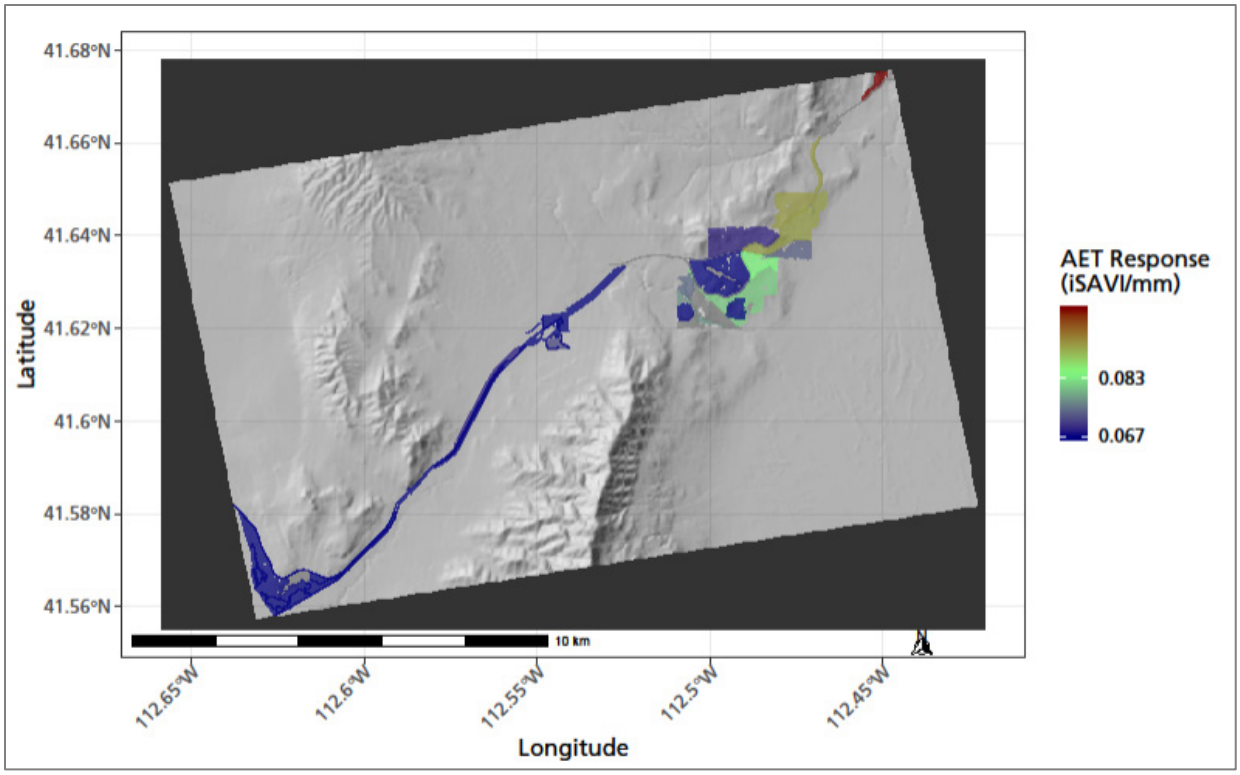


Figure 50. Sensitivity of growing season vegetation production to actual evapotranspiration, where the relationship was significant (p-value < 0.05). Climate data summarized by water year.

NPS / DAVID THOMA

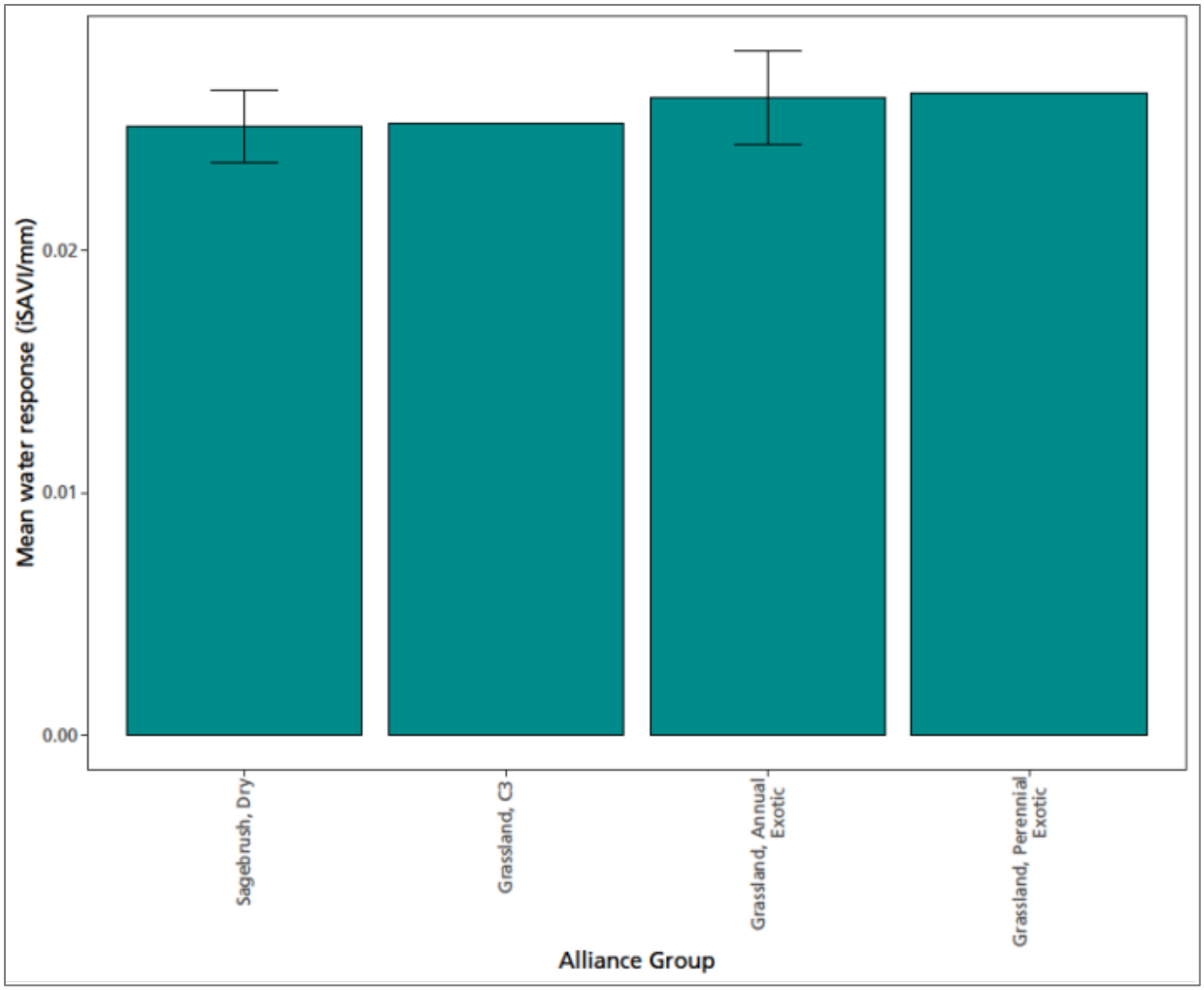


Figure 51. Sensitivity of growing season vegetation production to water in polygons, where the relationship was significant (p-value < 0.05). Climate data summarized by water year.

NPS / DAVID THOMA

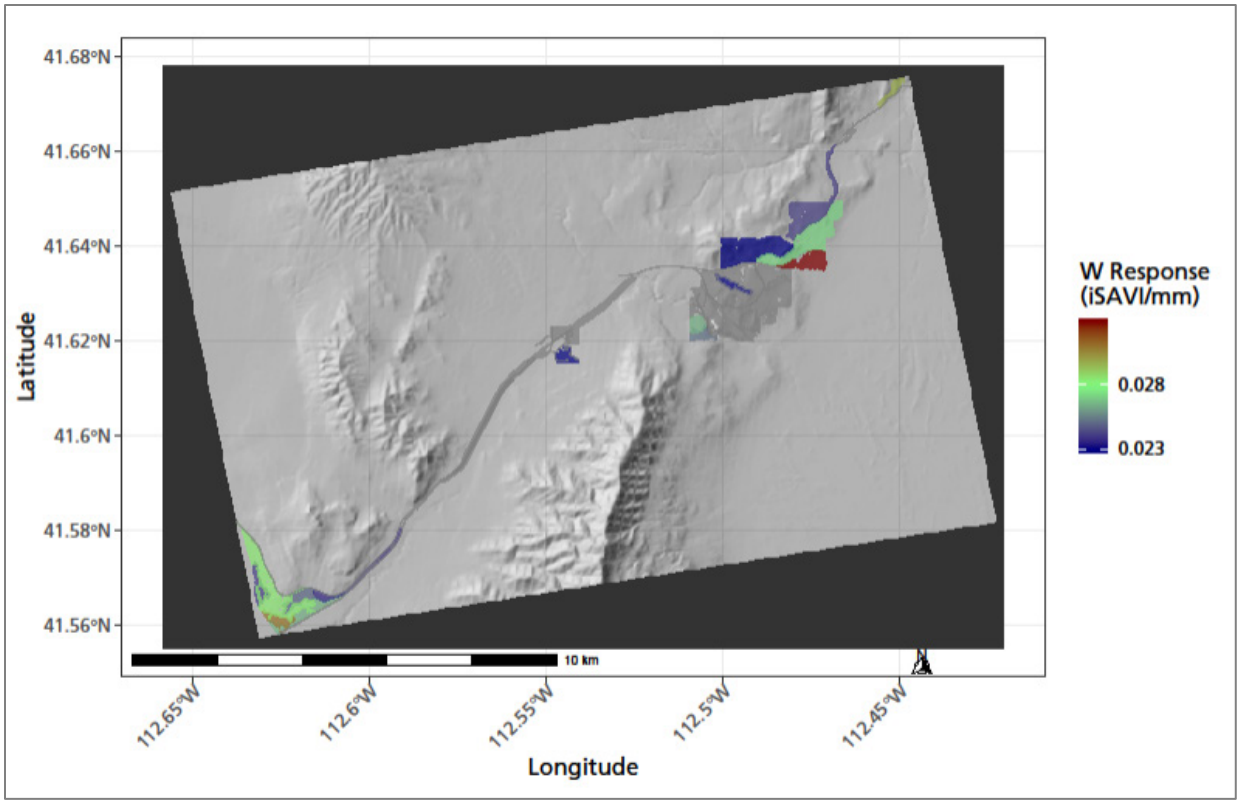


Figure 52. Sensitivity of growing season vegetation production to water, where the relationship was significant (p-value < 0.05). Climate data summarized by water year.

NPS / DAVID THOMA

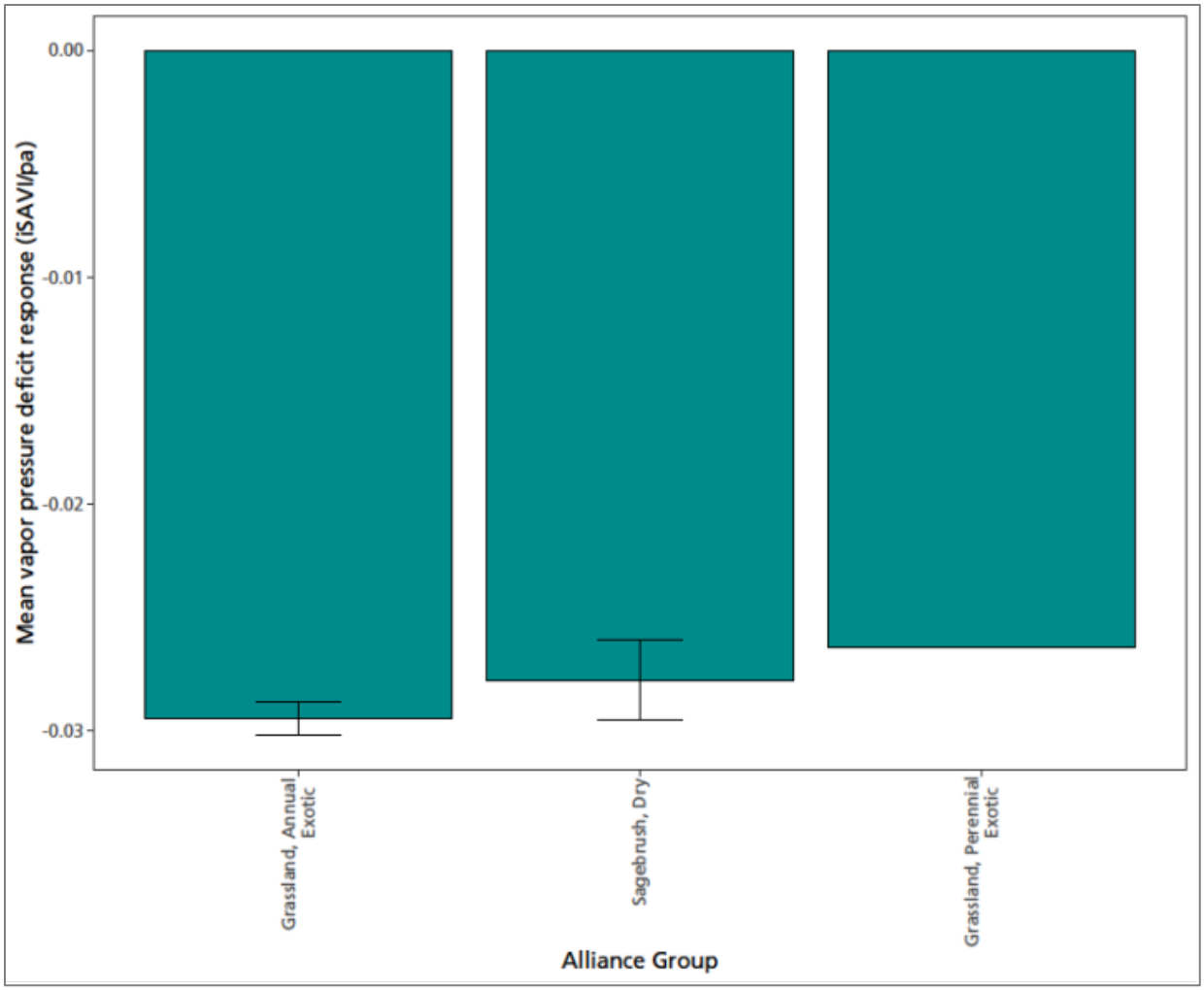


Figure 53. Sensitivity of growing season vegetation production to vapor pressure deficit in polygons, where the relationship was significant (p-value < 0.05). Climate data summarized by water year.
NPS / DAVID THOMA

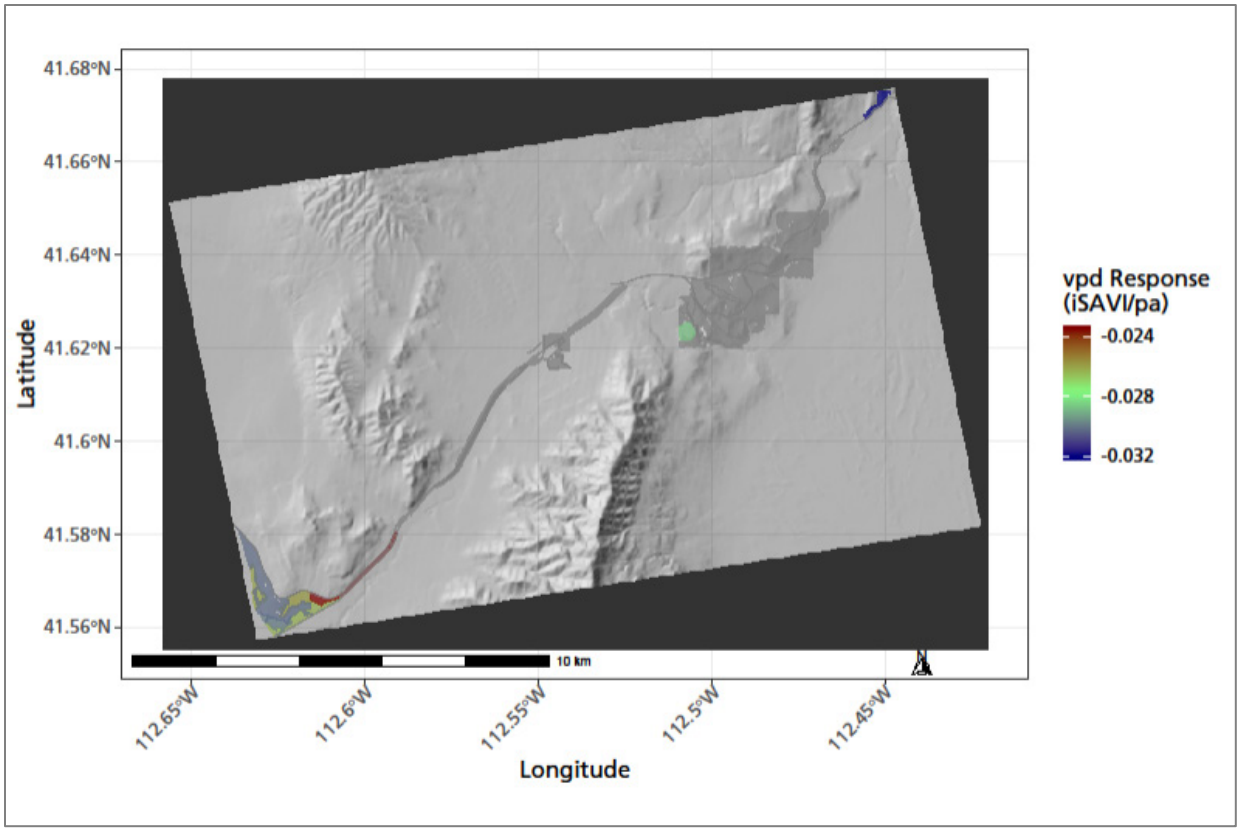


Figure 54. A map showing the sensitivity of growing season vegetation production to vapor pressure deficit in polygons where the relationship was significant (p-value < 0.05). Climate data summarized by water year.

NPS / DAVID THOMA

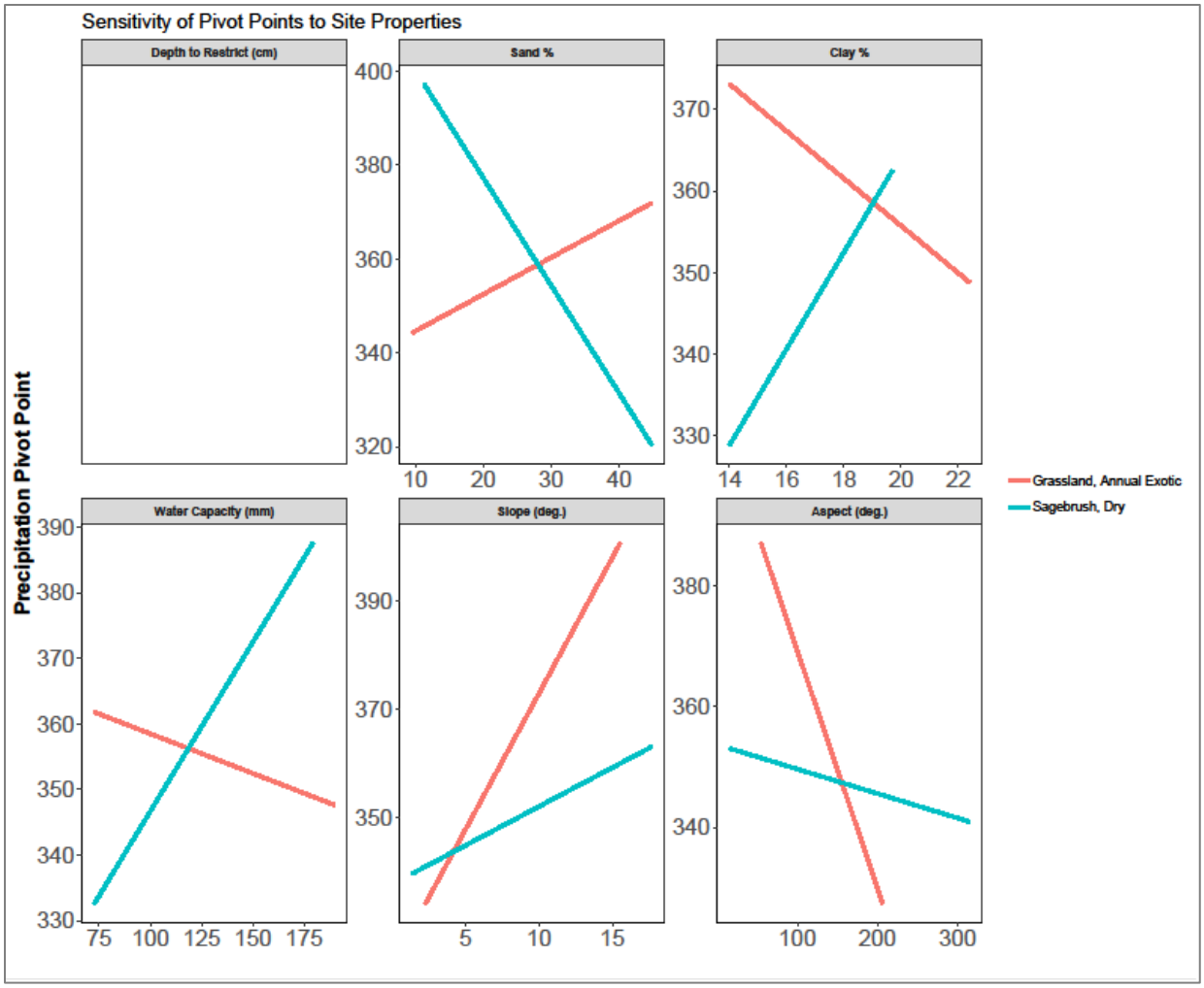


Figure 55. Variation in precipitation pivot points as related to soil and site characteristics. Steeper slopes indicate greater sensitivity of pivot points to site properties. These site properties are important modifiers of climate because they control water retention and distribution in the soil profile and, in the case of site slope and aspect, because they affect the heat load on vegetation.

NPS / DAVID THOMA

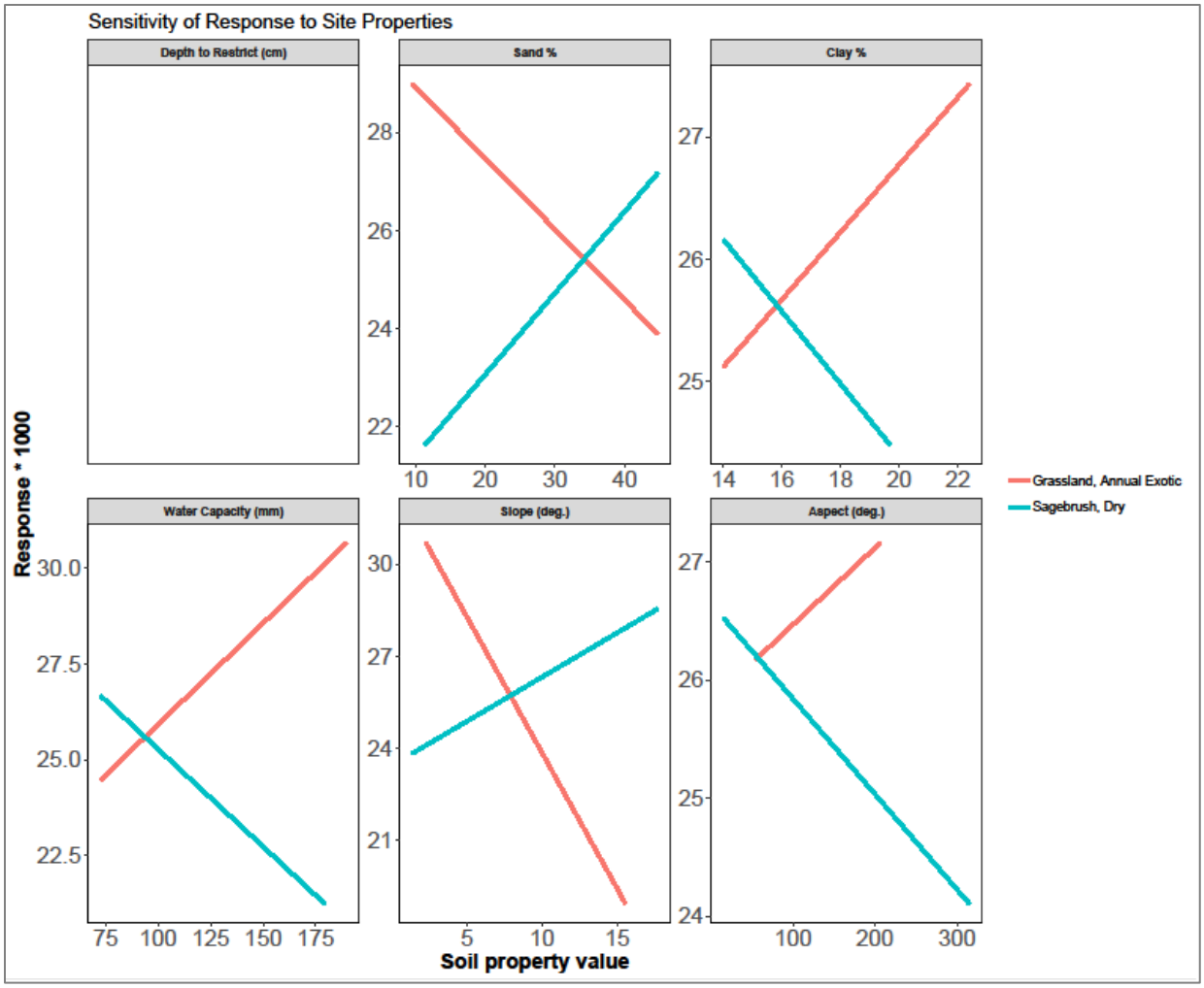


Figure 56. Variation in responses to precipitation as related to soil and site characteristics. Steeper slopes indicate greater sensitivity of responses to site properties. These site properties are important modifiers of climate because they control water retention and distribution in the soil profile and in the case of site slope and aspect because they affect the heat load on vegetation.

NPS / DAVID THOMA

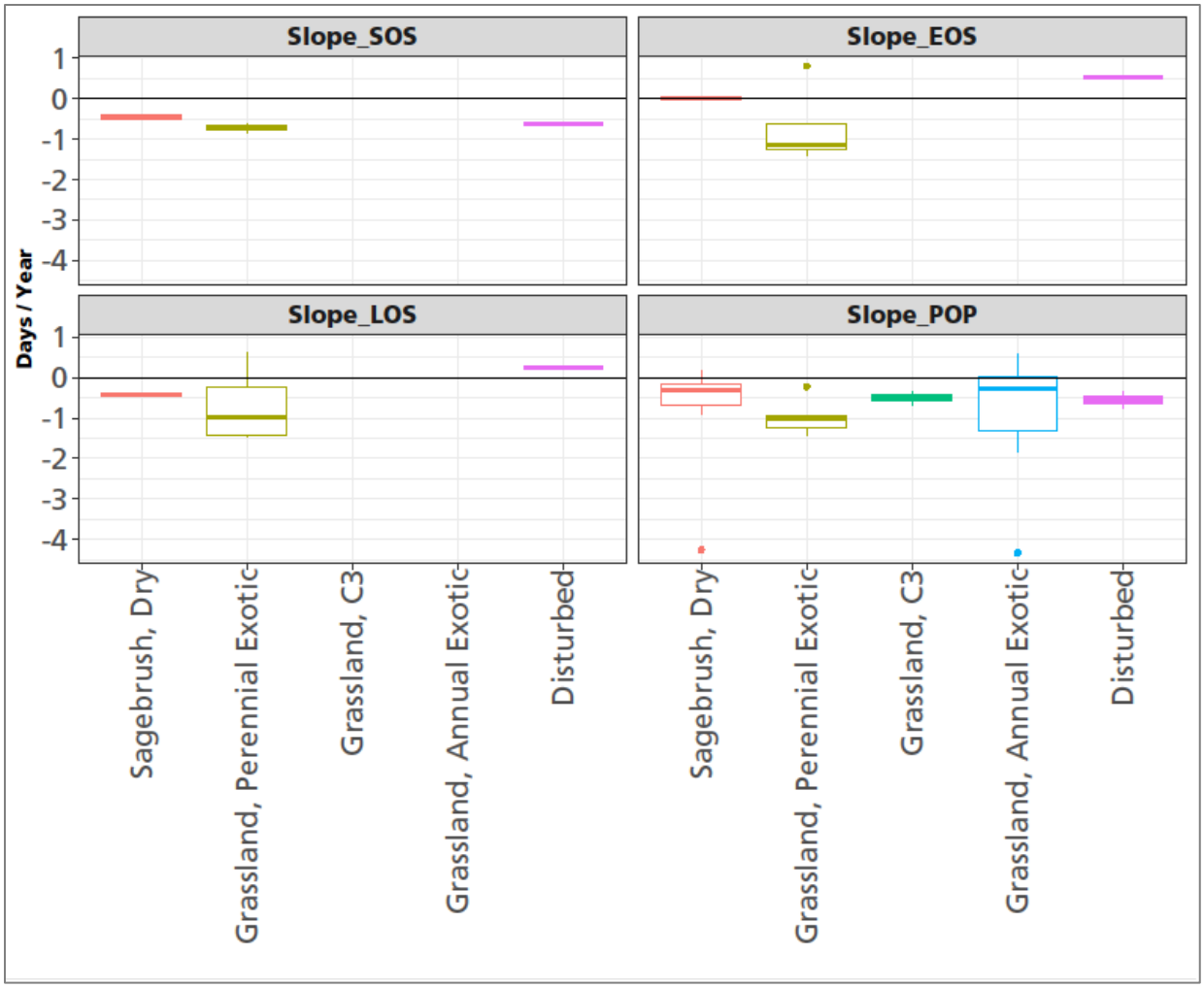


Figure 57. Direction and magnitude of change in land surface phenology metrics, shown as ± days per year, for each vegetation alliance group. Metrics include the start of season (Slope SOS), end of season (Slope EOS), length of season (Slope LOS), and timing of peak SAVI (Slope POP). Slope refers to the slope of linear regression of each phenology metric versus year for the period 2000–2019.

NPS / DAVID THOMA

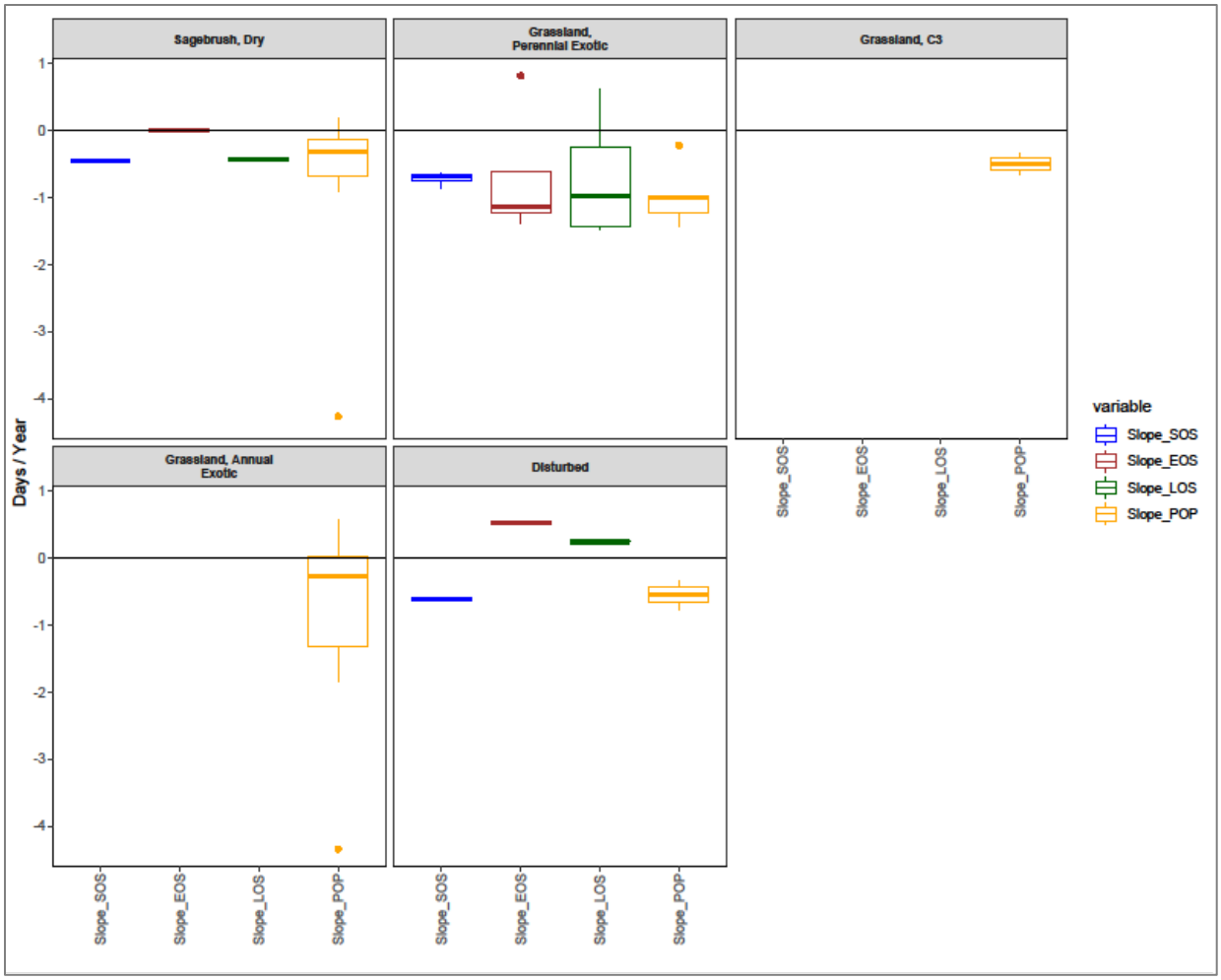


Figure 58. Direction and magnitude of change in land surface phenology metrics, shown as ± days per year, grouped by metric. Each panel shows change rates for SOS, EOS, LOS, and POP across alliance groups. Slope refers to the slope of linear regression of each phenology metric versus year for the period 2000–2019.

NPS / DAVID THOMA

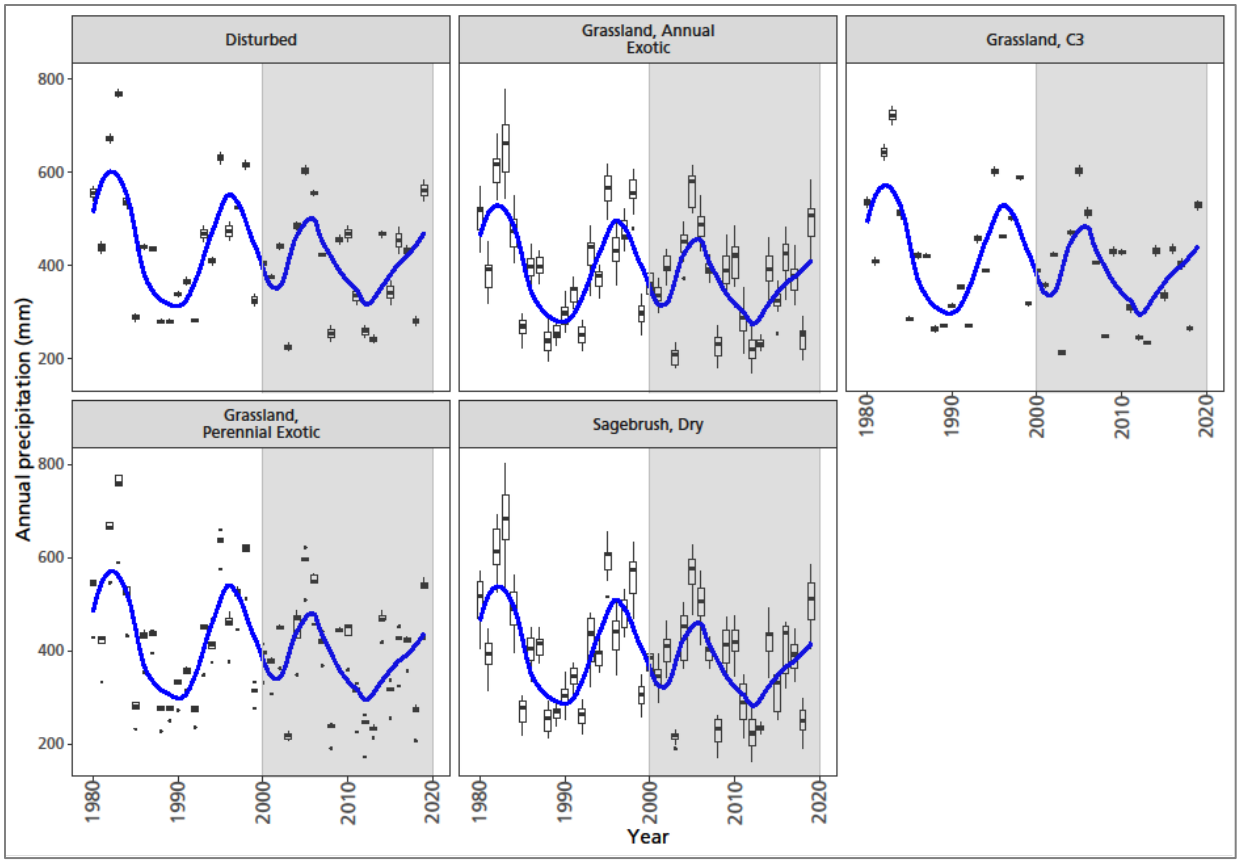


Figure 59. Cumulative annual precipitation over time (1980 to 2019) in vegetation alliance groups. Box plots demonstrate the range of variation within alliance groups by year. The blue line is a loess smooth with a 25 percent span to illustrate multi-year patterns. Gray shaded area includes the period investigated for relationships between production and climate when satellite imagery and climate data were both available.

NPS / DAVID THOMA

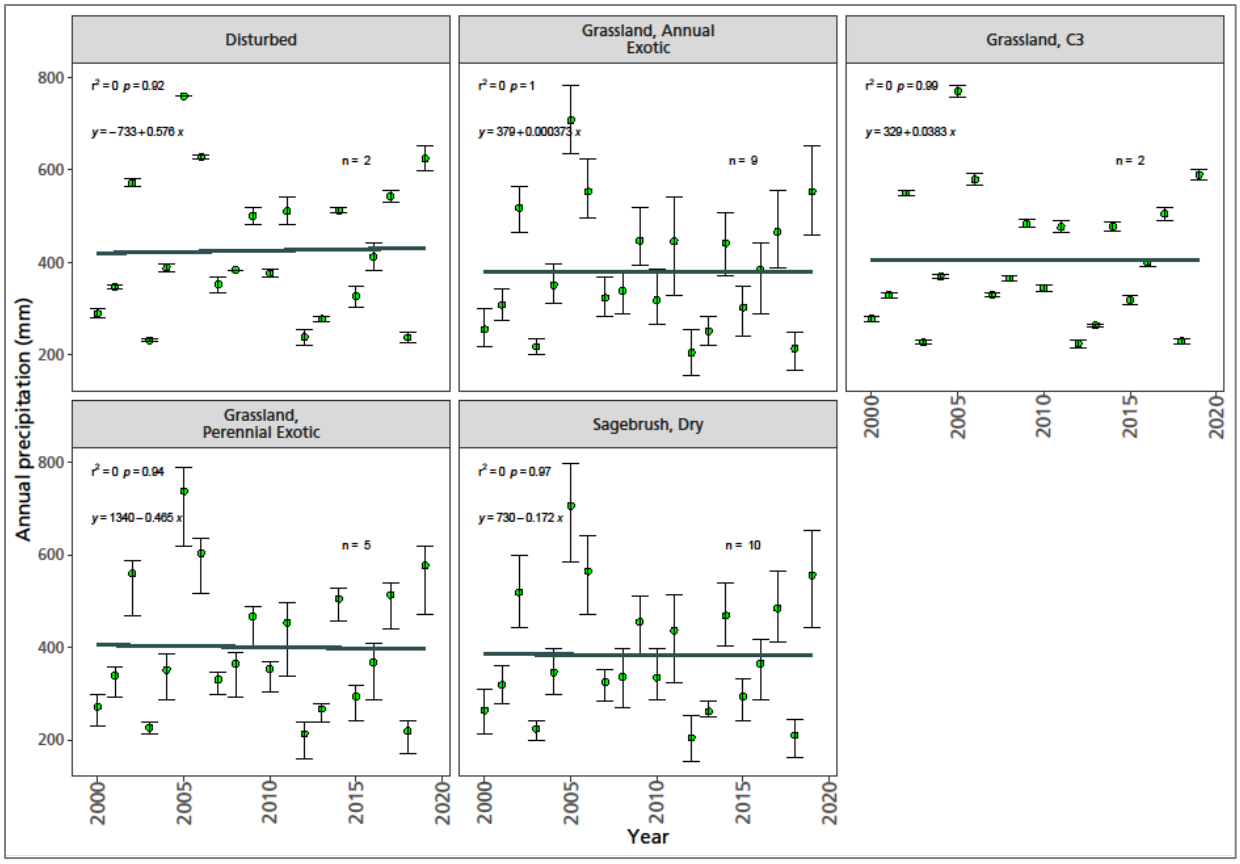


Figure 60. Cumulative annual precipitation over time (2000 to 2019) in vegetation alliance groups. The trend over time is shown for the period in gray in the previous figure. Error bars are standard error.
NPS / DAVID THOMA

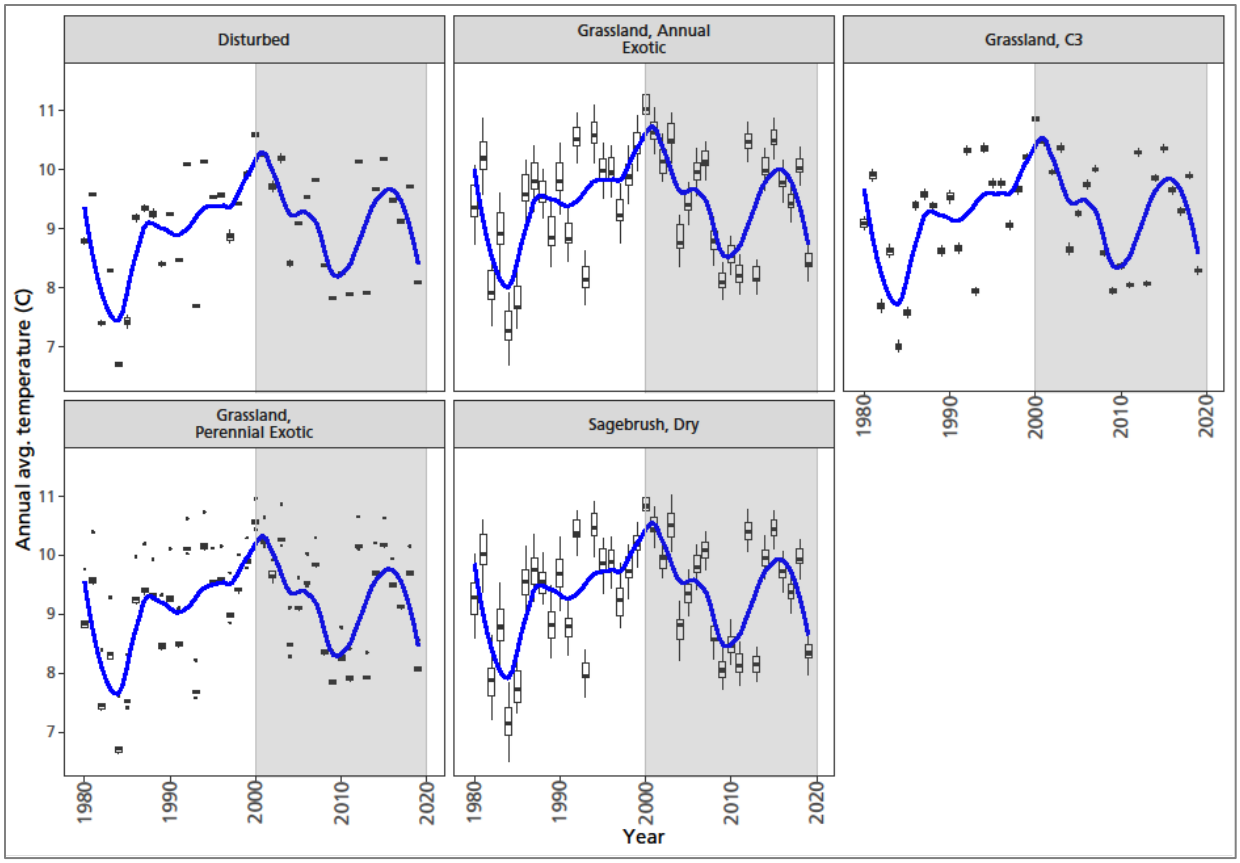


Figure 61. Annual average temperature over time (1980 to 2019) in vegetation alliance groups. Box plots demonstrate the range of variation within alliance groups by year. The blue line is a loess smooth with a 25 percent span to illustrate multi-year patterns. Gray shaded area includes the period investigated for relationships between production and climate when satellite imagery and climate data were both available.

NPS / DAVID THOMA

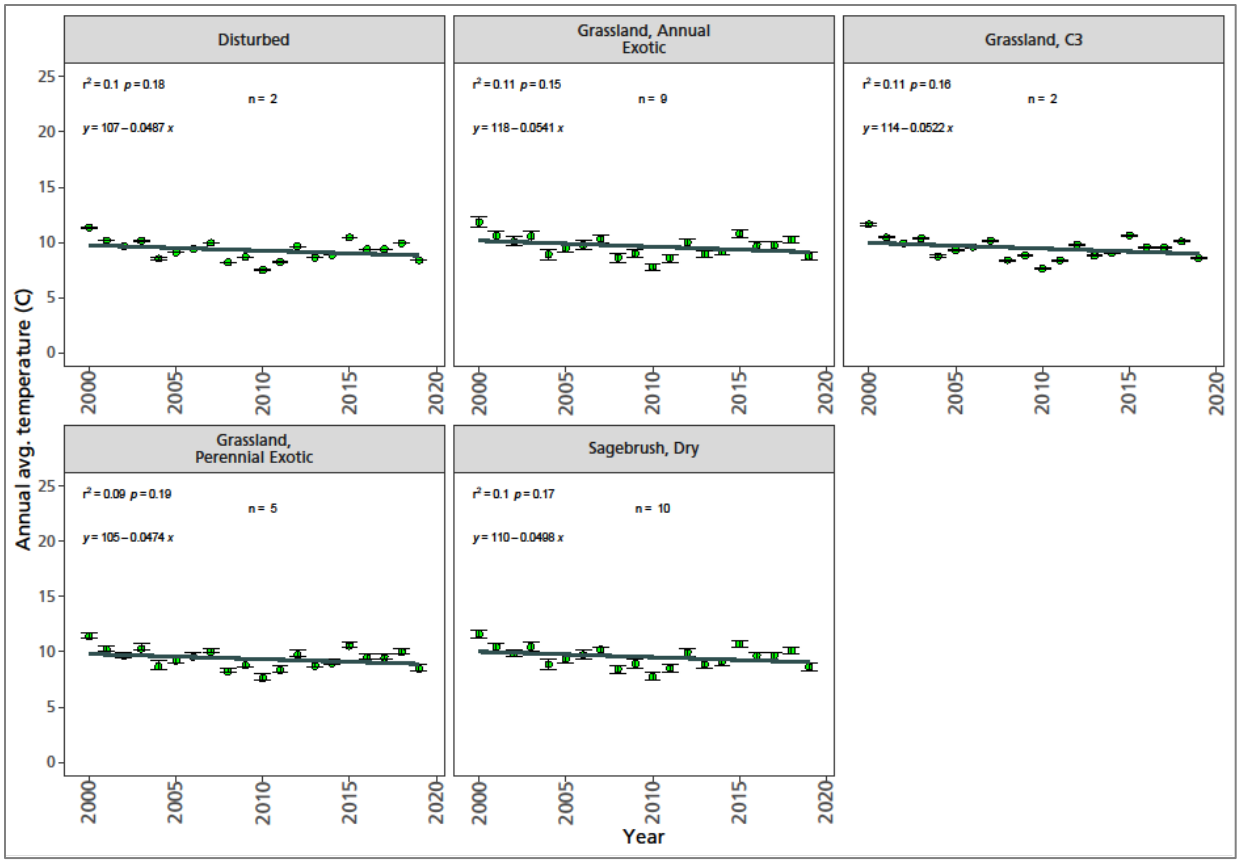


Figure 62. Annual average temperature over time (2000 to 2019) in vegetation alliance groups. The trend over time is shown for the period in gray in the previous figure. Error bars are standard error.

NPS / DAVID THOMA

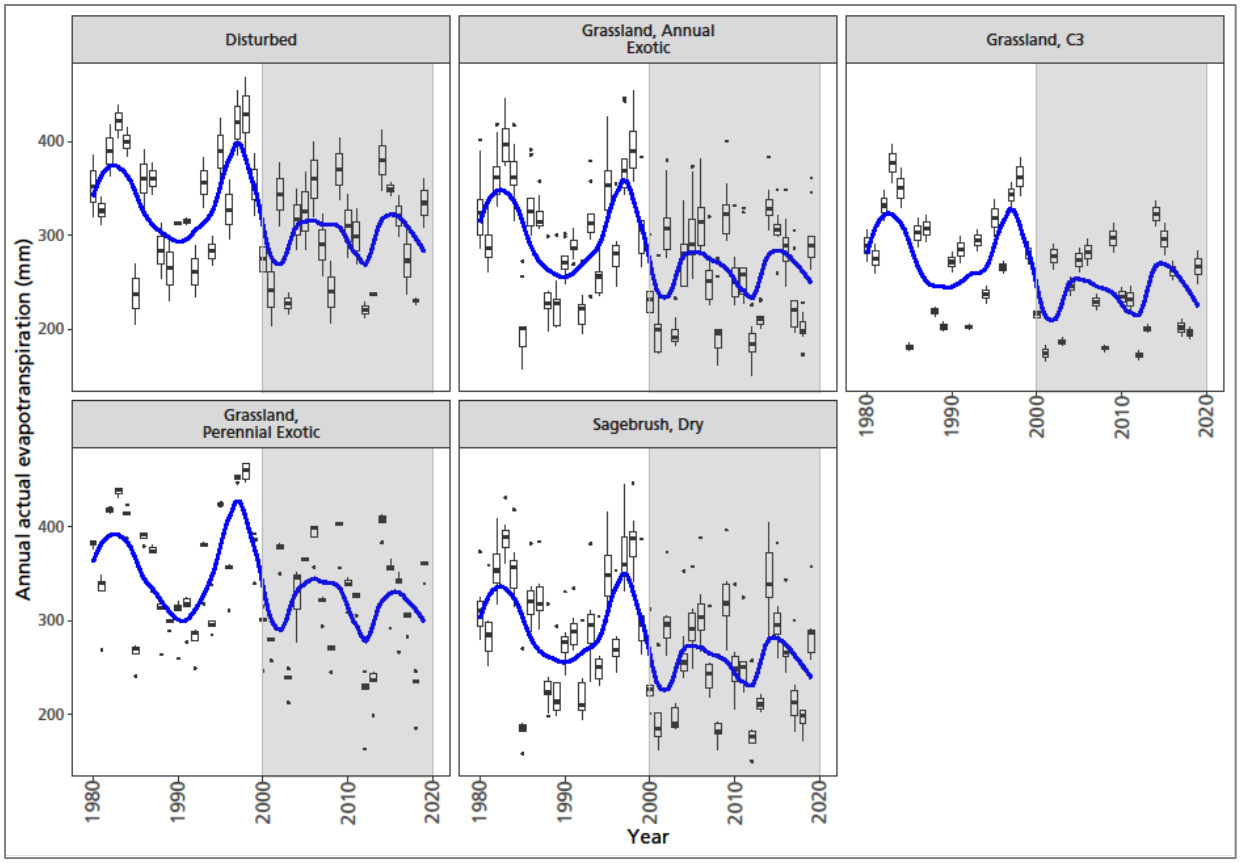


Figure 63. Cumulative annual actual evapotranspiration over time (1980 to 2019) in vegetation alliance groups. Box plots demonstrate the range of variation within alliance groups by year. The blue line is a loess smooth with a 25 percent span to illustrate multi-year patterns. Gray shaded area includes the period investigated for relationships between production and climate when satellite imagery and climate data were both available.

NPS / DAVID THOMA

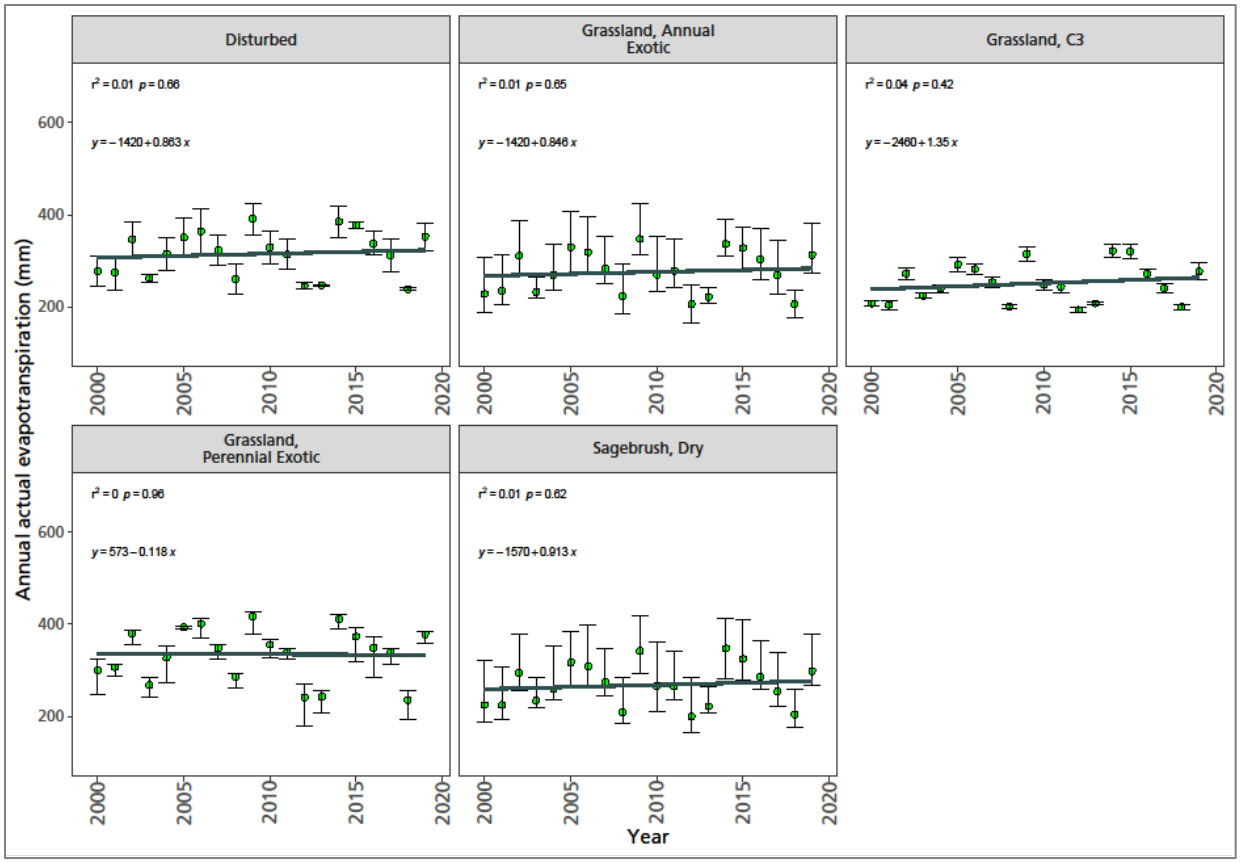


Figure 64. Cumulative annual actual evapotranspiration over time (2000 to 2019) in vegetation alliance groups. The trend over time is shown for the period in gray in the previous figure. Error bars are standard error.

NPS / DAVID THOMA

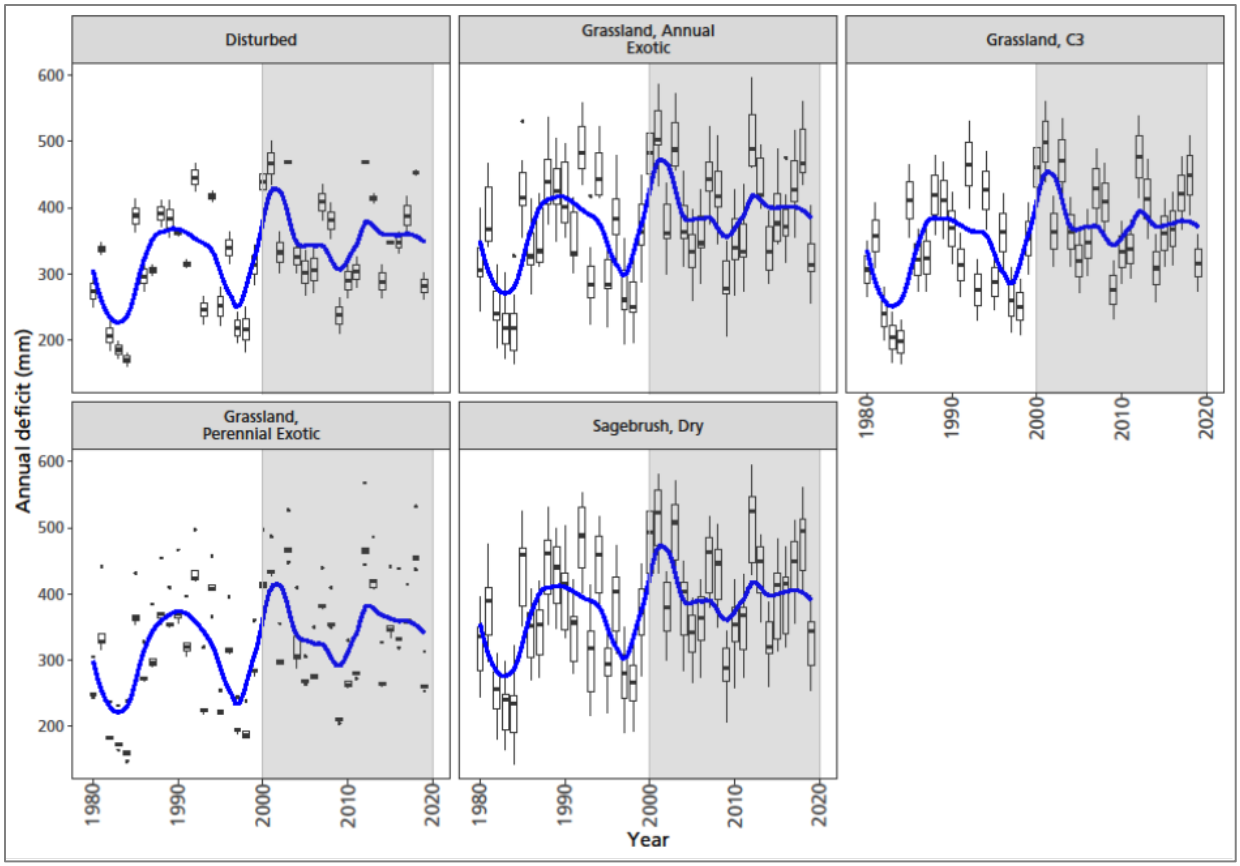


Figure 65. Cumulative annual water deficit over time (1980 to 2019) in vegetation alliance groups. Box plots demonstrate the range of variation within alliance groups by year. The blue line is a loess smooth with a 25 percent span to illustrate multi-year patterns. Gray shaded area includes the period investigated for relationships between production and climate when satellite imagery and climate data were both available.

NPS / DAVID THOMA

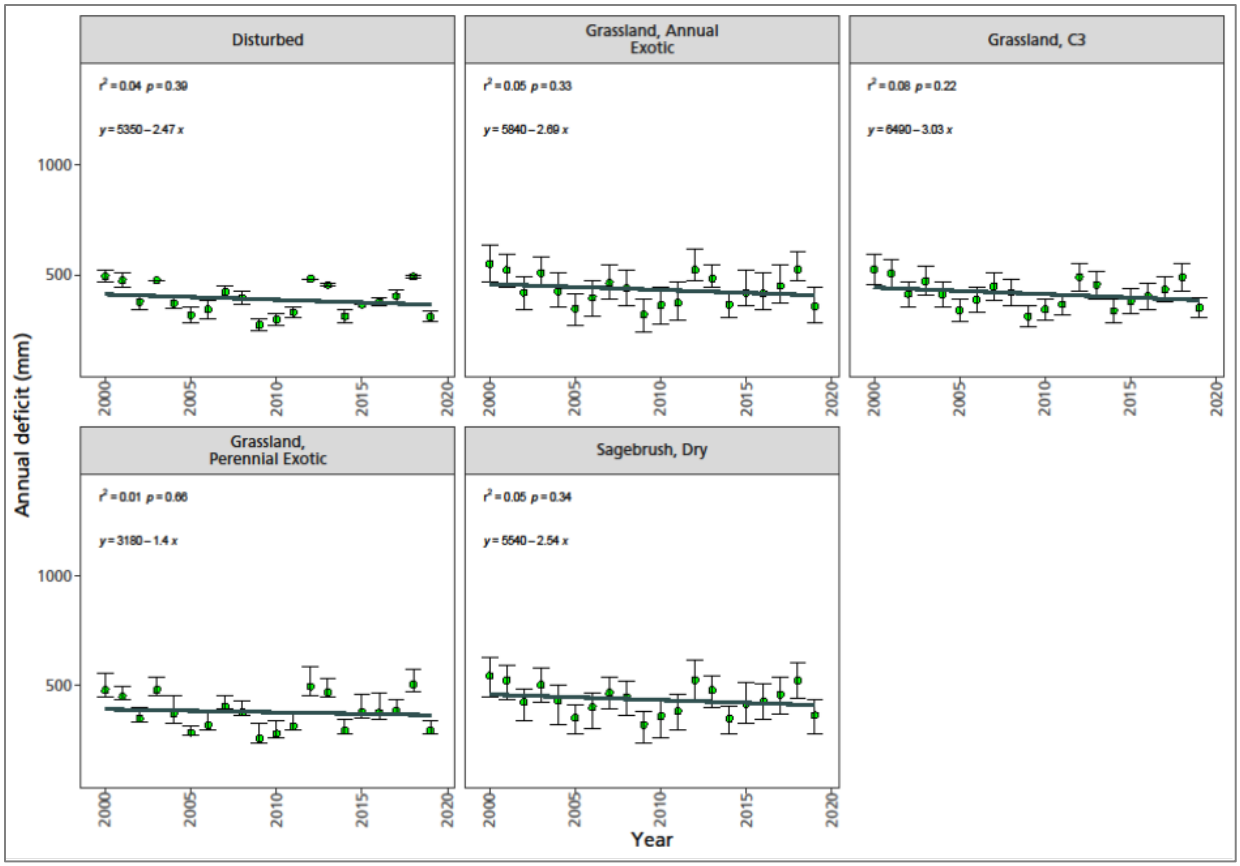


Figure 66. Cumulative annual water deficit over time (2000 to 2019) in vegetation alliance groups. The trend over time is shown for the period in gray in the previous figure. Error bars are standard error.
NPS / DAVID THOMA

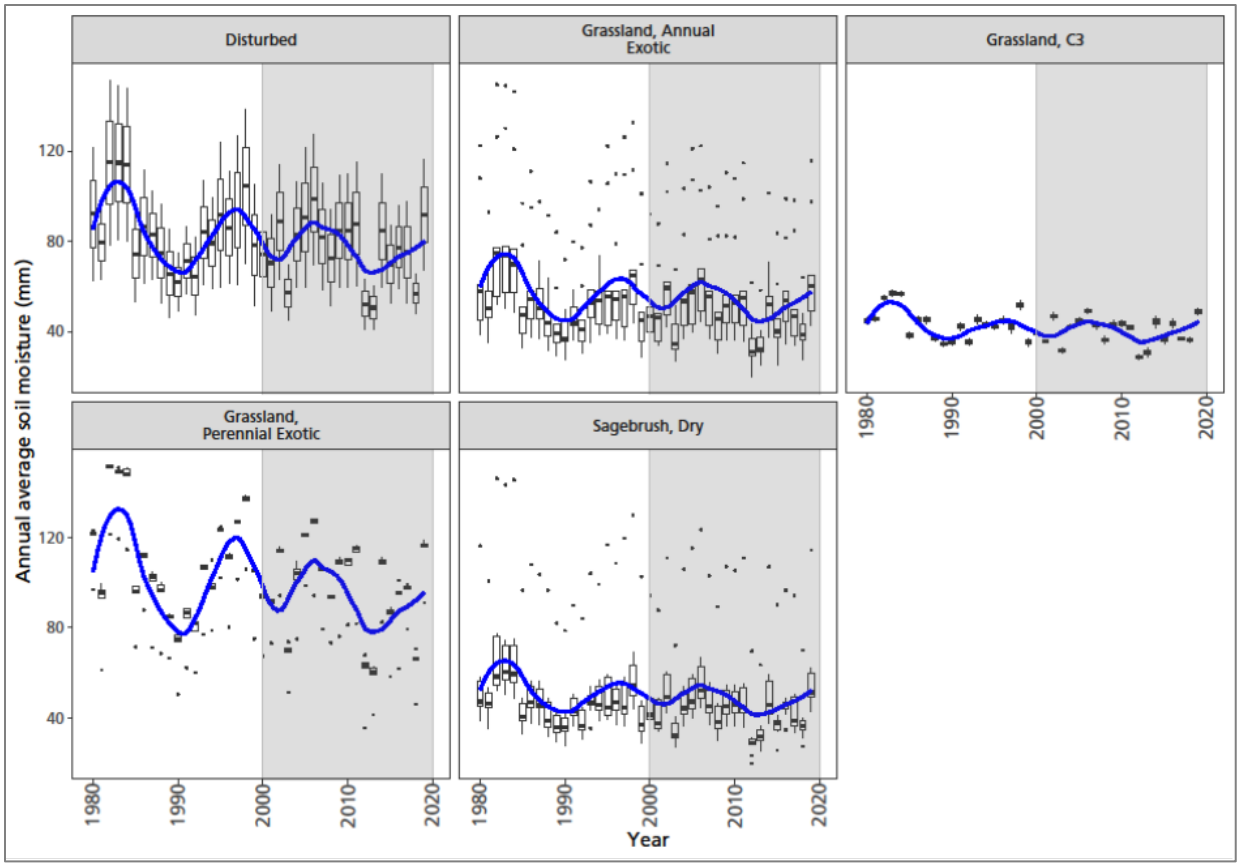


Figure 67. Annual average soil moisture over time (1980 to 2019) in vegetation alliance groups. Box plots demonstrate the range of variation within alliance groups by year. The blue line is a loess smooth with a 25 percent span to illustrate multi-year patterns. Gray shaded area includes the period investigated for relationships between production and climate when satellite imagery and climate data were both available.

NPS / DAVID THOMA

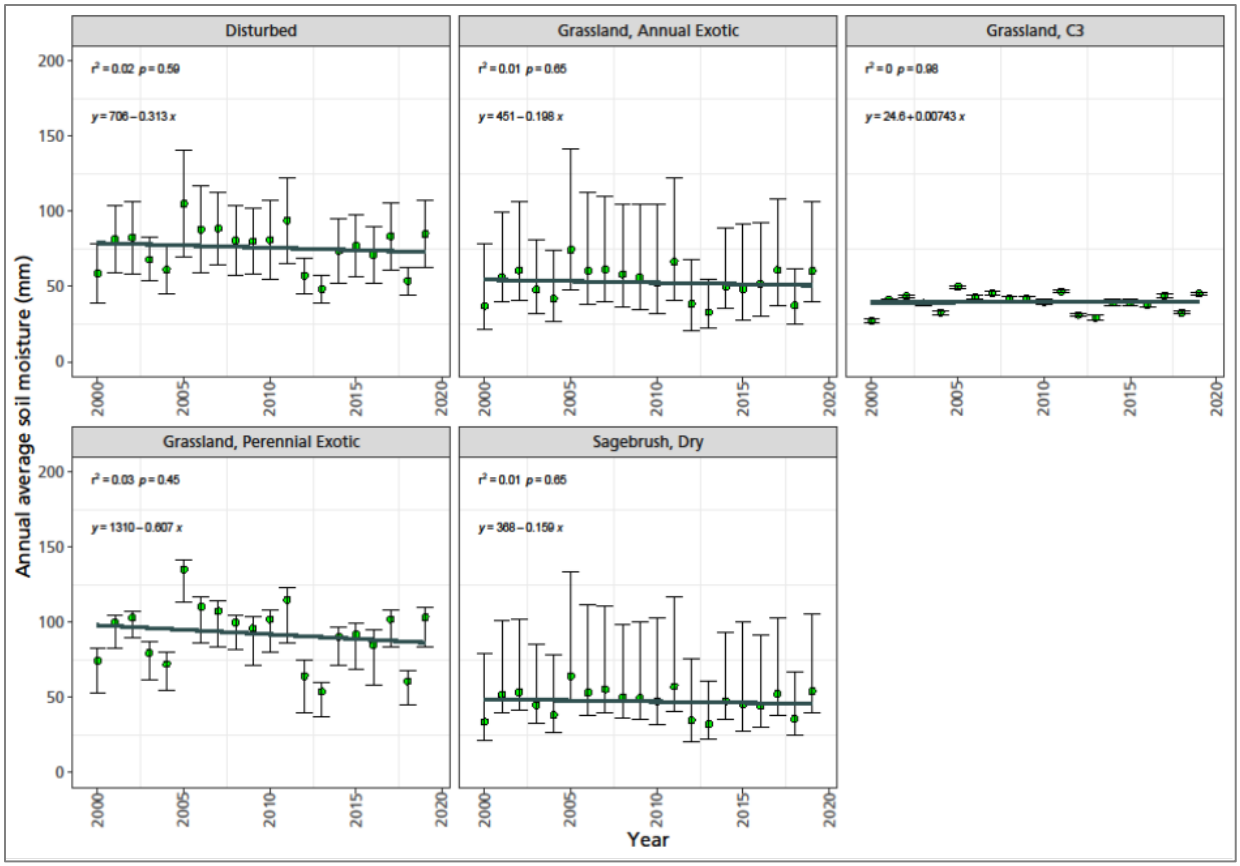


Figure 68. Annual average soil moisture over time (2000 to 2019) in vegetation alliance groups. The trend over time is shown for the period in gray in the previous figure. Error bars are standard error. *NPS / DAVID THOMA*

National Park Service
U.S. Department of the Interior

Science Report NPS/SR—2025/324
https://doi.org/10.36967/2313756



Natural Resource Stewardship and Science
1201 Oakridge Drive, Suite 150
Fort Collins, CO 80525

NPS 431/197327, June 2025